Supplementary Information

Gene expression dynamics of human and mouse craniofacial development at the single-cell level

Nagham Khouri-Farah[1,*], Alexandra Manchel[2,*], Emma Wentworth Winchester[1], Brian M. Schilder[3,4], Kelsey Robinson[5], Sarah W. Curtis[5], Nathan G. Skene[3,4], Elizabeth J. Leslie-Clarkson[5], Justin Cotney[2,6,#]

[1] Graduate Program in Genetics and Developmental Biology, UConn Health, Farmington, CT 06030, USA

[2] Department of Surgery, Children's Hospital of Philadelphia, Philadelphia, PA 19104, USA

[3] Department of Brain Sciences, Faculty of Medicine, Imperial College London, London, W12 0BZ, UK

[4] UK Dementia Research Institute at Imperial College London, London, W12 0BZ, UK

[5] Department of Human Genetics, Emory University School of Medicine, Atlanta, GA 30322, USA

[6] Department of Genetics, Perelman School of Medicine, University of Pennsylvania, Philadelphia, PA 19104, USA

* These authors contributed equally to this work.

Corresponding author: cotneyj@chop.edu

Contents:

1. Supplementary Note

2. Supplementary Figures and Captions

3. Supplementary References

1. Supplementary Note

Initial Filtering of Non-Craniofacial Cell Types

To characterize the cellular landscape of human craniofacial development we performed snRNA-seq analysis of 24 individual human embryos across 6 distinct time points, encompassing major milestones of human craniofacial development from 4 to 8 post conception weeks (Fig. 1A). We profiled the entire craniofacial prominence from multiple biological replicates at each time point resulting in 130,427 nuclei after filtering for doublets and nuclei quality. Our initial clustering analysis revealed a total of 24 distinct clusters (Supplementary Fig. 1A), which was higher than the main cell types identified in mouse craniofacial developmental studies[1-3]. When we examined the contributions of each Carnegie Stage to these clusters, we found several clusters to be biased towards early vs. later time points (Supplementary Fig. 1B). We sought to clarify the identity of the 24 cell populations by first generating module scores for neuronal and radial glia cell populations. We generated module scores for neurons and radial glia using their gene markers from Eze et al. 2021[4] and labeled these cell types in our data when the module scores were above the median (Supplementary Fig.1C-D). We reasoned these clusters were derived from developing brain tissue and thus excluded these nuclei from downstream analyses. This resulted in a total of 95,892 remaining nuclei with an average of 3,996 nuclei from each sample (Supplementary Fig. 2A) and a median of 6,890 counts from 2,988 genes per nucleus (Supplementary Fig. 2B,C). We observed that early samples had consistently higher mitochondrial reads (Supplementary Fig. 2D), however, this was not due to increased apoptosis as tested by generating an apoptosis module score using gene markers from the Hallmark Apoptosis gene set within the human MSigDB Core Collection[5] (Supplementary Fig. 2D). The sex of each embryo was identified using known sex determination genes for males (*UTY, DDX3Y, KDM5D*, and *NLGN4Y*) and females (*XIST* and *TSIX*) (Supplementary Fig. 2E), and each of the main cell type clusters contained roughly the same number of male and female samples (Supplementary Fig. 2F). We observed that early samples had consistently higher mitochondrial reads (Supplementary Fig. 2D), however, this was not due to increased apoptosis based on expression of Hallmark Apoptosis genes from human MSigDB Core Collection[5] (Supplementary Fig. 2F). The sex of each embryo was identified using known sex determination genes for males (*UTY, DDX3Y, KDM5D*, and *NLGN4Y*) and females (*XIST* and *TSIX*) (Supplementary Fig. 2E), and each of the main cell type clusters contained roughly the same number of male and female samples (Supplementary Fig. 2F). We then re-clustered the data after removing the neuronal and radial glia populations and identified eight major clusters, which we projected into two dimensions using Uniform Manifold Approximation and Projection (UMAP)[6] (Fig. 1C).

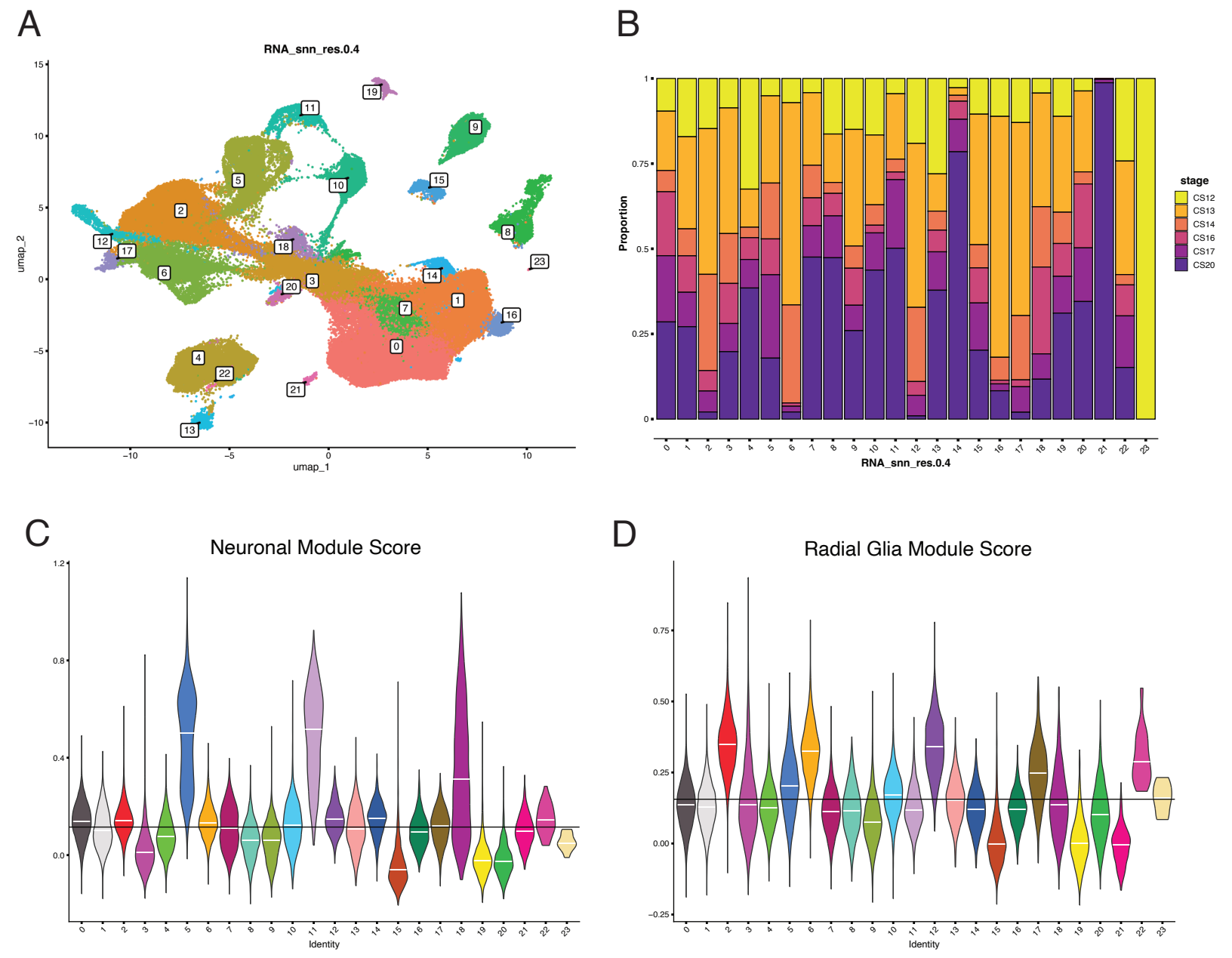
Characterization of the human *SOX2+/SOX10-* early progenitor cell subtypes

We next subclustered the *SOX2+/SOX10-* early progenitor cell population resulting in 20 subtype clusters with several exhibiting stage-specific bias (Supplementary Fig. 36A-C). To annotate each subtype, we generated multiple module scores using marker genes from publicly available databases and literature. First, we utilized the neural progenitor markers genes from the ScType database[7] and identified 5 enriched subclusters (NeuralProg_1-5). Similarly, we used the neural stem cell marker genes from Wang et al. 2024[8] and identified 6 enriched subclusters (NeuralStem_1-6). Lastly, we generated module scores for mesenchymal progenitors using markers from Wang et al. 2024[8] and epithelial progenitors using markers from the human CellMarker2.0 database[9] to label the final subclusters (Supplementary Fig. 36D,E). Additionally, when we analyzed the marker genes for each of the progenitor subtypes, we again find enrichment of many transcription factors. Transcription factor marker genes were identified showing enrichment of *SNAI1, FOXC1*, and *BARX1* for the Prog_1 subtype; *TFAP2A, ALX3*, and *BARX1* for the MesenchymalLikeProg_1 subtype; *FEZF2, EMX1, EMX2*, and *DMRTA2* for NeuralProg_2; *RAX* for NeuralProg_3; *GLIS1* and *GLIS3* for NeuralStem_5; *PITX1* for MesenchymalProg_2; and *EMX1, FEZF2, DMRT3,* and *NEUROG2* for NeuralProg.5 (Supplementary Fig. 36F, Supplementary Data 17).

Gene ontology analyses revealed enrichment of cell-cell junctions, pattern specification process, and epithelial cell development in the epithelial progenitor subtype, connective tissue development in mesenchymal progenitor populations, axonogenesis, neuron migration and gliogenesis in neural progenitor populations, and the synaptic membrane in neural stem cells (Supplementary Fig. 37, Supplementary Data 18). We also identified enrichment of various carcinomas and eye abnormalities associated with the epithelial progenitor subtype, while craniofacial abnormalities were associated mesenchymal-like progenitor populations (Supplementary Fig. 37F).

Next, we examined markers of the early progenitor population including *SOX2, PAX6, POU3F2,* and *FGFBP3* in the CS13 human spatial transcriptomics, which were all fairly specific to the facial and putative neural tube regions (Supplementary Fig. 38A) When we examined some of the subtype marker genes, we found much more localized expression, with *FEZF2, DMRTA2*, and *DMRT3* mostly restricted to the face (Supplementary Fig. 38B). Module scores for each progenitor subtype were also analyzed, revealing specific localization of progenitor subtypes to the face, neural tube, and pharyngeal arch regions (Supplementary Fig. 38C).

2. Supplementary Figures and Captions


A
RNA_snn_res.0.4
umap_1
umap_2
B
Proportion
RNA_snn_res.0.4
stage
CS12
CS13
CS14
CS16
CS17
CS20
C
Neuronal Module Score
Identity
D
Radial Glia Module Score
Identity

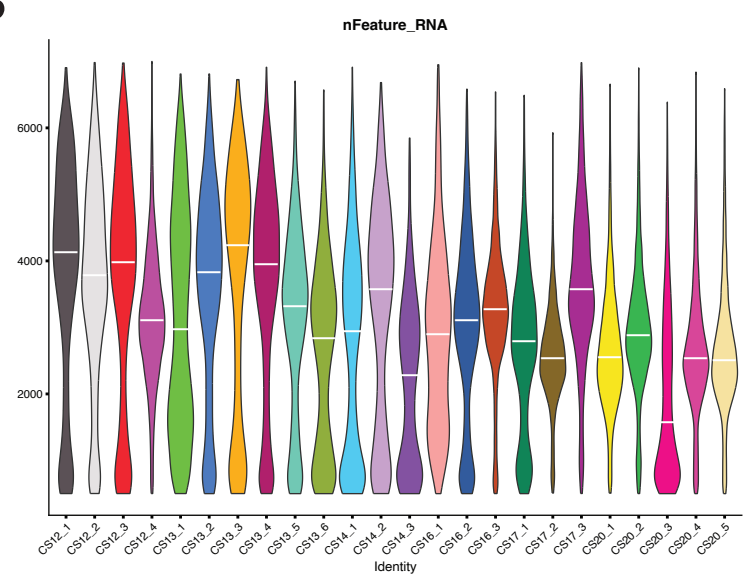
Supplementary Figure 1. Initial human craniofacial cell clustering prior to removal of neuronal and radial glia populations.

A). UMAP projection of all clustered cells with resolution parameter set to 0.4. B). Proportion of cells from each stage across the clusters. C). Violin plot of neuronal module score across the clusters. D). Same as C but for the radial glia module score.

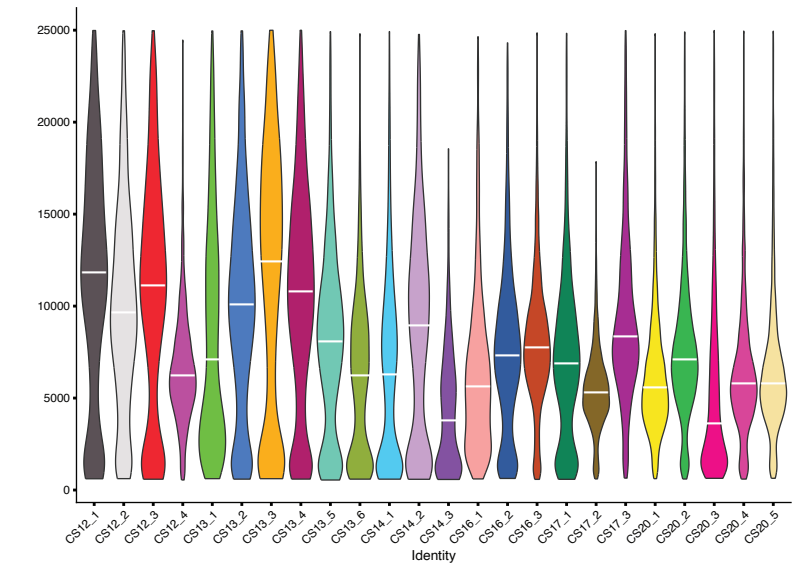
A

	Stage						
Replicate	CS12	CS13	CS14	CS16	CS17	CS20	
CS12_1	2235	0	0	0	0	0	
CS12_2	2997	0	0	0	0	0	
CS12_3	2563	0	0	0	0	0	
CS12_4	5263	0	0	0	0	0	
CS13_1	0	4072	0	0	0	0	
CS13_2	0	4364	0	0	0	0	
CS13_3	0	2198	0	0	0	0	
CS13_4	0	5281	0	0	0	0	
CS13_5	0	3655	0	0	0	0	
CS13_6	0	2710	0	0	0	0	
CS14_1	0	0	3559	0	0	0	
CS14_2	0	0	2838	0	0	0	
CS14_3	0	0	732	0	0	0	
CS16_1	0	0	0	2971	0	0	
CS16_2	0	0	0	2866	0	0	
CS16_3	0	0	0	5569	0	0	
CS17_1	0	0	0	0	2972	0	
CS17_2	0	0	0	0	4413	0	
CS17_3	0	0	0	0	4467	0	
CS20_1	0	0	0	0	0	5745	
CS20_2	0	0	0	0	0	6257	
CS20_3	0	0	0	0	0	4417	
CS20_4	0	0	0	0	0	7449	
CS20_5	0	0	0	0	0	6299	
	13058	22280	7179	11406	11852	30167	95892

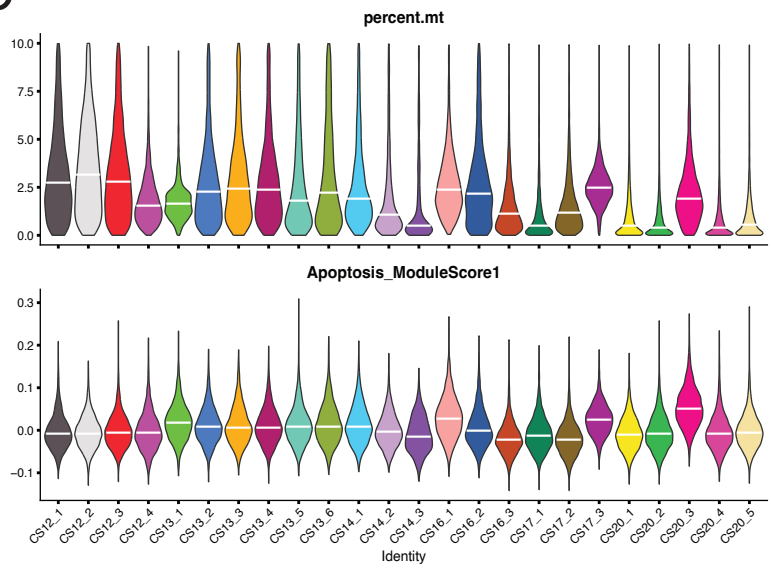
B



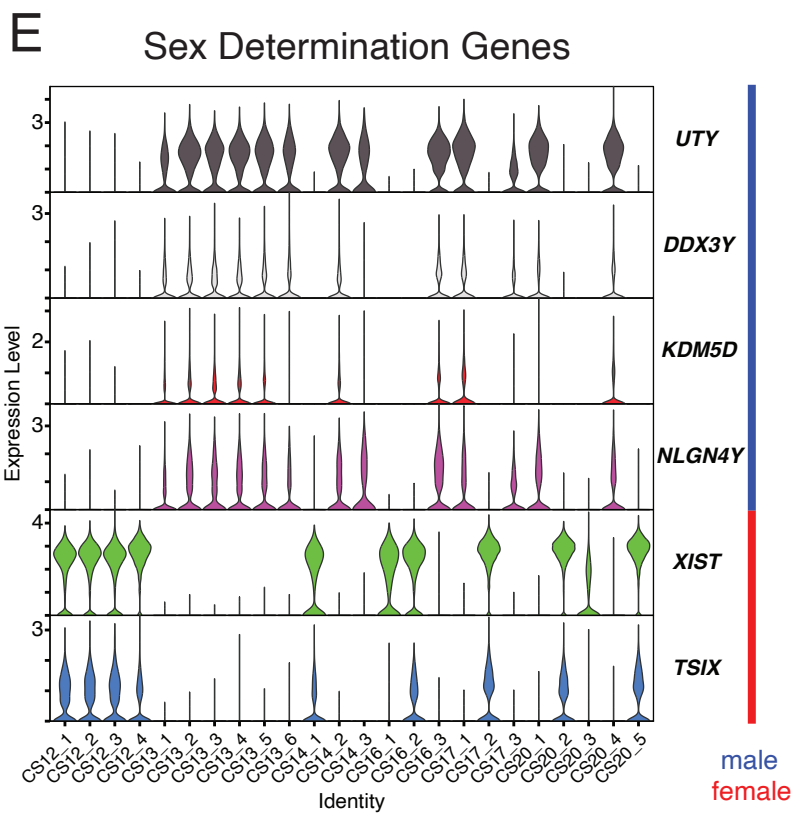
C



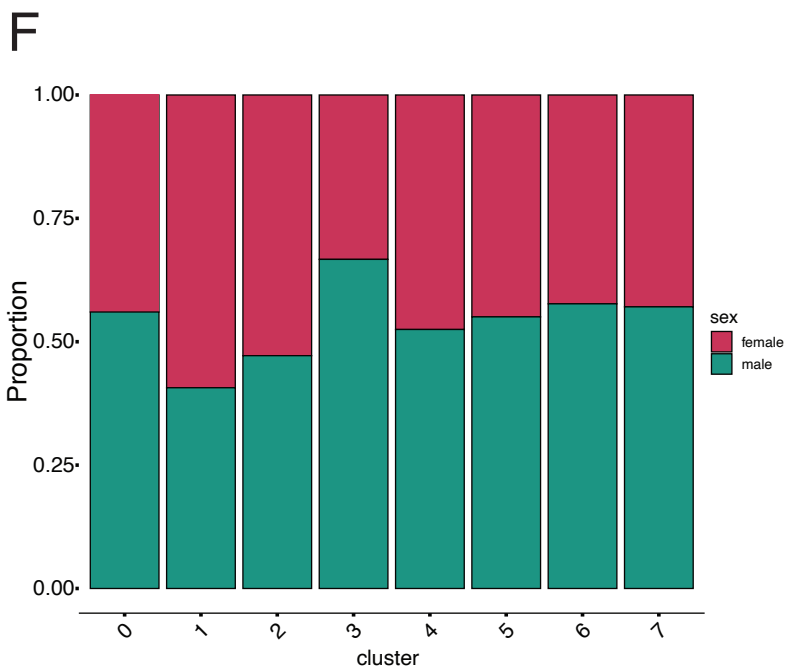
D



E

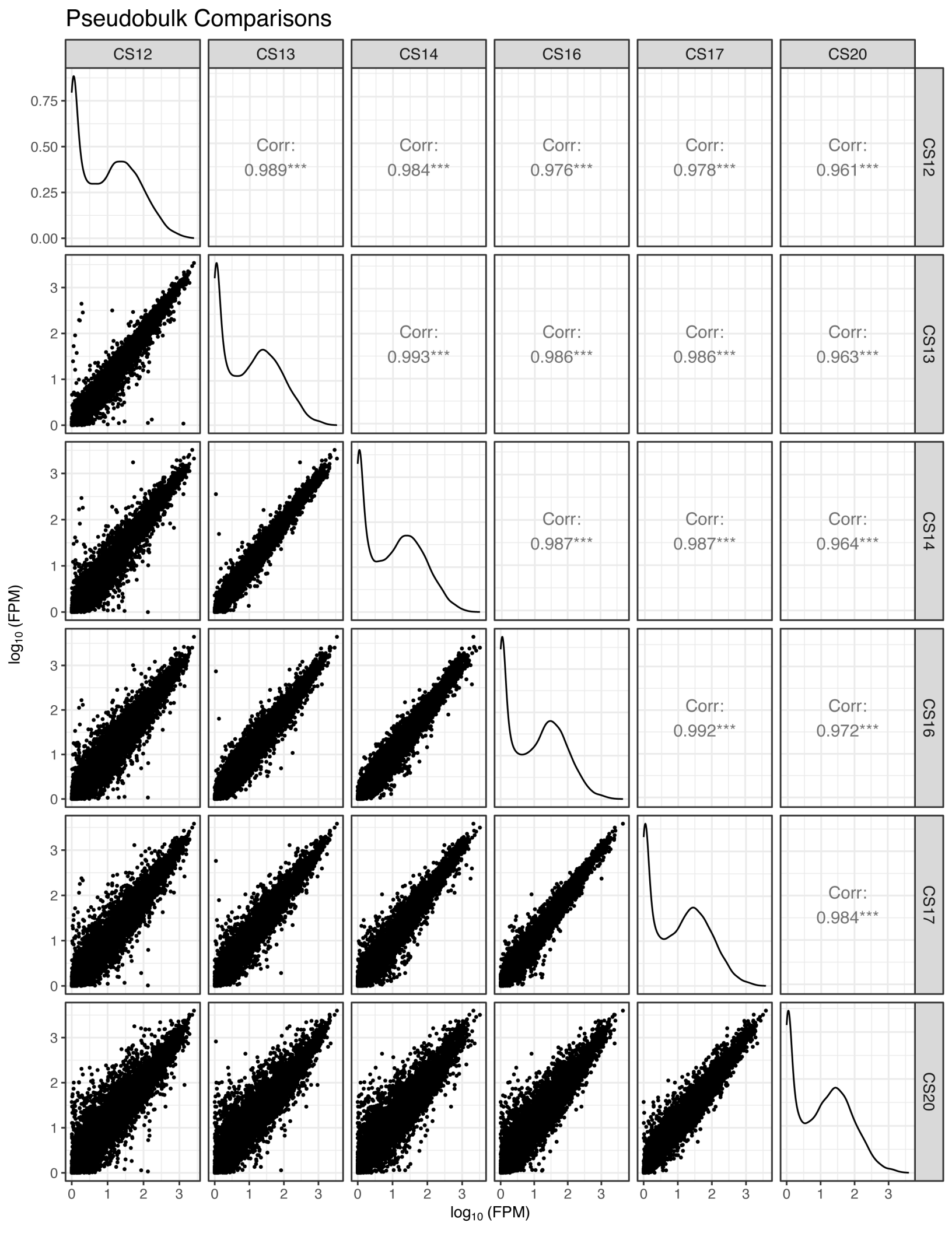


F

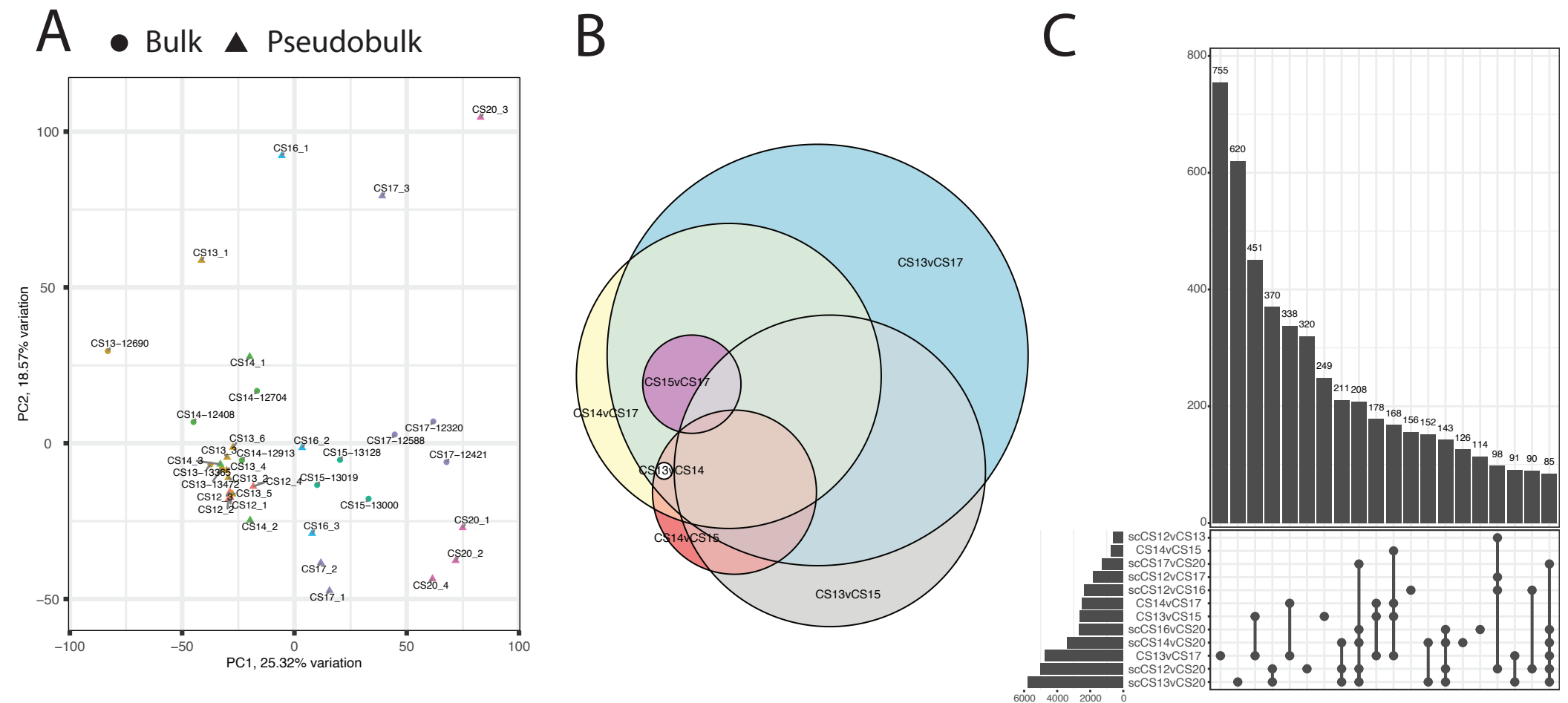


Supplementary Figure 2. QC for cell clusters after filtering out neuronal and radial glia populations.

A). Number of cells split by sample and stage following removal of neuronal and radial glia populations. B). Violin plot for number of features across samples. C). same as B but for number of counts. D). Violin plots for mitochondrial read percentage and apoptosis module scores across samples. E). Stacked bar plot of male (*UTY, DDX3Y, KDM5D, NLGN4Y*) and female (*XIST, TSIX*) genes across samples. F). Proportion of males and females across main cell type clusters from Fig. 1C.

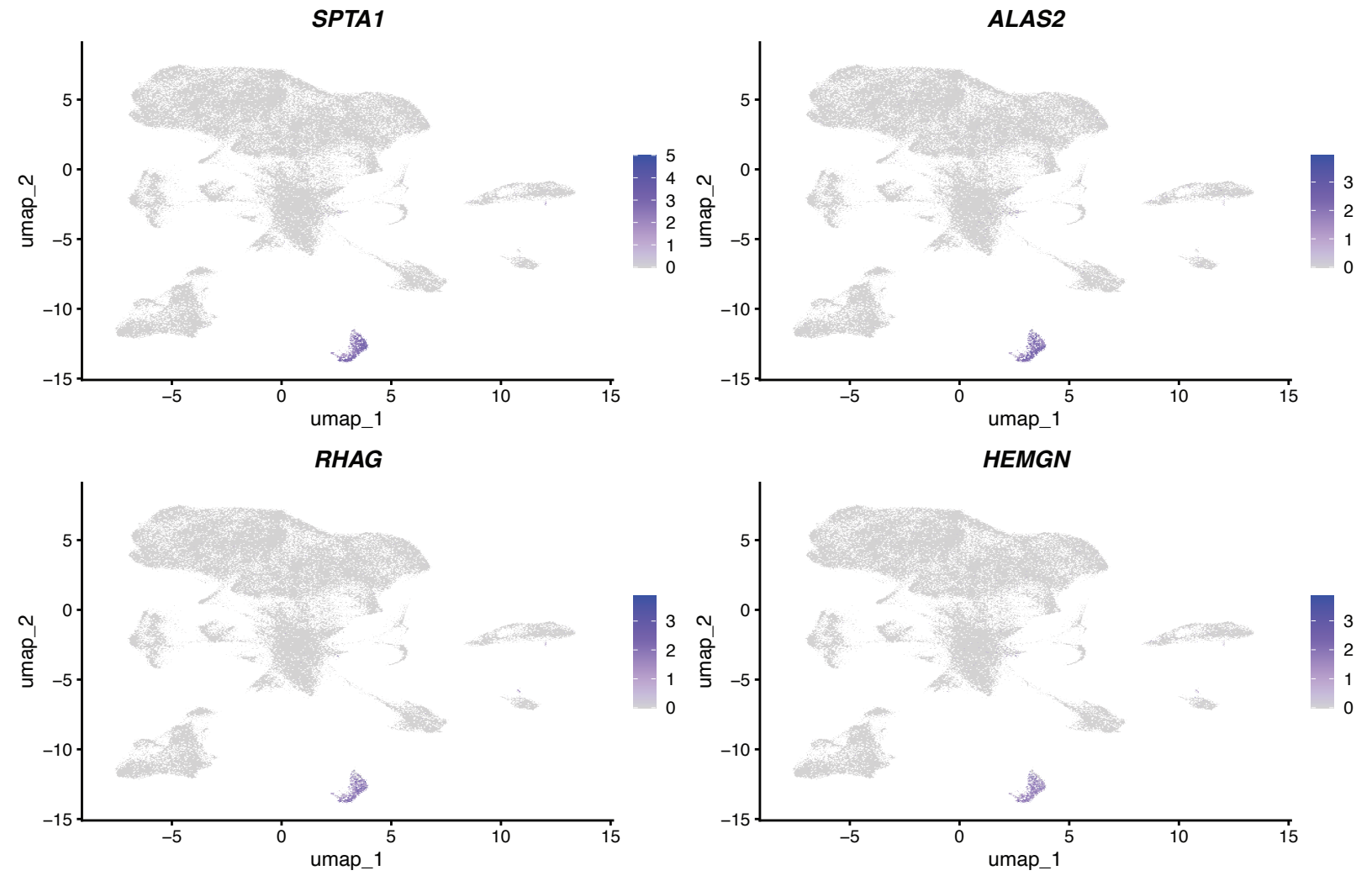

Pseudobulk Comparisons
CS12
CS13
CS14
CS16
CS17
CS20
Corr:
0.989***
Corr:
0.984***
Corr:
0.976***
Corr:
0.978***
Corr:
0.961***
Corr:
0.993***
Corr:
0.986***
Corr:
0.986***
Corr:
0.963***
Corr:
0.987***
Corr:
0.987***
Corr:
0.964***
Corr:
0.992***
Corr:
0.972***
Corr:
0.984***
log10 (FPM)
log10 (FPM)

Supplementary Figure 3. Correlations across single cell data pseudo-bulked by stage. FPM = fragments per million.

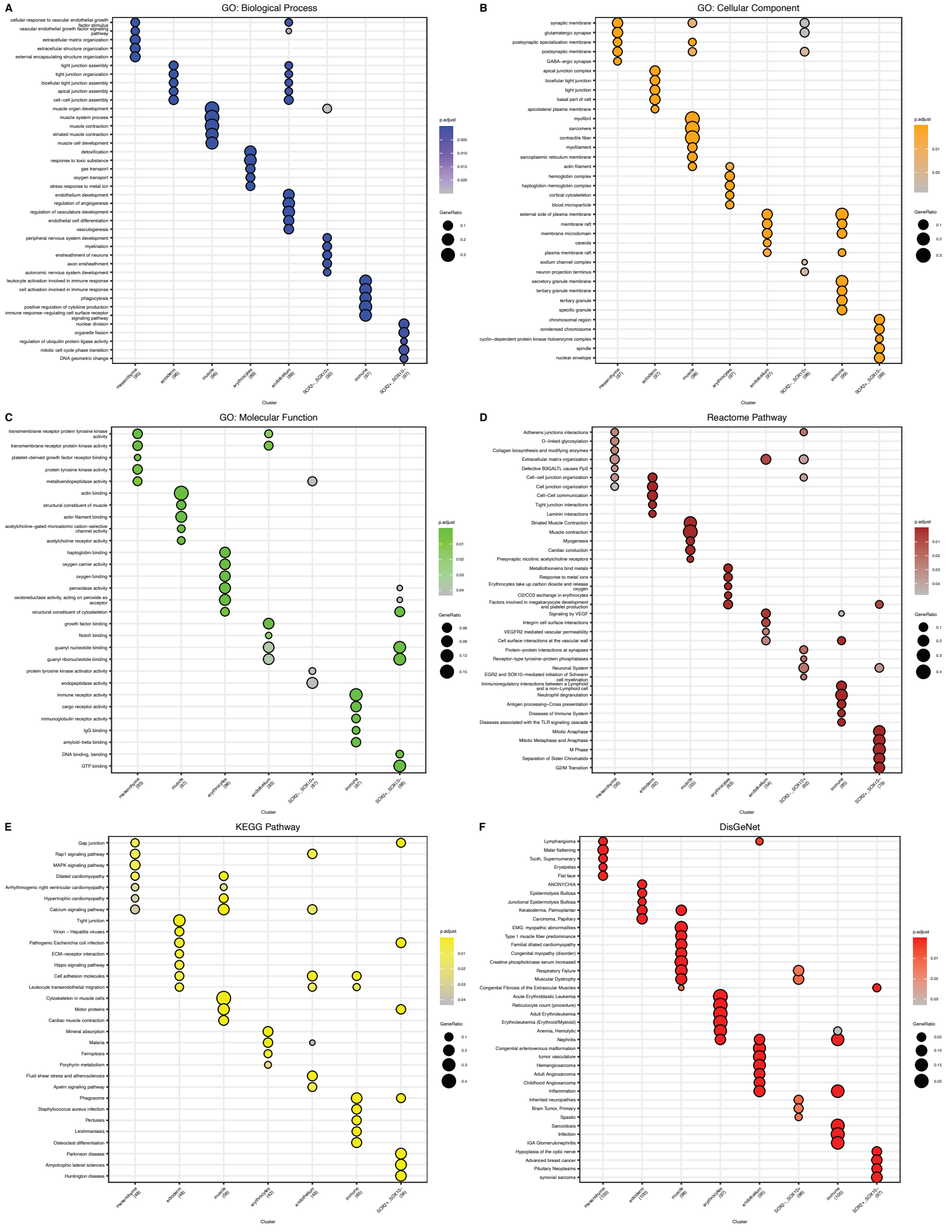

A
Bulk
Pseudobulk
PC2, 18.57% variation
PC1, 25.32% variation
CS20_3
CS16_1
CS17_3
CS13_1
CS13−12690
CS14_1
CS14−12704
CS14−12408
CS17−12320
CS13_6
CS16_2
CS17−12588
CS13_3
CS14−12913
CS15−13128
CS17−12421
CS14_3
CS13_4
CS13−13365
CS13_2
CS12_4
CS15−13019
CS13−13472
CS13_5
CS12_3
CS12_2
CS12_1
CS15−13000
CS20_1
CS14_2
CS16_3
CS20_2
CS17_2
CS20_4
CS17_1
B
CS13vCS17
CS15vCS17
CS14vCS17
CS13vCS14
CS14vCS15
CS13vCS15
C
755
620
451
370
338
320
249
211
208
178
168
156
152
143
126
114
98
91
90
85
scCS12vCS13
CS14vCS15
scCS17vCS20
scCS12vCS17
scCS12vCS16
CS14vCS17
CS13vCS15
scCS16vCS20
scCS14vCS20
CS13vCS17
scCS12vCS20
scCS13vCS20

Supplementary Figure 4. Comparisons between bulk and single cell human craniofacial data.

A). PCA of replicated from our previous bulk[3] and pseudo-bulked single cell data (this manuscript). B). Venn diagram of bulk differentially expressed genes between stages. C). Upset plot for single cell and bulk differentially expressed gene by stage.

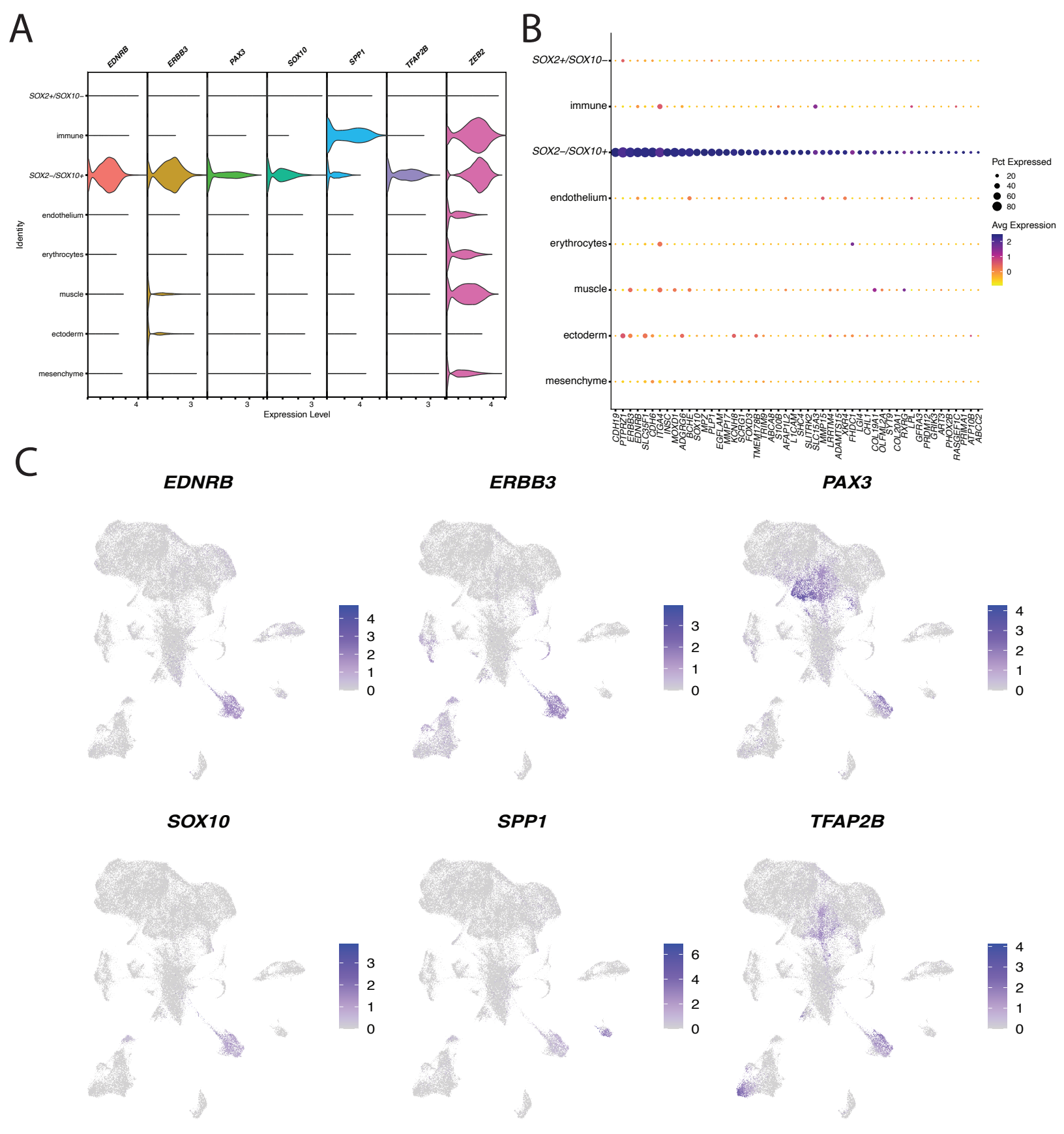

SPTA1
ALAS2
RHAG
HEMGN
umap_1
umap_2
5
4
3
2
1
0
−5
0
5
10
15
−10
−15

Supplementary Figure 5. Feature plots of initial clustering UMAP projection from Fig. 1C for erythrocyte marker genes including *SPTA1, ALAS2, RHAG,* and *HEMGN*.


A
GO: Biological Process
cellular response to vascular endothelial growth factor stimulus
vascular endothelial growth factor signaling pathway
extracellular matrix organization
extracellular structure organization
external encapsulating structure organization
tight junction assembly
tight junction organization
bicellular tight junction assembly
apical junction assembly
cell–cell junction assembly
muscle organ development
muscle system process
muscle contraction
striated muscle contraction
muscle cell development
detoxification
response to toxic substance
gas transport
oxygen transport
stress response to metal ion
endothelium development
regulation of angiogenesis
regulation of vasculature development
endothelial cell differentiation
vasculogenesis
peripheral nervous system development
myelination
ensheathment of neurons
axon ensheathment
autonomic nervous system development
leukocyte activation involved in immune response
cell activation involved in immune response
phagocytosis
positive regulation of cytokine production
immune response–regulating cell surface receptor signaling pathway
nuclear division
organelle fission
regulation of ubiquitin protein ligase activity
mitotic cell cycle phase transition
DNA geometric change
mesenchyme (69)
ectoderm (66)
muscle (68)
erythrocytes (68)
endothelium (68)
SOX2−_SOX10+ (62)
immune (67)
SOX2+_SOX10− (67)
Cluster
p.adjust
0.005
0.010
0.015
0.020
GeneRatio
0.1
0.2
0.3
B
GO: Cellular Component
synaptic membrane
glutamatergic synapse
postsynaptic specialization membrane
postsynaptic membrane
GABA–ergic synapse
apical junction complex
bicellular tight junction
tight junction
basal part of cell
apicolateral plasma membrane
myofibril
sarcomere
contractile fiber
myofilament
sarcoplasmic reticulum membrane
actin filament
hemoglobin complex
haptoglobin–hemoglobin complex
cortical cytoskeleton
blood microparticle
external side of plasma membrane
membrane raft
membrane microdomain
caveola
plasma membrane raft
sodium channel complex
neuron projection terminus
secretory granule membrane
tertiary granule membrane
tertiary granule
specific granule
chromosomal region
condensed chromosome
cyclin–dependent protein kinase holoenzyme complex
spindle
nuclear envelope
mesenchyme (97)
ectoderm (91)
muscle (98)
erythrocytes (97)
endothelium (97)
SOX2−_SOX10+ (96)
immune (98)
SOX2+_SOX10− (89)
Cluster
p.adjust
0.01
0.02
GeneRatio
0.1
0.2
0.3
C
GO: Molecular Function
transmembrane receptor protein tyrosine kinase activity
transmembrane receptor protein kinase activity
platelet–derived growth factor receptor binding
protein tyrosine kinase activity
metalloendopeptidase activity
actin binding
structural constituent of muscle
actin filament binding
acetylcholine–gated monoatomic cation–selective channel activity
acetylcholine receptor activity
haptoglobin binding
oxygen carrier activity
oxygen binding
peroxidase activity
oxidoreductase activity, acting on peroxide as acceptor
structural constituent of cytoskeleton
growth factor binding
Notch binding
guanyl nucleotide binding
guanyl ribonucleotide binding
protein tyrosine kinase activator activity
endopeptidase activity
immune receptor activity
cargo receptor activity
immunoglobulin receptor activity
IgG binding
amyloid–beta binding
DNA binding, bending
GTP binding
mesenchyme (69)
muscle (97)
erythrocytes (96)
endothelium (88)
SOX2−_SOX10+ (87)
immune (97)
SOX2+_SOX10− (96)
Cluster
p.adjust
0.01
0.02
0.03
0.04
GeneRatio
0.06
0.09
0.12
0.15
D
Reactome Pathway
Adherens junctions interactions
O–linked glycosylation
Collagen biosynthesis and modifying enzymes
Extracellular matrix organization
Defective B3GALTL causes PpS
Cell–cell junction organization
Cell junction organization
Cell–Cell communication
Tight junction interactions
Laminin interactions
Striated Muscle Contraction
Muscle contraction
Myogenesis
Cardiac conduction
Presynaptic nicotinic acetylcholine receptors
Metallothioneins bind metals
Response to metal ions
Erythrocytes take up carbon dioxide and release oxygen
O2/CO2 exchange in erythrocytes
Factors involved in megakaryocyte development and platelet production
Signaling by VEGF
Integrin cell surface interactions
VEGFR2 mediated vascular permeability
Cell surface interactions at the vascular wall
Protein–protein interactions at synapses
Receptor–type tyrosine–protein phosphatases
Neuronal System
EGR2 and SOX10–mediated initiation of Schwann cell myelination
Immunoregulatory interactions between a Lymphoid and a non–Lymphoid cell
Neutrophil degranulation
Antigen processing–Cross presentation
Diseases of Immune System
Diseases associated with the TLR signaling cascade
Mitotic Anaphase
Mitotic Metaphase and Anaphase
M Phase
Separation of Sister Chromatids
G2/M Transition
mesenchyme (58)
ectoderm (62)
muscle (55)
erythrocytes (63)
endothelium (54)
SOX2−_SOX10+ (62)
immune (68)
SOX2+_SOX10− (19)
Cluster
p.adjust
0.01
0.02
0.03
0.04
GeneRatio
0.1
0.2
0.3
0.4
E
KEGG Pathway
Gap junction
Rap1 signaling pathway
MAPK signaling pathway
Dilated cardiomyopathy
Arrhythmogenic right ventricular cardiomyopathy
Hypertrophic cardiomyopathy
Calcium signaling pathway
Tight junction
Virion – Hepatitis viruses
Pathogenic Escherichia coli infection
ECM–receptor interaction
Hippo signaling pathway
Cell adhesion molecules
Leukocyte transendothelial migration
Cytoskeleton in muscle cells
Motor proteins
Cardiac muscle contraction
Mineral absorption
Malaria
Ferroptosis
Porphyrin metabolism
Fluid shear stress and atherosclerosis
Apelin signaling pathway
Phagosome
Staphylococcus aureus infection
Pertussis
Leishmaniasis
Osteoclast differentiation
Parkinson disease
Amyotrophic lateral sclerosis
Huntington disease
mesenchyme (48)
ectoderm (48)
muscle (56)
erythrocytes (42)
endothelium (49)
immune (55)
SOX2+_SOX10− (56)
Cluster
p.adjust
0.01
0.02
0.03
0.04
GeneRatio
0.1
0.2
0.3
0.4
F
DisGeNet
Lymphangioma
Malar flattening
Tooth, Supernumerary
Erysipelas
Flat face
ANONYCHIA
Epidermolysis Bullosa
Junctional Epidermolysis Bullosa
Keratoderma, Palmoplantar
Carcinoma, Papillary
EMG: myopathic abnormalities
Type 1 muscle fiber predominance
Familial dilated cardiomyopathy
Congenital myopathy (disorder)
Creatine phosphokinase serum increased
Respiratory Failure
Muscular Dystrophy
Congenital Fibrosis of the Extraocular Muscles
Acute Erythroblastic Leukemia
Reticulocyte count (procedure)
Adult Erythroleukemia
Erythroleukemia (Erythroid/Myeloid)
Anemia, Hemolytic
Nephritis
Congenital arteriovenous malformation
tumor vasculature
Hemangiosarcoma
Adult Angiosarcoma
Childhood Angiosarcoma
Inflammation
Inherited neuropathies
Brain Tumor, Primary
Spastic
Sarcoidosis
Infection
IGA Glomerulonephritis
Hypoplasia of the optic nerve
Advanced breast cancer
Pituitary Neoplasms
synovial sarcoma
mesenchyme (100)
ectoderm (100)
muscle (98)
erythrocytes (97)
endothelium (95)
SOX2−_SOX10+ (96)
immune (100)
SOX2+_SOX10− (97)
Cluster
p.adjust
0.01
0.02
0.03
GeneRatio
0.05
0.10
0.15
0.20

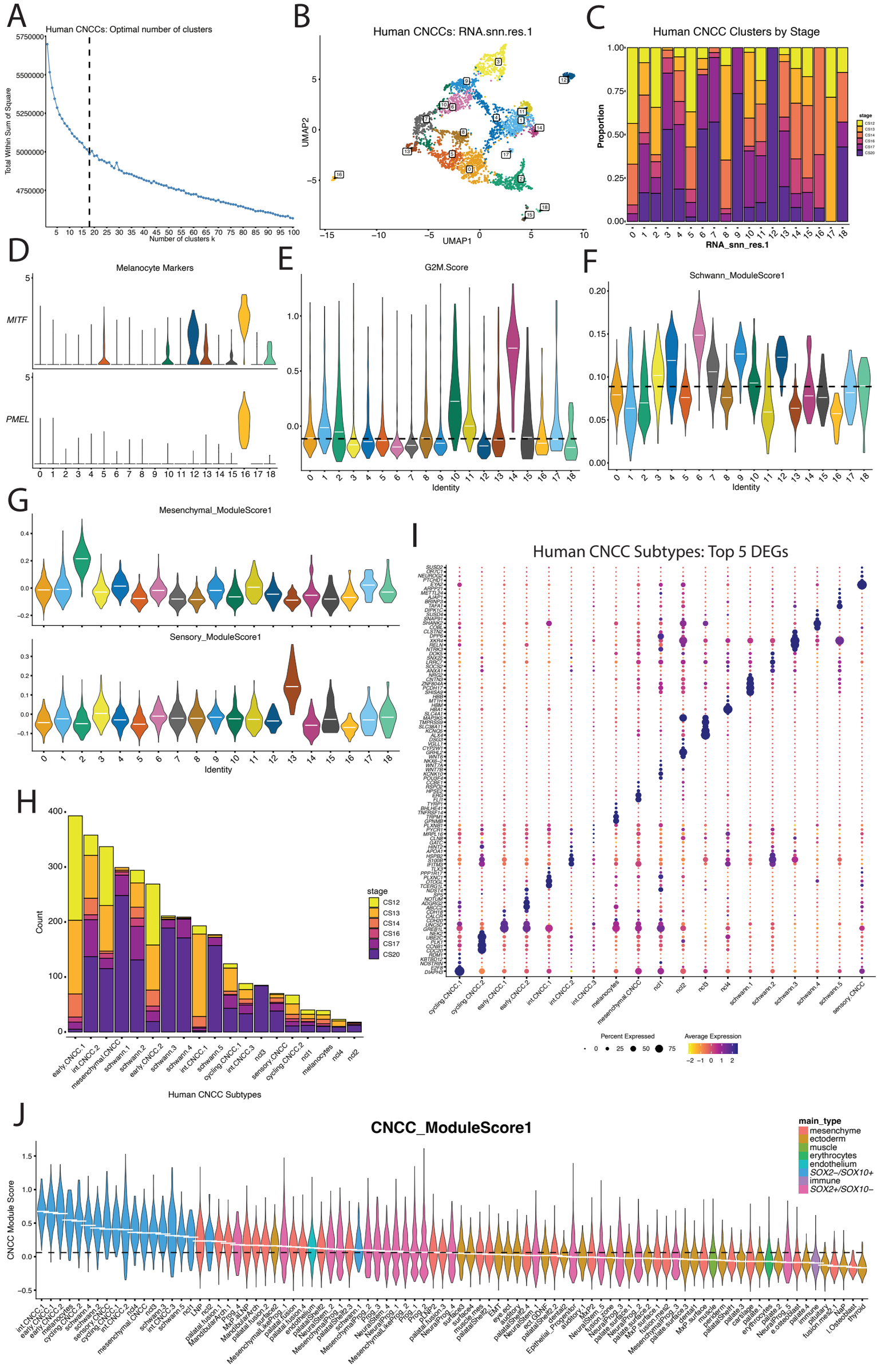
Supplementary Figure 6. Functional annotation enrichment for main cell types using the top 100 marker genes.

A). Gene Ontology for Biological Processes. B). Gene Ontology for Cellular Components. C). Gene Ontology for Molecular Functions. D). Reactome Pathways. E). KEGG pathways. F). DisGeNet.


A
EDNRB
ERBB3
PAX3
SOX10
SPP1
TFAP2B
ZEB2
SOX2+/SOX10−
immune
SOX2−/SOX10+
endothelium
erythrocytes
muscle
ectoderm
mesenchyme
Identity
Expression Level
B
CDH19
PTPRZ1
ERBB3
EDNRB
SLC35F1
CDH6
ITGA4
INSC
MOXD1
ADGRG6
BCHE
SOX10
MPZ
PLP1
EGFLAM
MMP17
KCNH8
SCRG1
LOXL3
TMEM132B
TRIM9
ABCA8
S100B
AFAP1L2
CADM4
SHC4
SLITRK2
SLC15A3
MMP15
LRRC4
ADAMTS15
XKR4
FHDC1
LGI4
HAS1
COL11A1
OLFML2A
SYT9
COL20A1
RXFP1
GFRA3
PRDM12
GRIK3
AR13
PHACTR3
RASGEF1C
PRIMA1
ATP10B
ABCC2
Pct Expressed
20
40
60
80
Avg Expression
2
1
0
C
EDNRB
ERBB3
PAX3
SOX10
SPP1
TFAP2B

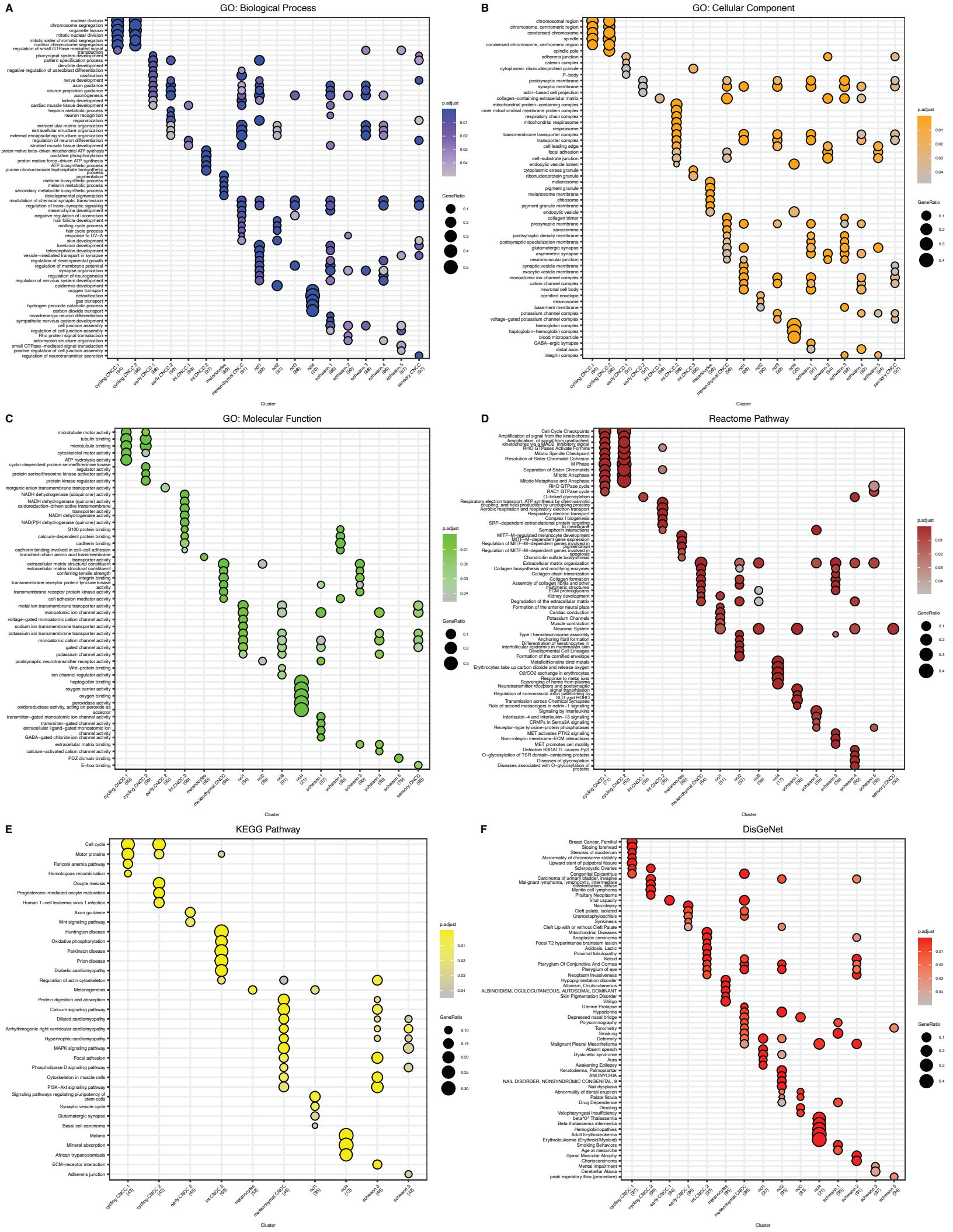
Supplementary Figure 7. General CNCC marker gene expression in main cell types.

A). Stacked violin plot of known CNCC marker genes across main cell types. B). Average and percent expression of CNCC marker genes across main cell types. C). Feature plots of known CNCC genes using UMAP projection from Fig. 1C.


A
Human CNCCs: Optimal number of clusters
Total Within Sum of Square
Number of clusters k
B
Human CNCCs: RNA.snn.res.1
UMAP1
UMAP2
C
Human CNCC Clusters by Stage
Proportion
RNA_snn_res.1
stage
CS12
CS13
CS14
CS16
CS17
CS20
D
Melanocyte Markers
MITF
PMEL
E
G2M.Score
Identity
F
Schwann_ModuleScore1
Identity
G
Mesenchymal_ModuleScore1
Sensory_ModuleScore1
Identity
H
Count
Human CNCC Subtypes
stage
I
Human CNCC Subtypes: Top 5 DEGs
Percent Expressed
Average Expression
J
CNCC_ModuleScore1
CNCC Module Score
main_type
mesenchyme
ectoderm
muscle
erythrocytes
endothelium
SOX2−/SOX10+
immune
SOX2+/SOX10−

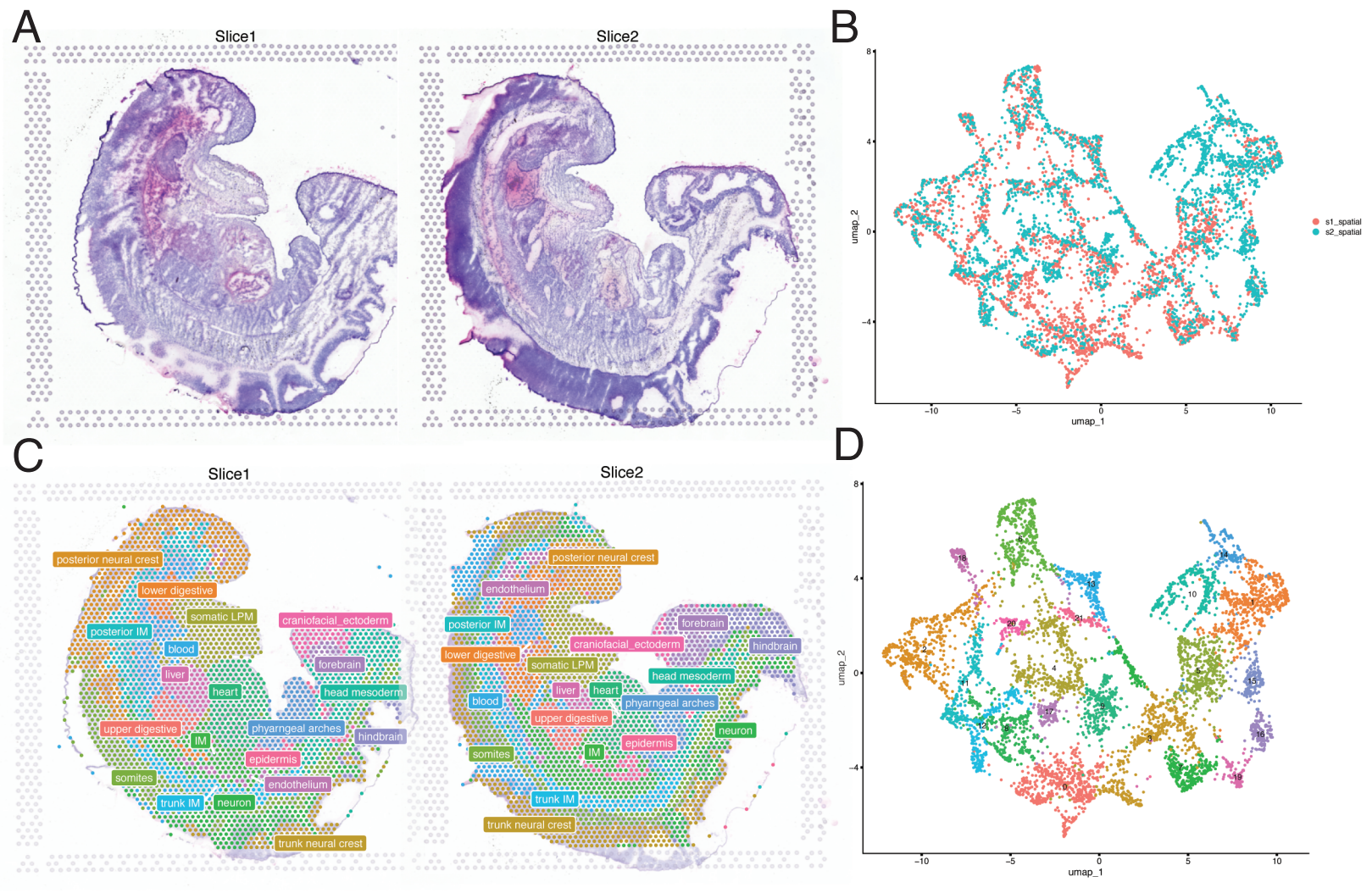
Supplementary Figure 8. Characterizing human *SOX2-/SOX10+* putative CNCC subtypes.

A). Elbow plot with optimal number of subclusters for human putative CNCC's. B). UMAP projection of putative CNCC subclusters with resolution set to 1. C). Proportion of putative CNNCs from each stage across the clusters D). Stacked violin plot of melanocyte gene markers *MITF* and *PMEL* across the putative CNCC subclusters. D). Same as C but for the radial glia module score. E). Violin plot of G2M cell cycle module score across the putative CNCC subclusters. F) Same as E but for Schwann cell module scores. G) Stacked violin plot of mesenchymal and sensory CNCC module scores across the putative CNCC subclusters. H) Distribution of putative CNNCs from each stage across the defined subtypes. I). Average and percent expression of top 5 DEGs for each of the defined putative CNCC subtypes. J). Violin plot for all cells across subtypes based on CNCC module score of curated neural crest genes calculated by Seurat.


A
GO: Biological Process
nuclear division
chromosome segregation
organelle fission
mitotic nuclear division
mitotic sister chromatid segregation
nuclear chromosome segregation
regulation of small GTPase mediated signal transduction
pharyngeal system development
pattern specification process
dendrite development
negative regulation of osteoblast differentiation
ossification
nerve development
axon guidance
neuron projection guidance
axonogenesis
kidney development
cardiac muscle tissue development
heparin metabolic process
neuron recognition
regionalization
extracellular matrix organization
extracellular structure organization
external encapsulating structure organization
regulation of neuron differentiation
striated muscle tissue development
proton motive force−driven mitochondrial ATP synthesis
oxidative phosphorylation
proton motive force−driven ATP synthesis
ATP biosynthetic process
purine ribonucleoside triphosphate biosynthetic process
pigmentation
melanin biosynthetic process
melanin metabolic process
secondary metabolite biosynthetic process
developmental pigmentation
modulation of chemical synaptic transmission
regulation of trans−synaptic signaling
mesenchyme development
negative regulation of locomotion
hair follicle development
molting cycle process
hair cycle process
response to UV−A
skin development
forebrain development
telencephalon development
vesicle−mediated transport in synapse
regulation of developmental growth
regulation of membrane potential
synapse organization
regulation of neurogenesis
regulation of nervous system development
epidermis development
oxygen transport
detoxification
gas transport
hydrogen peroxide catabolic process
carbon dioxide transport
noradrenergic neuron differentiation
sympathetic nervous system development
cell junction assembly
regulation of cell junction assembly
Rho protein signal transduction
actomyosin structure organization
small GTPase−mediated signal transduction
positive regulation of cell junction assembly
regulation of neurotransmitter secretion
p.adjust
0.01
0.02
0.03
0.04
GeneRatio
0.1
0.2
0.3
0.4
0.5
cycling CNCC_1 (94)
cycling CNCC_2 (90)
early CNCC_1 (66)
early CNCC_2 (63)
int.CNCC_1 (55)
int.CNCC_2 (97)
melanocytes (89)
mesenchymal CNCC (91)
nc1 (92)
nc2 (91)
nc3 (88)
nc4 (20)
schwann_1 (86)
schwann_2 (30)
schwann_3 (88)
schwann_4 (86)
schwann_5 (87)
sensory CNCC (97)
Cluster
B
GO: Cellular Component
chromosomal region
chromosome, centromeric region
condensed chromosome
spindle
condensed chromosome, centromeric region
spindle pole
adherens junction
catenin complex
cytoplasmic ribonucleoprotein granule
P−body
postsynaptic membrane
synaptic membrane
actin−based cell projection
collagen−containing extracellular matrix
mitochondrial protein−containing complex
inner mitochondrial membrane protein complex
respiratory chain complex
mitochondrial respirasome
respirasome
transmembrane transporter complex
transporter complex
cell leading edge
focal adhesion
cell−substrate junction
endocytic vesicle lumen
cytoplasmic stress granule
ribonucleoprotein granule
melanosome
pigment granule
melanosome membrane
chitosome
pigment granule membrane
endocytic vesicle
collagen trimer
presynaptic membrane
sarcolemma
postsynaptic density membrane
postsynaptic specialization membrane
glutamatergic synapse
asymmetric synapse
neuromuscular junction
synaptic vesicle membrane
exocytic vesicle membrane
monoatomic ion channel complex
cation channel complex
neuronal cell body
cornified envelope
desmosome
basement membrane
potassium channel complex
voltage−gated potassium channel complex
hemoglobin complex
haptoglobin−hemoglobin complex
blood microparticle
GABA−ergic synapse
distal axon
integrin complex
p.adjust
0.01
0.02
0.03
0.04
GeneRatio
0.1
0.2
0.3
0.4
cycling CNCC_1 (94)
cycling CNCC_2 (90)
early CNCC_1 (66)
early CNCC_2 (63)
int.CNCC_1 (55)
int.CNCC_2 (97)
int.CNCC_3 (66)
melanocytes (89)
mesenchymal CNCC (91)
nc1 (89)
nc2 (90)
nc3 (92)
nc4 (20)
schwann_1 (91)
schwann_2 (94)
schwann_3 (92)
schwann_4 (92)
schwann_5 (94)
sensory CNCC (97)
Cluster
C
GO: Molecular Function
microtubule motor activity
tubulin binding
microtubule binding
cytoskeletal motor activity
ATP hydrolysis activity
cyclin−dependent protein serine/threonine kinase regulator activity
protein serine/threonine kinase activator activity
protein kinase regulator activity
inorganic anion transmembrane transporter activity
NADH dehydrogenase (ubiquinone) activity
NADH dehydrogenase (quinone) activity
oxidoreduction−driven active transmembrane transporter activity
NADH dehydrogenase activity
NAD(P)H dehydrogenase (quinone) activity
S100 protein binding
calcium−dependent protein binding
cadherin binding
cadherin binding involved in cell−cell adhesion
branched−chain amino acid transmembrane transporter activity
extracellular matrix structural constituent
extracellular matrix structural constituent conferring tensile strength
integrin binding
transmembrane receptor protein tyrosine kinase activity
transmembrane receptor protein kinase activity
cell adhesion mediator activity
metal ion transmembrane transporter activity
monoatomic ion channel activity
voltage−gated monoatomic cation channel activity
sodium ion transmembrane transporter activity
potassium ion transmembrane transporter activity
monoatomic cation channel activity
gated channel activity
potassium channel activity
postsynaptic neurotransmitter receptor activity
Wnt−protein binding
ion channel regulator activity
haptoglobin binding
oxygen carrier activity
oxygen binding
peroxidase activity
oxidoreductase activity, acting on peroxide as acceptor
transmitter−gated monoatomic ion channel activity
transmitter−gated channel activity
extracellular ligand−gated monoatomic ion channel activity
GABA−gated chloride ion channel activity
extracellular matrix binding
calcium−activated cation channel activity
PDZ domain binding
E−box binding
p.adjust
0.01
0.02
0.03
0.04
GeneRatio
0.1
0.2
0.3
cycling CNCC_1 (92)
cycling CNCC_2 (96)
early CNCC_1 (66)
early CNCC_2 (65)
int.CNCC_1 (68)
int.CNCC_2 (97)
melanocytes (90)
mesenchymal CNCC (94)
nc1 (84)
nc2 (89)
nc3 (91)
nc4 (21)
schwann_1 (87)
schwann_2 (88)
schwann_3 (90)
schwann_4 (85)
schwann_5 (79)
sensory CNCC (95)
Cluster
D
Reactome Pathway
Cell Cycle Checkpoints
Amplification of signal from the kinetochores
Amplification of signal from unattached kinetochores via a MAD2 inhibitory signal
RHO GTPases Activate Formins
Mitotic Spindle Checkpoint
Resolution of Sister Chromatid Cohesion
M Phase
Separation of Sister Chromatids
Mitotic Anaphase
Mitotic Metaphase and Anaphase
RHO GTPase cycle
RAC1 GTPase cycle
O−linked glycosylation
Respiratory electron transport, ATP synthesis by chemiosmotic coupling, and heat production by uncoupling proteins
Aerobic respiration and respiratory electron transport
Respiration electron transport
Complex I biogenesis
SRP−dependent cotranslational protein targeting to membrane
Semaphorin interactions
MITF−M−regulated melanocyte development
MITF−M−dependent gene expression
Regulation of MITF−M−dependent genes involved in pigmentation
Regulation of MITF−M−dependent genes involved in apoptosis
Chondroitin sulfate biosynthesis
Extracellular matrix organization
Collagen biosynthesis and modifying enzymes
Collagen chain trimerization
Collagen formation
Assembly of collagen fibrils and other multimeric structures
ECM proteoglycans
Kidney development
Degradation of the extracellular matrix
Formation of the anterior neural plate
Cardiac conduction
Potassium Channels
Muscle contraction
Neuronal System
Type I hemidesmosome assembly
Anchoring fibril formation
Differentiation of keratinocytes in interfollicular epidermis in mammalian skin
Developmental Cell Lineages
Formation of the cornified envelope
Metallothioneins bind metals
Erythrocytes take up carbon dioxide and release oxygen
O2/CO2 exchange in erythrocytes
Response to metal ions
Scavenging of heme from plasma
Neurotransmitter receptors and postsynaptic signal transmission
Regulation of commissural axon pathfinding by SLIT and ROBO
Transmission across Chemical Synapses
Role of second messengers in netrin−1 signaling
Signaling by Interleukins
Interleukin−4 and Interleukin−13 signaling
CRMPs in Sema3A signaling
Receptor−type tyrosine−protein phosphatases
MET activates PTK2 signaling
Non−integrin membrane−ECM interactions
MET promotes cell motility
Defective B3GALTL causes PpS
O−glycosylation of TSR domain−containing proteins
Diseases of glycosylation
Diseases associated with O−glycosylation of proteins
p.adjust
0.01
0.02
0.03
0.04
GeneRatio
0.1
0.2
0.3
0.4
cycling CNCC_1 (71)
cycling CNCC_2 (63)
int.CNCC_1 (59)
int.CNCC_2 (85)
melanocytes (62)
mesenchymal CNCC (64)
nc1 (51)
nc2 (57)
nc3 (59)
nc4 (17)
schwann_1 (58)
schwann_2 (59)
schwann_3 (59)
schwann_4 (60)
schwann_5 (58)
sensory CNCC (50)
Cluster
E
KEGG Pathway
Cell cycle
Motor proteins
Fanconi anemia pathway
Homologous recombination
Oocyte meiosis
Progesterone−mediated oocyte maturation
Human T−cell leukemia virus 1 infection
Axon guidance
Wnt signaling pathway
Huntington disease
Oxidative phosphorylation
Parkinson disease
Prion disease
Diabetic cardiomyopathy
Regulation of actin cytoskeleton
Melanogenesis
Protein digestion and absorption
Calcium signaling pathway
Dilated cardiomyopathy
Arrhythmogenic right ventricular cardiomyopathy
Hypertrophic cardiomyopathy
MAPK signaling pathway
Focal adhesion
Phospholipase D signaling pathway
Cytoskeleton in muscle cells
PI3K−Akt signaling pathway
Signaling pathways regulating pluripotency of stem cells
Synaptic vesicle cycle
Glutamatergic synapse
Basal cell carcinoma
Malaria
Mineral absorption
African trypanosomiasis
ECM−receptor interaction
Adherens junction
p.adjust
0.01
0.02
0.03
0.04
GeneRatio
0.10
0.15
0.20
0.25
0.30
cycling CNCC_1 (48)
cycling CNCC_2 (47)
early CNCC_2 (45)
int.CNCC_2 (68)
melanocytes (62)
mesenchymal CNCC (46)
nc1 (35)
nc4 (12)
schwann_3 (46)
schwann_5 (42)
Cluster
F
DisGeNet
Breast Cancer, Familial
Sloping forehead
Stenosis of duodenum
Abnormality of chromosome stability
Upward slant of palpebral fissure
Sclerocystic Ovaries
Congenital Epicanthus
Carcinoma of urinary bladder, invasive
Malignant lymphoma, lymphocytic, intermediate differentiation, diffuse
Mantle cell lymphoma
Pituitary Neoplasms
Vital capacity
Narcolepsy
Cleft palate, isolated
Uranostaphyloschisis
Synkinesis
Cleft Lip with or without Cleft Palate
Mitochondrial Diseases
Anaplastic carcinoma
Focal T2 hyperintense brainstem lesion
Acidosis, Lactic
Proximal tubulopathy
Keloid
Pterygium Of Conjunctiva And Cornea
Pterygium of eye
Neoplasm Invasiveness
Hypopigmentation disorder
Albinism, Oculocutaneous
ALBINOIDISM, OCULOCUTANEOUS, AUTOSOMAL DOMINANT
Skin Pigmentation Disorder
Vitiligo
Uterine Prolapse
Hypodontia
Depressed nasal bridge
Polysomnography
Tonometry
Smoking
Deformity
Malignant Pleural Mesothelioma
Absent speech
Dyskinetic syndrome
Aura
Awakening Epilepsy
Keratoderma, Palmoplantar
ANONYCHIA
NAIL DISORDER, NONSYNDROMIC CONGENITAL, 9
Nail dysplasia
Abnormality of dental eruption
Palate fistula
Drug Dependence
Drooling
Velopharyngeal Insufficiency
beta^0^ Thalassemia
Beta thalassemia intermedia
Hemoglobinopathies
Adult Erythroleukemia
Erythroleukemia (Erythroid/Myeloid)
Smoking Behaviors
Age at menarche
Spinal Muscular Atrophy
Choriocarcinoma
Mental impairment
Cerebellar Ataxia
peak expiratory flow (procedure)
p.adjust
0.01
0.02
0.03
0.04
GeneRatio
0.1
0.2
0.3
0.4
cycling CNCC_1 (97)
cycling CNCC_2 (96)
early CNCC_1 (64)
early CNCC_2 (96)
int.CNCC_2 (65)
melanocytes (95)
mesenchymal CNCC (98)
nc1 (97)
nc2 (89)
nc3 (93)
nc4 (21)
schwann_1 (65)
schwann_2 (91)
schwann_3 (97)
schwann_5 (94)
Cluster

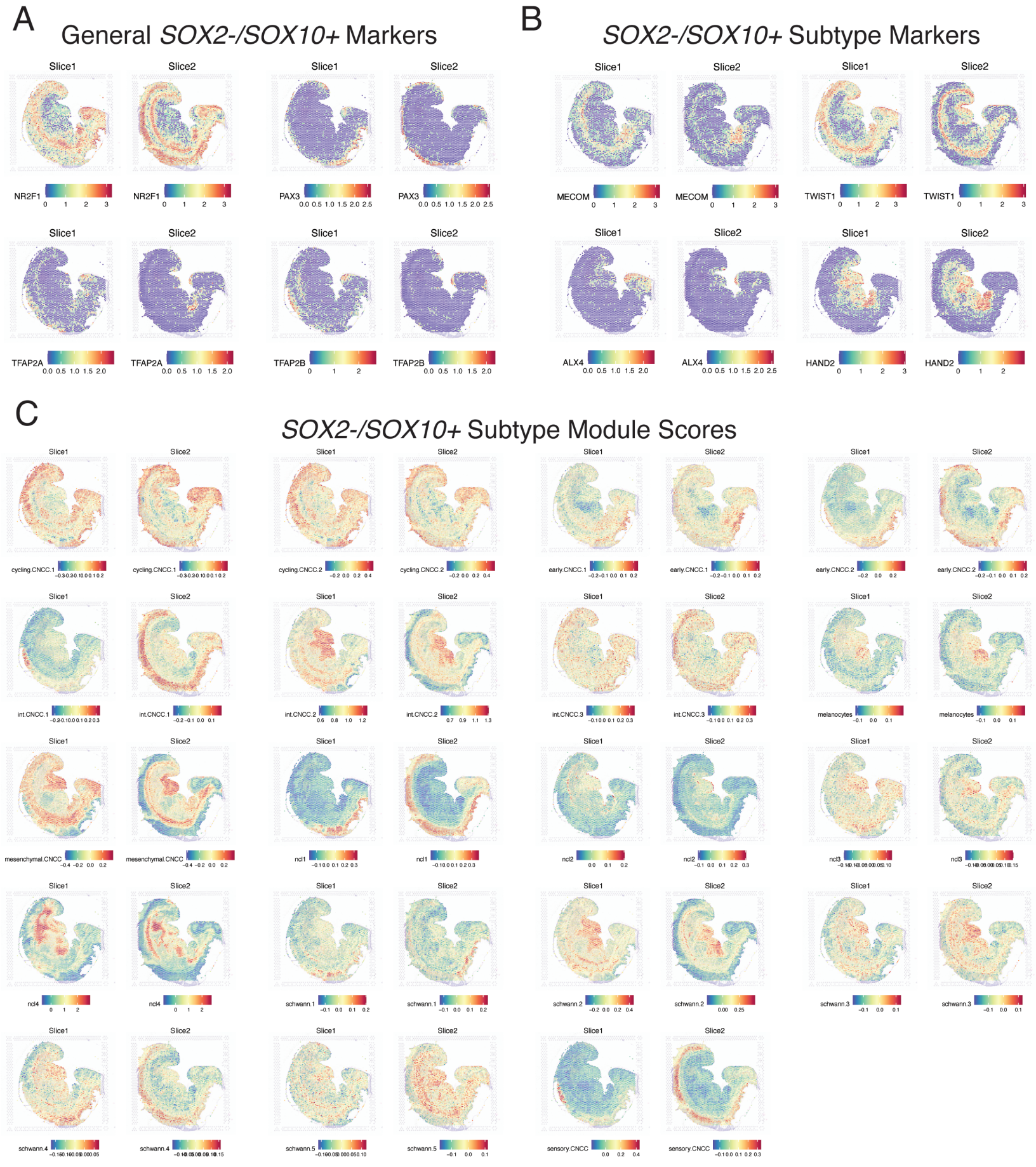
Supplementary Figure 9. Functional annotation enrichment for human putative CNCC subtypes using the top 100 marker genes.

A). Gene Ontology for Biological Processes. B). Gene Ontology for Cellular Components. C). Gene Ontology for Molecular Functions. D). Reactome Pathways. E). KEGG pathways. F). DisGeNet.


A
Slice1
Slice2
B
umap_2
umap_1
s1_spatial
s2_spatial
C
Slice1
Slice2
posterior neural crest
lower digestive
somatic LPM
posterior IM
craniofacial_ectoderm
blood
forebrain
liver
heart
head mesoderm
upper digestive
pharyngeal arches
IM
hindbrain
epidermis
somites
endothelium
trunk IM
neuron
trunk neural crest
endothelium
forebrain
hindbrain
neuron
epidermis
pharyngeal arches
D
umap_2
umap_1

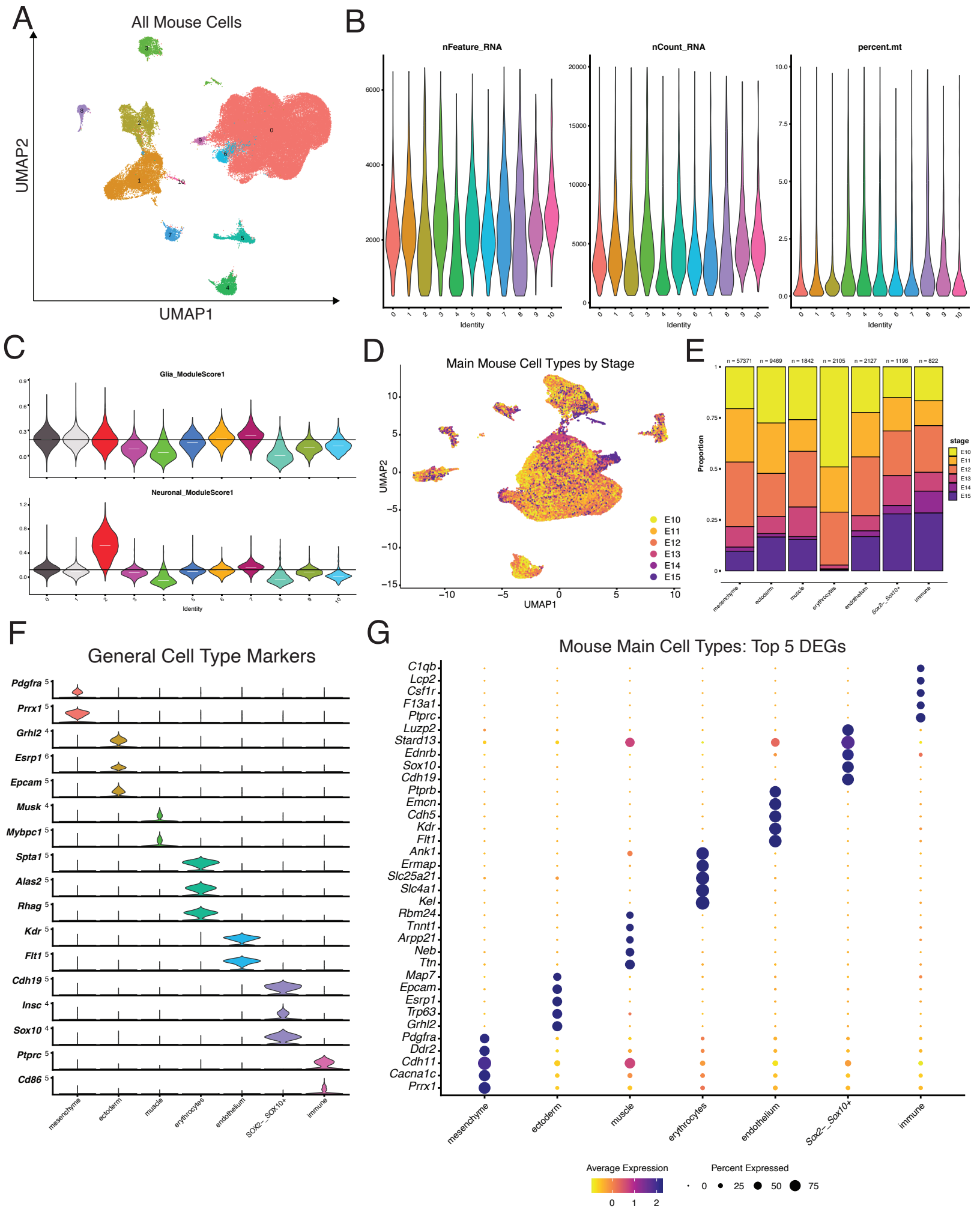
Supplementary Figure 10. Processing and re-analysis of spatial transcriptomics data from two sections of a human CS13 embryo[10].

A) Hematoxylin & Eosin-stained images of both sections of the CS13 embryo used for generating spatial transcriptomics data. B). UMAP projection of spatial transcriptomic spots integrated from both sections of the CS13 embryo. C). Spatial plot for both sections of the data with spots annotated based on cluster in D).


A
General SOX2-/SOX10+ Markers
Slice1
Slice2
NR2F1
PAX3
B
SOX2-/SOX10+ Subtype Markers
MECOM
TWIST1
TFAP2A
TFAP2B
ALX4
HAND2
C
SOX2-/SOX10+ Subtype Module Scores
cycling.CNCC.1
cycling.CNCC.2
early.CNCC.1
early.CNCC.2
int.CNCC.1
int.CNCC.2
int.CNCC.3
melanocytes
mesenchymal.CNCC
ncl1
ncl2
ncl3
ncl4
schwann.1
schwann.2
schwann.3
schwann.4
schwann.5
sensory.CNCC

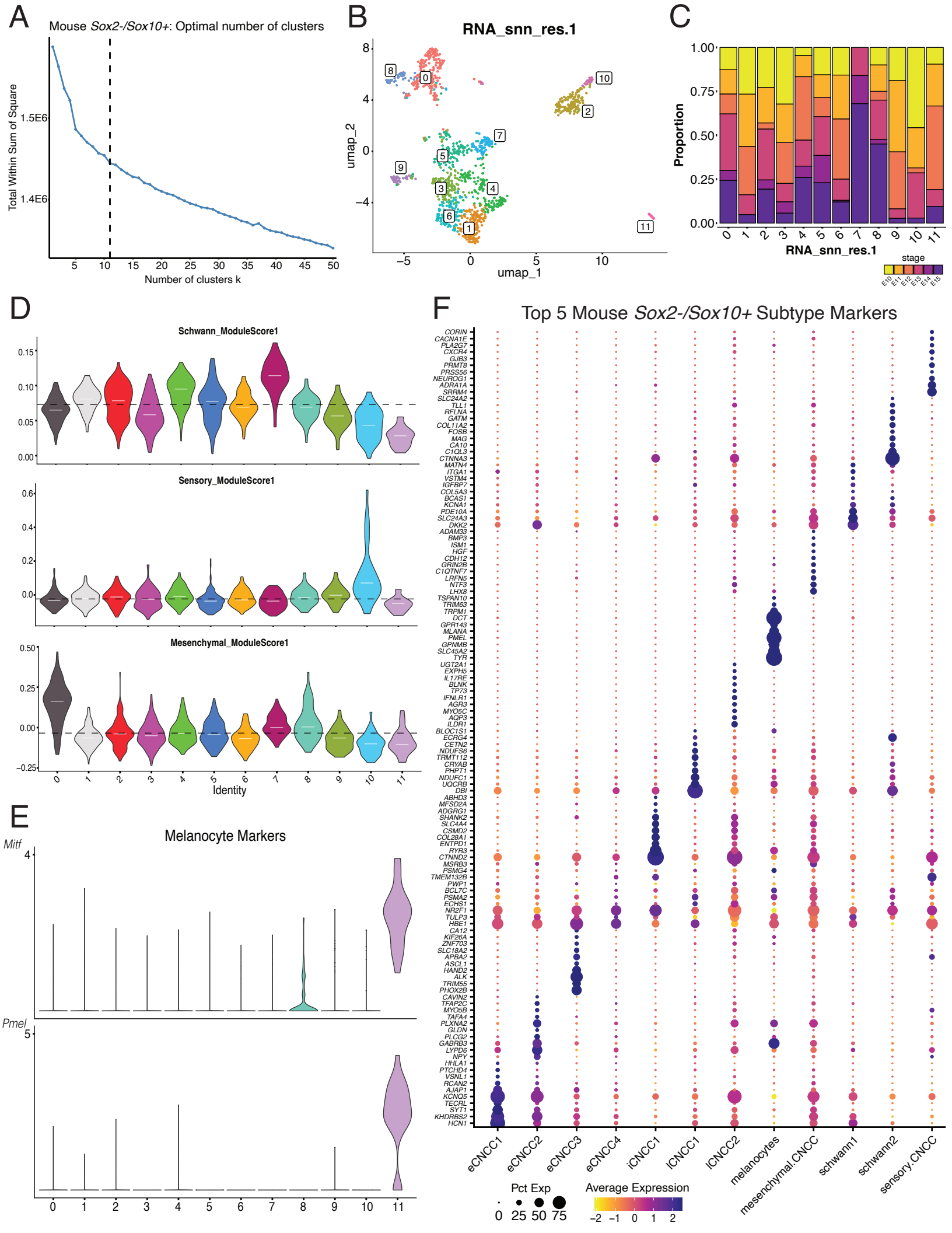
Supplementary Figure 11. Spatial feature plots of human *SOX2-/SOX10+* putative CNCC genes and module scores from two sections of a human CS13 embryo[10].

A). General *SOX2-/SOX10+* putative CNCC gene markers. B). *SOX2-/SOX10+* putative CNCC subtype markers. C). *SOX2-/SOX10+* putative CNCC subtype module scores.


A
All Mouse Cells
UMAP2
UMAP1
B
nFeature_RNA
nCount_RNA
percent.mt
Identity
C
Glia_ModuleScore1
Neuronal_ModuleScore1
Identity
D
Main Mouse Cell Types by Stage
UMAP2
UMAP1
E10
E11
E12
E13
E14
E15
E
n = 57371
n = 9469
n = 1842
n = 2105
n = 2127
n = 1196
n = 822
Proportion
stage
mesenchyme
ectoderm
muscle
erythrocytes
endothelium
Sox2-_Sox10+
immune
F
General Cell Type Markers
Pdgfra
Prrx1
Grhl2
Esrp1
Epcam
Musk
Mybpc1
Spta1
Alas2
Rhag
Kdr
Flt1
Cdh19
Insc
Sox10
Ptprc
Cd86
mesenchyme
ectoderm
muscle
erythrocytes
endothelium
SOX2-_SOX10+
immune
G
Mouse Main Cell Types: Top 5 DEGs
C1qb
Lcp2
Csf1r
F13a1
Ptprc
Luzp2
Stard13
Ednrb
Sox10
Cdh19
Ptprb
Emcn
Cdh5
Kdr
Flt1
Ank1
Ermap
Slc25a21
Slc4a1
Kel
Rbm24
Tnnt1
Arpp21
Neb
Ttn
Map7
Epcam
Esrp1
Trp63
Grhl2
Pdgfra
Ddr2
Cdh11
Cacna1c
Prrx1
mesenchyme
ectoderm
muscle
erythrocytes
endothelium
Sox2-_Sox10+
immune
Average Expression
Percent Expressed
0
25
50
75

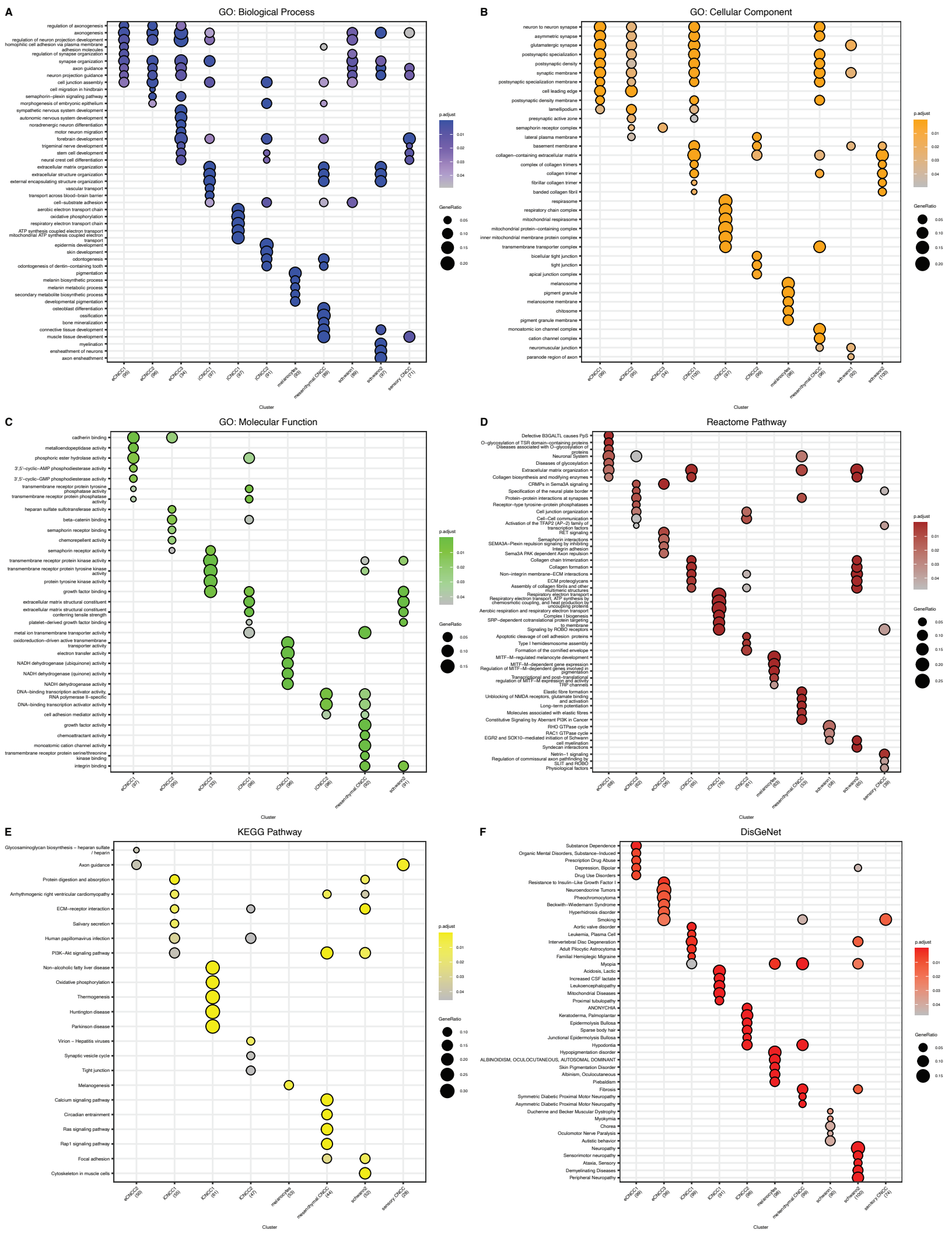
Supplementary Figure 12. Clustering and annotating mouse main cell types.

A). UMAP projection of all mouse cells clustered prior to neuronal and radial glia filtering. B). Violin plots of QC metrics including nFeature_RNA, nCount_RNA, and percent.mt. C). Violin plots of radial glia and neuronal module scores for each cluster. D). Distribution of cells following the removal of the neuronal cell population from each stage across the UMAP projection in Fig. 4A. E). Distribution of cells obtained at each stage for each cluster identified in Fig. 4A. F). Stacked violin plot of general cell type markers. G). Average and percent expression for the top 5 DEGs identified in each mouse main cell type.


A
Mouse Sox2-/Sox10+: Optimal number of clusters
Total Within Sum of Square
1.5E6
1.4E6
5 10 15 20 25 30 35 40 45 50
Number of clusters k
B
RNA_snn_res.1
umap_2
umap_1
C
Proportion
1.00
0.75
0.50
0.25
0.00
0 1 2 3 4 5 6 7 8 9 10 11
RNA_snn_res.1
stage
E10 E11 E12 E13 E14 E15
D
Schwann_ModuleScore1
Sensory_ModuleScore1
Mesenchymal_ModuleScore1
Identity
F
Top 5 Mouse Sox2-/Sox10+ Subtype Markers
CORIN
CACNA1E
PLA2G7
CXCR4
GJB3
PRMT8
PRSS56
NEUROG1
ADRA1A
SRRM4
SLC24A2
TLL1
RFLNA
GATM
COL11A2
FOSB
MAG
CA10
C1QL3
CTNNA3
MATN4
ITGA1
VSTM4
IGFBP7
COL5A3
BCAS1
KCNA1
PDE10A
SLC24A3
DKK2
ADAM33
BMP3
ISM1
HGF
CDH12
GRIN2B
C1QTNF7
LRFN5
NTF3
LHX8
TSPAN10
TRIM63
TRPM1
DCT
GPR143
MLANA
PMEL
GPNMB
SLC45A2
TYR
UGT2A1
EXPH5
IL17RE
BLNK
TP73
IFNLR1
AGR3
MYO5C
AQP3
ILDR1
BLOC1S1
ECRG4
CETN2
NDUFS6
TRMT112
CRYAB
PHPT1
NDUFC1
UQCRB
DBI
ABHD3
MFSD2A
ADGRG1
SHANK2
SLC4A4
CSMD2
COL28A1
ENTPD1
RYR3
CTNND2
MSRB3
PSMG4
TMEM132B
PWP1
BCL7C
PSMA3
ECHS1
NR2F1
TULP3
HBE1
CA12
KIF26A
ZNF703
SLC18A2
APBA2
ASCL1
HAND2
ALK
TRIM55
PHOX2B
CAVIN2
TAPT1
MYO5B
TAFA4
PLXNA2
GLDN
PLCG2
GABRB3
LYPD6
NPY
HHLA1
PTCHD4
VSNL1
RCAN2
AJAP1
KCNQ5
TECRL
SYT1
KHDRBS2
HCN1
eCNCC1
eCNCC2
eCNCC3
eCNCC4
iCNCC1
lCNCC1
lCNCC2
melanocytes
mesenchymal.CNCC
schwann1
schwann2
sensory.CNCC
Pct Exp
0 25 50 75
Average Expression
−2 −1 0 1 2
E
Melanocyte Markers
Mitf
Pmel
0 1 2 3 4 5 6 7 8 9 10 11

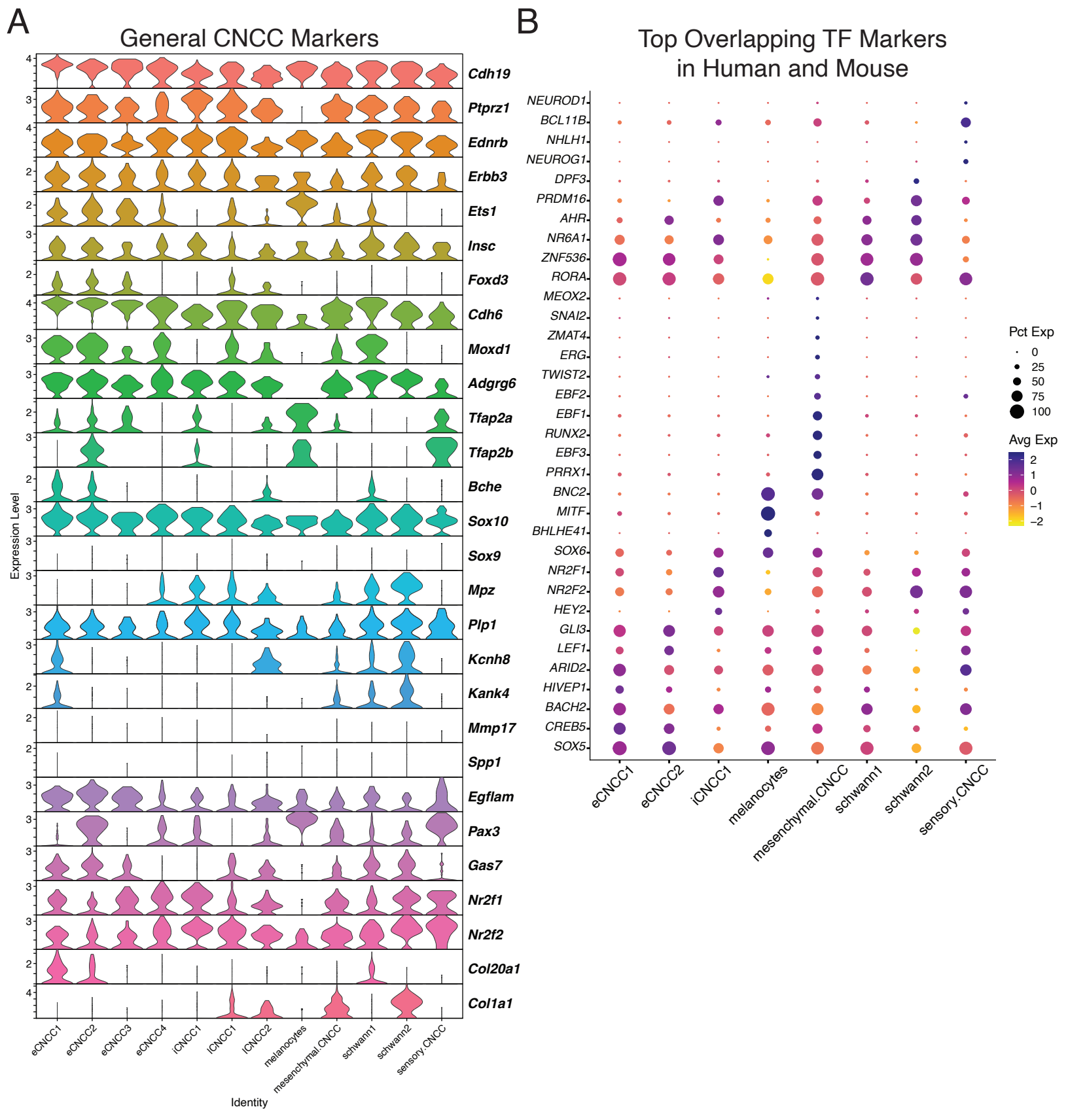
Supplementary Figure 13. Characterizing mouse *Sox2-/Sox10+* putative CNCC subtypes.

A). Elbow plot with optimal number of subclusters for mouse putative CNCC's. B). UMAP projection of putative CNCC subclusters with resolution set to 1. C). Proportion of putative CNNCs from each stage across the clusters D). Stacked violin plot of Schwann cell, sensory CNCC, and mesenchymal CNCC module scores across the clusters. E). Stacked violin plot of melanocyte gene markers *Mitf* and *Pmel* across the putative CNCC subclusters. F) Average and percent expression of the top 5 DEGs for the mouse putative CNCC subtypes.


A
GO: Biological Process
regulation of axonogenesis
axonogenesis
regulation of neuron projection development
homophilic cell adhesion via plasma membrane adhesion molecules
regulation of synapse organization
synapse organization
axon guidance
neuron projection guidance
cell junction assembly
cell migration in hindbrain
semaphorin−plexin signaling pathway
morphogenesis of embryonic epithelium
sympathetic nervous system development
autonomic nervous system development
noradrenergic neuron differentiation
motor neuron migration
forebrain development
trigeminal nerve development
stem cell development
neural crest cell differentiation
extracellular matrix organization
extracellular structure organization
external encapsulating structure organization
vascular transport
transport across blood−brain barrier
cell−substrate adhesion
aerobic electron transport chain
oxidative phosphorylation
respiratory electron transport chain
ATP synthesis coupled electron transport
mitochondrial ATP synthesis coupled electron transport
epidermis development
skin development
odontogenesis
odontogenesis of dentin−containing tooth
pigmentation
melanin biosynthetic process
melanin metabolic process
secondary metabolite biosynthetic process
developmental pigmentation
osteoblast differentiation
ossification
bone mineralization
connective tissue development
muscle tissue development
myelination
ensheathment of neurons
axon ensheathment
eCNCC1 (95)
eCNCC2 (99)
eCNCC3 (34)
iCNCC1 (97)
iCNCC2 (97)
iCNCC3 (91)
melanocytes (93)
mesenchymal CNCC (89)
schwann1 (89)
schwann2 (97)
sensory CNCC (71)
Cluster
p.adjust
0.01
0.02
0.03
0.04
GeneRatio
0.05
0.10
0.15
0.20
B
GO: Cellular Component
neuron to neuron synapse
asymmetric synapse
glutamatergic synapse
postsynaptic specialization
postsynaptic density
synaptic membrane
postsynaptic specialization membrane
cell leading edge
postsynaptic density membrane
lamellipodium
presynaptic active zone
semaphorin receptor complex
lateral plasma membrane
basement membrane
collagen−containing extracellular matrix
complex of collagen trimers
collagen trimer
fibrillar collagen trimer
banded collagen fibril
respirasome
respiratory chain complex
mitochondrial respirasome
mitochondrial protein−containing complex
inner mitochondrial membrane protein complex
transmembrane transporter complex
bicellular tight junction
tight junction
apical junction complex
melanosome
pigment granule
melanosome membrane
chitosome
pigment granule membrane
monoatomic ion channel complex
cation channel complex
neuromuscular junction
paranode region of axon
eCNCC1 (98)
eCNCC2 (93)
eCNCC3 (34)
iCNCC1 (100)
iCNCC2 (97)
iCNCC3 (99)
melanocytes (98)
mesenchymal CNCC (98)
schwann1 (93)
schwann2 (100)
Cluster
p.adjust
0.01
0.02
0.03
0.04
GeneRatio
0.05
0.10
0.15
0.20
C
GO: Molecular Function
cadherin binding
metalloendopeptidase activity
phosphoric ester hydrolase activity
3',5'−cyclic−AMP phosphodiesterase activity
3',5'−cyclic−GMP phosphodiesterase activity
transmembrane receptor protein tyrosine phosphatase activity
transmembrane receptor protein phosphatase activity
heparan sulfate sulfotransferase activity
beta−catenin binding
semaphorin receptor binding
chemorepellent activity
semaphorin receptor activity
transmembrane receptor protein kinase activity
transmembrane receptor protein tyrosine kinase activity
protein tyrosine kinase activity
growth factor binding
extracellular matrix structural constituent
extracellular matrix structural constituent conferring tensile strength
platelet−derived growth factor binding
metal ion transmembrane transporter activity
oxidoreduction−driven active transmembrane transporter activity
electron transfer activity
NADH dehydrogenase (ubiquinone) activity
NADH dehydrogenase (quinone) activity
NADH dehydrogenase activity
DNA−binding transcription activator activity, RNA polymerase II−specific
DNA−binding transcription activator activity
cell adhesion mediator activity
growth factor activity
chemoattractant activity
monoatomic cation channel activity
transmembrane receptor protein serine/threonine kinase binding
integrin binding
eCNCC1 (97)
eCNCC2 (99)
eCNCC3 (93)
iCNCC1 (98)
iCNCC2 (98)
iCNCC3 (98)
mesenchymal CNCC (92)
schwann2 (91)
Cluster
p.adjust
0.01
0.02
0.03
0.04
GeneRatio
0.05
0.10
0.15
D
Reactome Pathway
Defective B3GALTL causes PpS
O−glycosylation of TSR domain−containing proteins
Diseases associated with O−glycosylation of proteins
Neuronal System
Diseases of glycosylation
Extracellular matrix organization
Collagen biosynthesis and modifying enzymes
CRMPs in Sema3A signaling
Specification of the neural plate border
Protein−protein interactions at synapses
Receptor−type tyrosine−protein phosphatases
Cell junction organization
Cell−Cell communication
Activation of the TFAP2 (AP−2) family of transcription factors
RET signaling
Semaphorin interactions
SEMA3A−Plexin repulsion signaling by inhibiting Integrin adhesion
Sema3A PAK dependent Axon repulsion
Collagen chain trimerization
Collagen formation
Non−integrin membrane−ECM interactions
ECM proteoglycans
Assembly of collagen fibrils and other multimeric structures
Respiratory electron transport
Respiratory electron transport, ATP synthesis by chemiosmotic coupling, and heat production by uncoupling proteins
Aerobic respiration and respiratory electron transport
Complex I biogenesis
SRP−dependent cotranslational protein targeting to membrane
Signaling by ROBO receptors
Apoptotic cleavage of cell adhesion proteins
Type I hemidesmosome assembly
Formation of the cornified envelope
MITF−M−regulated melanocyte development
MITF−M−dependent gene expression
Regulation of MITF−M−dependent genes involved in pigmentation
Transcriptional and post−translational regulation of MITF−M expression and activity
TRP channels
Elastic fibre formation
Unblocking of NMDA receptors, glutamate binding and activation
Long−term potentiation
Molecules associated with elastic fibres
Constitutive Signaling by Aberrant PI3K in Cancer
RHO GTPase cycle
RAC1 GTPase cycle
EGR2 and SOX10−mediated initiation of Schwann cell myelination
Syndecan interactions
Netrin−1 signaling
Regulation of commissural axon pathfinding by SLIT and ROBO
Physiological factors
eCNCC1 (69)
eCNCC2 (65)
eCNCC3 (58)
iCNCC1 (65)
iCNCC1 (76)
iCNCC2 (61)
melanocytes (63)
mesenchymal CNCC (53)
schwann1 (58)
schwann2 (65)
sensory CNCC (58)
Cluster
p.adjust
0.01
0.02
0.03
0.04
GeneRatio
0.05
0.10
0.15
0.20
0.25
E
KEGG Pathway
Glycosaminoglycan biosynthesis − heparan sulfate / heparin
Axon guidance
Protein digestion and absorption
Arrhythmogenic right ventricular cardiomyopathy
ECM−receptor interaction
Salivary secretion
Human papillomavirus infection
PI3K−Akt signaling pathway
Non−alcoholic fatty liver disease
Oxidative phosphorylation
Thermogenesis
Huntington disease
Parkinson disease
Virion − Hepatitis viruses
Synaptic vesicle cycle
Tight junction
Melanogenesis
Calcium signaling pathway
Circadian entrainment
Ras signaling pathway
Rap1 signaling pathway
Focal adhesion
Cytoskeleton in muscle cells
eCNCC2 (50)
iCNCC1 (55)
iCNCC1 (61)
iCNCC2 (47)
melanocytes (53)
mesenchymal CNCC (44)
schwann2 (52)
sensory CNCC (28)
Cluster
p.adjust
0.01
0.02
0.03
0.04
GeneRatio
0.10
0.15
0.20
0.25
0.30
F
DisGeNet
Substance Dependence
Organic Mental Disorders, Substance−Induced
Prescription Drug Abuse
Depression, Bipolar
Drug Use Disorders
Resistance to Insulin−Like Growth Factor I
Neuroendocrine Tumors
Pheochromocytoma
Beckwith−Wiedemann Syndrome
Hyperhidrosis disorder
Smoking
Aortic valve disorder
Leukemia, Plasma Cell
Intervertebral Disc Degeneration
Adult Pilocytic Astrocytoma
Familial Hemiplegic Migraine
Myopia
Acidosis, Lactic
Increased CSF lactate
Leukoencephalopathy
Mitochondrial Diseases
Proximal tubulopathy
ANONYCHIA
Keratoderma, Palmoplantar
Epidermolysis Bullosa
Sparse body hair
Junctional Epidermolysis Bullosa
Hypodontia
Hypopigmentation disorder
ALBINOIDISM, OCULOCUTANEOUS, AUTOSOMAL DOMINANT
Skin Pigmentation Disorder
Albinism, Oculocutaneous
Piebaldism
Fibrosis
Symmetric Diabetic Proximal Motor Neuropathy
Asymmetric Diabetic Proximal Motor Neuropathy
Duchenne and Becker Muscular Dystrophy
Myokymia
Chorea
Oculomotor Nerve Paralysis
Autistic behavior
Neuropathy
Sensorimotor neuropathy
Ataxia, Sensory
Demyelinating Diseases
Peripheral Neuropathy
eCNCC1 (99)
eCNCC3 (98)
iCNCC1 (99)
iCNCC1 (91)
iCNCC2 (98)
melanocytes (98)
mesenchymal CNCC (99)
schwann1 (98)
schwann2 (100)
sensory CNCC (74)
Cluster
p.adjust
0.01
0.02
0.03
0.04
GeneRatio
0.05
0.10
0.15

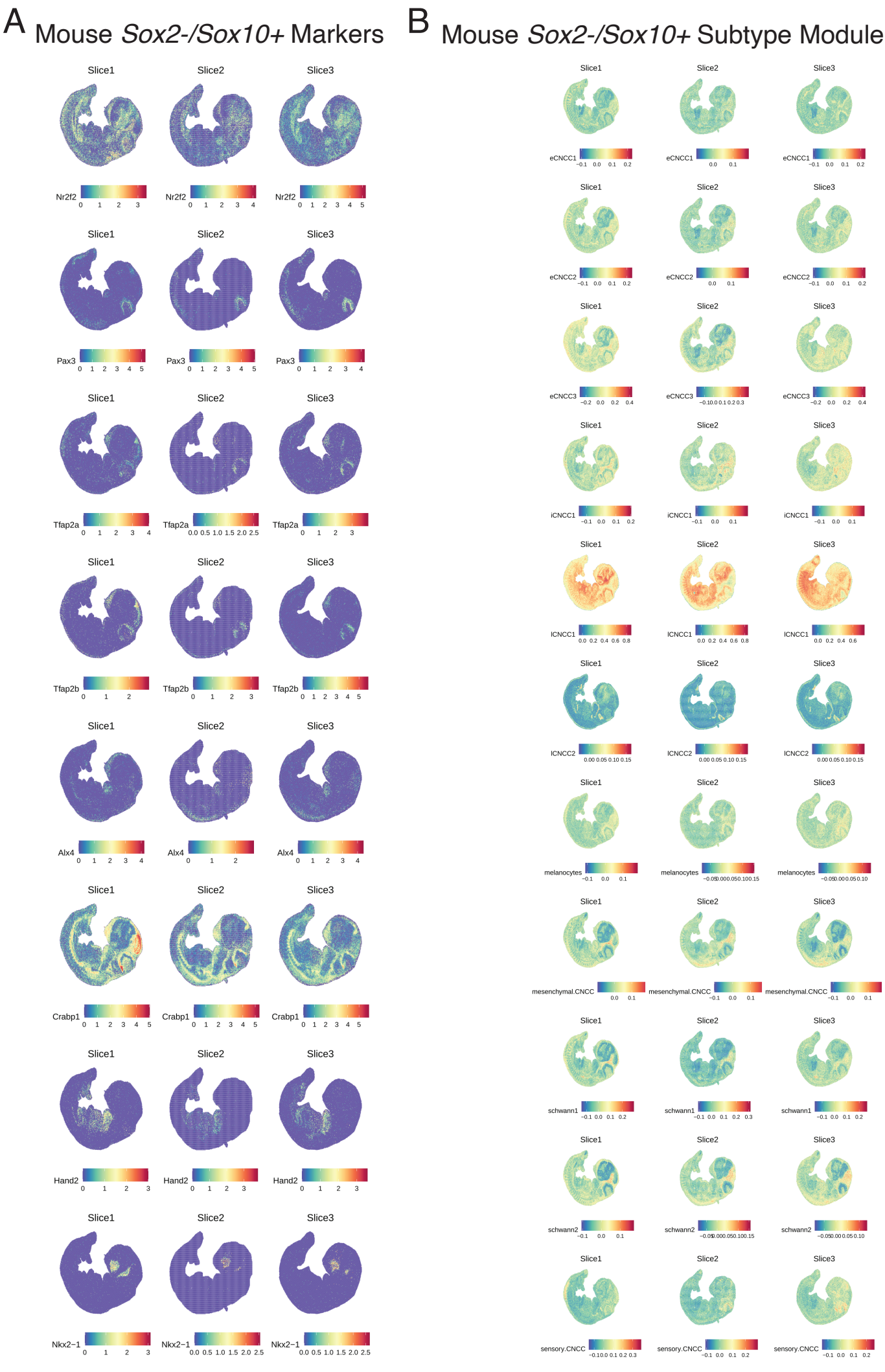
Supplementary Figure 14. Functional annotation enrichment for mouse putative CNCC subtypes using the top 100 marker genes.

A). Gene Ontology for Biological Processes. B). Gene Ontology for Cellular Components. C). Gene Ontology for Molecular Functions. D). Reactome Pathways. E). KEGG pathways. F). DisGeNet.


A
General CNCC Markers
Cdh19
Ptprz1
Ednrb
Erbb3
Ets1
Insc
Foxd3
Cdh6
Moxd1
Adgrg6
Tfap2a
Tfap2b
Bche
Sox10
Sox9
Mpz
Plp1
Kcnh8
Kank4
Mmp17
Spp1
Egflam
Pax3
Gas7
Nr2f1
Nr2f2
Col20a1
Col1a1
Expression Level
eCNCC1
eCNCC2
eCNCC3
eCNCC4
iCNCC1
iCNCC1
iCNCC2
melanocytes
mesenchymal.CNCC
schwann1
schwann2
sensory.CNCC
Identity
B
Top Overlapping TF Markers
in Human and Mouse
NEUROD1
BCL11B
NHLH1
NEUROG1
DPF3
PRDM16
AHR
NR6A1
ZNF536
RORA
MEOX2
SNAI2
ZMAT4
ERG
TWIST2
EBF2
EBF1
RUNX2
EBF3
PRRX1
BNC2
MITF
BHLHE41
SOX6
NR2F1
NR2F2
HEY2
GLI3
LEF1
ARID2
HIVEP1
BACH2
CREB5
SOX5
eCNCC1
eCNCC2
iCNCC1
melanocytes
mesenchymal.CNCC
schwann1
schwann2
sensory.CNCC
Pct Exp
0
25
50
75
100
Avg Exp
2
1
0
−1
−2

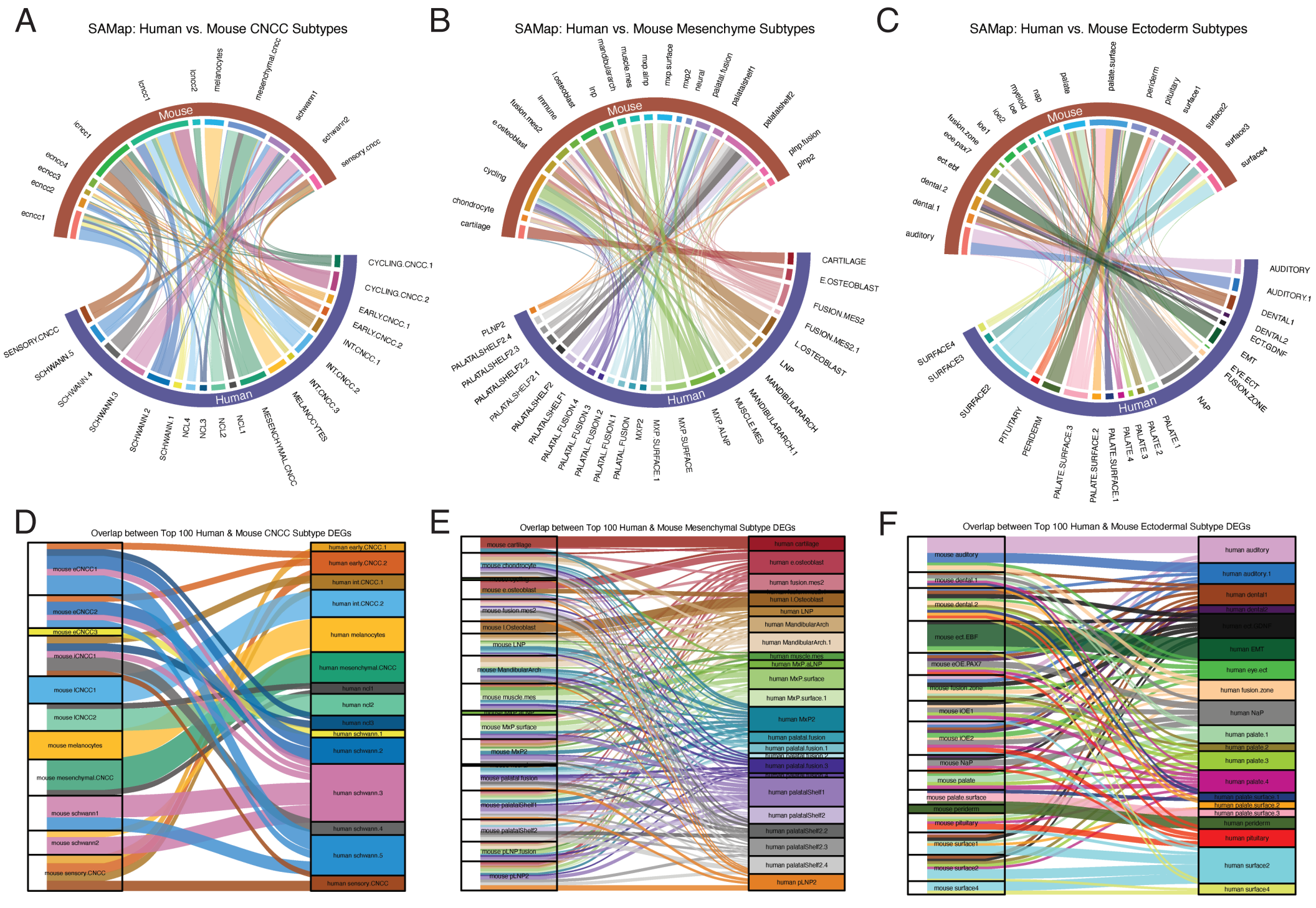
Supplementary Figure 15. Analysis of CNCC genes in mouse putative CNCC subtypes.

A). Violin plot of mouse orthologous neural crest marker genes from Fig. 3C for mouse putative CNCC subtypes. B). Average and percent expression of top overlapping TF DEGs between human and mouse for each orthologous putative CNCC subtype.


A
Mouse Sox2-/Sox10+ Markers
Slice1
Slice2
Slice3
Nr2f2
Pax3
Tfap2a
Tfap2b
Alx4
Crabp1
Hand2
Nkx2−1
B
Mouse Sox2-/Sox10+ Subtype Module Scores
eCNCC1
eCNCC2
eCNCC3
iCNCC1
lCNCC1
lCNCC2
melanocytes
mesenchymal.CNCC
schwann1
schwann2
sensory.CNCC

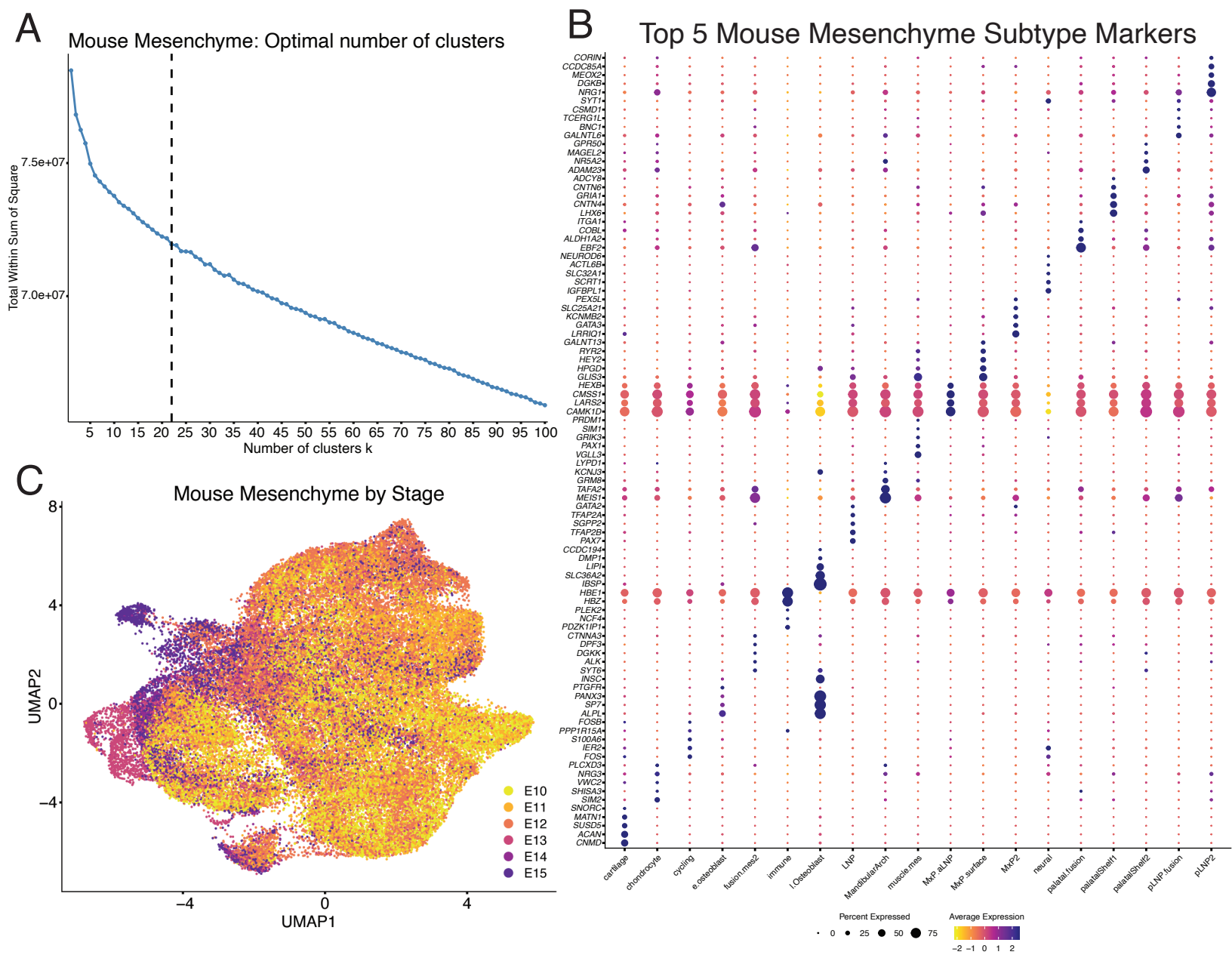
Supplementary Figure 16. Spatial feature plots of mouse *Sox2-/Sox10+* putative CNCC genes and module scores from 3 sections of mouse E11.5 embryos[11].

A). Mouse *Sox2-/Sox10+* putative CNCC gene markers. B). Mouse *Sox2-/Sox10+* putative CNCC subtype module scores.


A
SAMap: Human vs. Mouse CNCC Subtypes
Mouse
Human
icncc1
icncc2
melanocytes
mesenchymal.cncc
schwann1
schwann2
sensory.cncc
ecncc4
ecncc3
ecncc2
ecncc1
CYCLING.CNCC.1
CYCLING.CNCC.2
EARLY.CNCC.1
EARLY.CNCC.2
INT.CNCC.1
INT.CNCC.2
INT.CNCC.3
MELANOCYTES
MESENCHYMAL.CNCC
NCL1
NCL2
NCL3
NCL4
SCHWANN.1
SCHWANN.2
SCHWANN.3
SCHWANN.4
SCHWANN.5
SENSORY.CNCC
B
SAMap: Human vs. Mouse Mesenchyme Subtypes
Mouse
Human
mandibulararch
muscle.mes
mxp.alnp
mxp.surface
mxp2
neural
palatal.fusion
palatalshelf1
palatalshelf2
plnp.fusion
plnp2
l.osteoblast
lnp
immune
fusion.mes2
e.osteoblast
cycling
chondrocyte
cartilage
CARTILAGE
E.OSTEOBLAST
FUSION.MES2
FUSION.MES2.1
L.OSTEOBLAST
LNP
MANDIBULARARCH
MANDIBULARARCH.1
MUSCLE.MES
MXP.ALNP
MXP.SURFACE
MXP.SURFACE.1
MXP2
PALATAL.FUSION
PALATAL.FUSION.1
PALATAL.FUSION.2
PALATAL.FUSION.3
PALATAL.FUSION.4
PALATALSHELF1
PALATALSHELF2
PALATALSHELF2.1
PALATALSHELF2.2
PALATALSHELF2.3
PALATALSHELF2.4
PLNP2
C
SAMap: Human vs. Mouse Ectoderm Subtypes
Mouse
Human
palate.surface
periderm
pituitary
surface1
surface2
surface3
surface4
palate
nap
myeloid
loe
loe2
loe1
fusion.zone
eoe.pax7
ect.ebf
dental.2
dental.1
auditory
AUDITORY
AUDITORY.1
DENTAL1
DENTAL2
ECT.GDNF
EMT
EYE.ECT
FUSION.ZONE
NAP
PALATE.1
PALATE.2
PALATE.3
PALATE.4
PALATE.SURFACE.1
PALATE.SURFACE.2
PALATE.SURFACE.3
PERIDERM
PITUITARY
SURFACE2
SURFACE3
SURFACE4
D
Overlap between Top 100 Human & Mouse CNCC Subtype DEGs
mouse eCNCC1
mouse eCNCC2
mouse eCNCC3
mouse iCNCC1
mouse lCNCC1
mouse lCNCC2
mouse melanocytes
mouse mesenchymal.CNCC
mouse schwann1
mouse schwann2
mouse sensory.CNCC
human early.CNCC.1
human early.CNCC.2
human int.CNCC.1
human int.CNCC.2
human melanocytes
human mesenchymal.CNCC
human ncl1
human ncl2
human ncl3
human schwann.1
human schwann.2
human schwann.3
human schwann.4
human schwann.5
human sensory.CNCC
E
Overlap between Top 100 Human & Mouse Mesenchymal Subtype DEGs
mouse cartilage
mouse chondrocyte
mouse e.osteoblast
mouse fusion.mes2
mouse l.Osteoblast
mouse LNP
mouse MandibularArch
mouse muscle.mes
mouse MxP.surface
mouse MxP2
mouse palatal.fusion
mouse palatalShelf1
mouse palatalShelf2
mouse pLNP.fusion
mouse pLNP2
human cartilage
human e.osteoblast
human fusion.mes2
human l.Osteoblast
human LNP
human MandibularArch
human MandibularArch.1
human muscle.mes
human MxP.aLNP
human MxP.surface
human MxP.surface.1
human MxP2
human palatal.fusion
human palatal.fusion.1
human palatal.fusion.3
human palatalShelf1
human palatalShelf2
human palatalShelf2.2
human palatalShelf2.3
human palatalShelf2.4
human pLNP2
F
Overlap between Top 100 Human & Mouse Ectodermal Subtype DEGs
mouse auditory
mouse dental.1
mouse dental.2
mouse ect.EBF
mouse eOE.PAX7
mouse fusion.zone
mouse iOE1
mouse iOE2
mouse NaP
mouse palate
mouse palate.surface
mouse periderm
mouse pituitary
mouse surface1
mouse surface2
mouse surface4
human auditory
human auditory.1
human dental1
human dental2
human ect.GDNF
human EMT
human eye.ect
human fusion.zone
human NaP
human palate.1
human palate.2
human palate.3
human palate.4
human palate.surface.1
human palate.surface.2
human palate.surface.3
human periderm
human pituitary
human surface2
human surface4

Supplementary Figure 17. Comparing human and mouse cell subtype annotations.

Chord plots for mapping human to mouse SAMap similarity scores for A). putative CNCC subtypes, B). mesenchymal subtypes, and C). ectodermal subtypes. Alluvial plots showing overlap between top 100 human and mouse DEGs for D). putative CNCC subtypes, E). mesenchymal subtypes, and F). ectodermal subtypes.

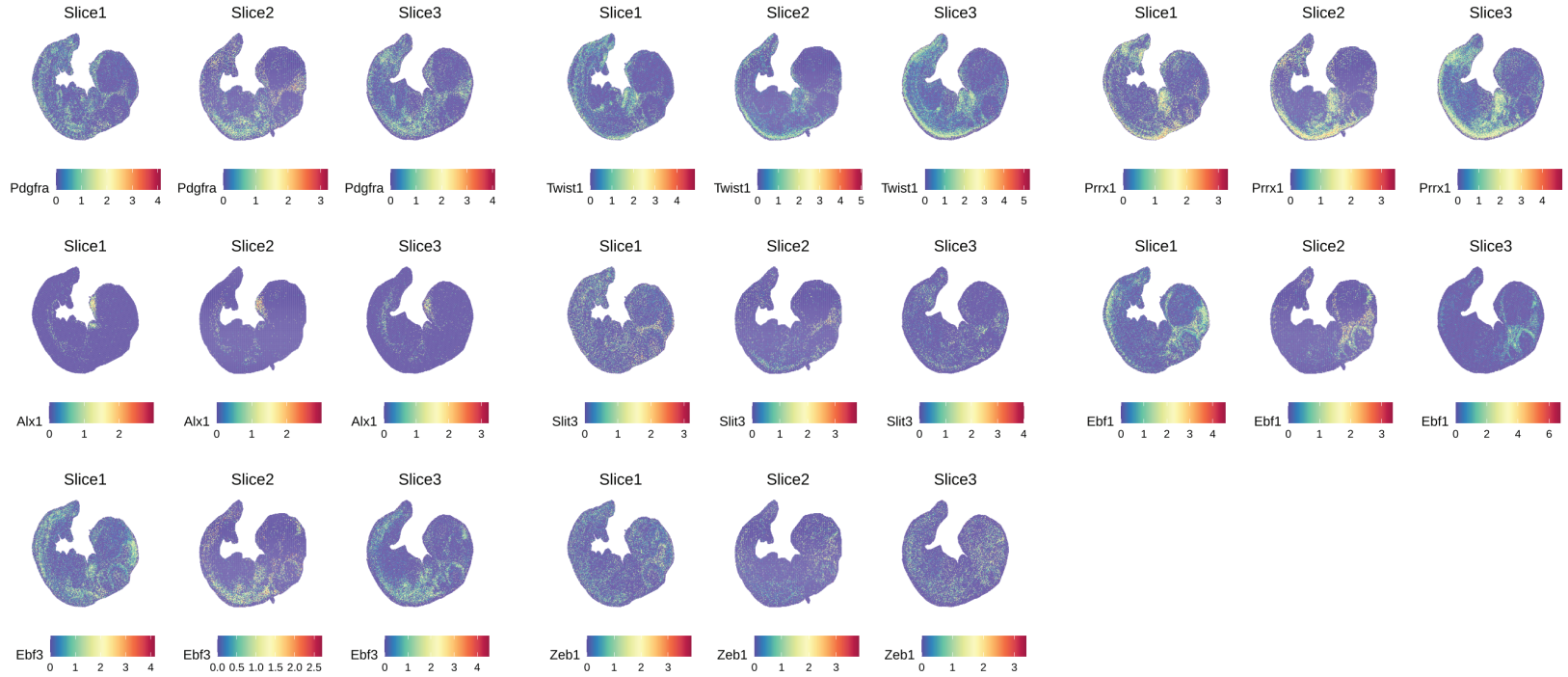

A
Mouse Mesenchyme: Optimal number of clusters
Total Within Sum of Square
7.5e+07
7.0e+07
5 10 15 20 25 30 35 40 45 50 55 60 65 70 75 80 85 90 95 100
Number of clusters k
B
Top 5 Mouse Mesenchyme Subtype Markers
CORIN
CCDC85A
MEOX2
DGKB
NRG1
SYT1
CSMD1
TCERG1L
BNC1
GALNTL6
GPR50
MAGEL2
NR5A2
ADAM23
ADCY8
CNTN6
GRIA1
CNTN4
LHX6
ITGA1
COBL
ALDH1A2
EBF2
NEUROD6
ACTL6B
SLC32A1
SCRT1
IGFBPL1
PEX5L
SLC25A21
KCNMB2
GATA3
LRRIQ1
GALNT13
RYR2
HEY2
HPGD
GLIS3
HEXB
CMSS1
LARS2
CAMK1D
PRDM1
SIM1
GRIK3
PAX1
VGLL3
LYPD1
KCNJ3
GRM8
TAFA2
MEIS1
GATA2
TFAP2A
SGPP2
TFAP2B
PAX7
CCDC194
DMP1
LIPI
SLC36A2
IBSP
HBE1
HBZ
PLEK2
NCF4
PDZK1IP1
CTNNA3
DPF3
DGKK
ALK
SYT6
INSC
PTGFR
PANX3
SP7
ALPL
FOSB
PPP1R15A
S100A6
IER2
FOS
PLCXD3
NRG3
VWC2
SHISA3
SIM2
SNORC
MATN1
SUSD5
ACAN
CNMD
cartilage
chondrocyte
cycling
e.osteoblast
fusion.mes2
immune
l.Osteoblast
LNP
MandibularArch
muscle.mes
MxP aLNP
MxP surface
MxP2
neural
palatal fusion
palatalShelf1
palatalShelf2
pLNP fusion
pLNP2
Percent Expressed
0 25 50 75
Average Expression
−2 −1 0 1 2
C
Mouse Mesenchyme by Stage
UMAP2
8
4
0
−4
−4
0
4
UMAP1
E10
E11
E12
E13
E14
E15

Supplementary Figure 18. Characterizing mouse mesenchymal subtypes.

A). Elbow plot with optimal number of subclusters for mouse mesenchyme. B). Average and percent expression of the top 5 DEGs for the mouse mesenchymal subtypes. C). Distribution of mouse mesenchymal cells from each stage across the UMAP projection.

A

Mouse Mesenchyme Markers



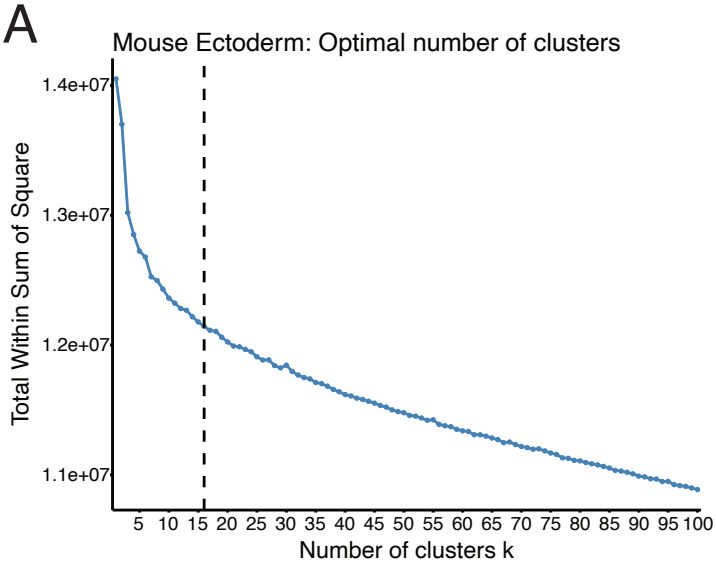
B

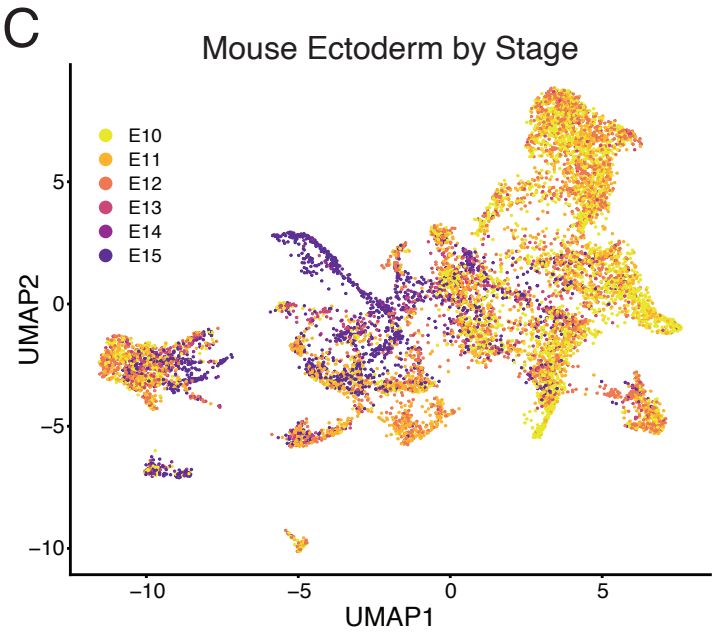
Mouse Mesenchyme Subtype Module Scores

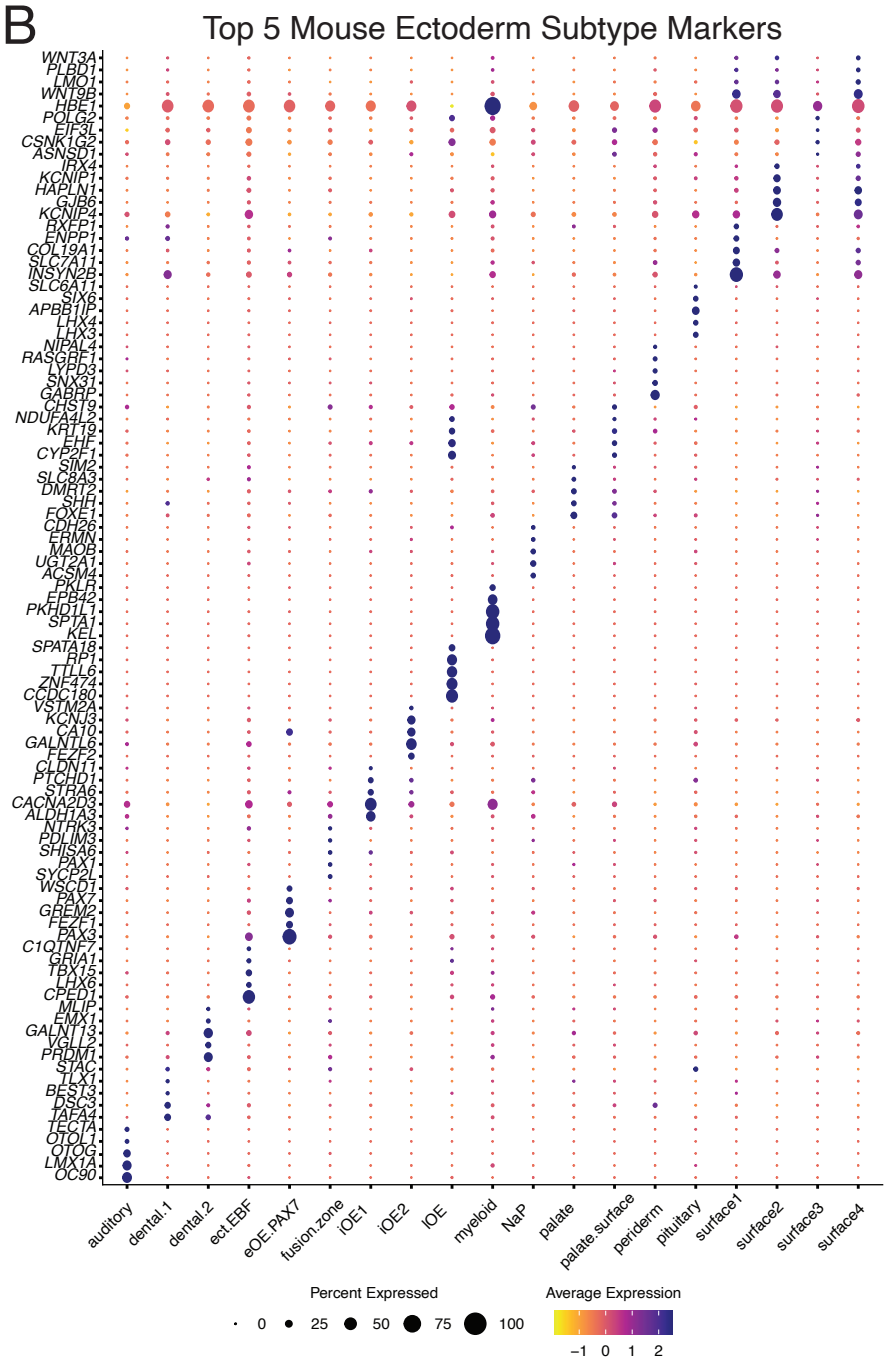


Supplementary Figure 19. Spatial feature plots of mouse mesenchymal genes and module scores from 3 sections of mouse E11.5 embryos[11].

A). Mouse mesenchyme gene markers. B). Mouse mesenchymal subtype module scores.


A
Mouse Ectoderm: Optimal number of clusters
Total Within Sum of Square
1.4e+07
1.3e+07
1.2e+07
1.1e+07
5 10 15 20 25 30 35 40 45 50 55 60 65 70 75 80 85 90 95 100
Number of clusters k


C
Mouse Ectoderm by Stage
E10
E11
E12
E13
E14
E15
UMAP2
5
0
−5
−10
−10
−5
0
5
UMAP1


B
Top 5 Mouse Ectoderm Subtype Markers
WNT3A
PLBD1
LMO1
WNT9B
HBE1
POLG2
EIF3L
CSNK1G2
ASNSD1
IRX4
KCNIP1
HAPLN1
GJB6
KCNIP4
RXFP1
ENPP1
COL19A1
SLC7A11
INSYN2B
SLC6A11
SIX6
APBB1IP
LHX4
LHX3
NPAL4
RASGRF1
LYPD3
SNX31
GABRP
CHST9
NDUFA4L2
KRT19
EHF
CYP2F1
SIM2
SLC8A3
DMRT2
SHH
FOXE1
CDH6
ERMN
MAOB
UGT2A1
ACSM4
PKLR
EPB42
PKHD1L1
SPTA1
KEL
SPATA18
RP1
TTLL6
ZNF474
CCDC180
VSTM2A
KCNJ3
CA10
GALNTL6
FEZF2
CLDN11
PTCHD1
STRA6
CACNA2D3
ALDH1A3
NTRK3
PDLIM3
SHISA6
PAX1
SYCP2L
WSCD1
PAX7
GREM2
FEZF1
PAX3
C1QTNF7
GRIA1
TBX15
LHX6
CPED1
MLIP
EMX1
GALNT13
VGLL2
PRDM1
STAC
TLX1
BEST3
DSC3
TAFA4
TECTA
OTOL1
OTOG
LMX1A
OC90
auditory
dental.1
dental.2
ect.EBF
eOE.PAX7
fusion.zone
iOE1
iOE2
lOE
myeloid
NaP
palate
palate.surface
periderm
pituitary
surface1
surface2
surface3
surface4
Percent Expressed
0
25
50
75
100
Average Expression
−1
0
1
2

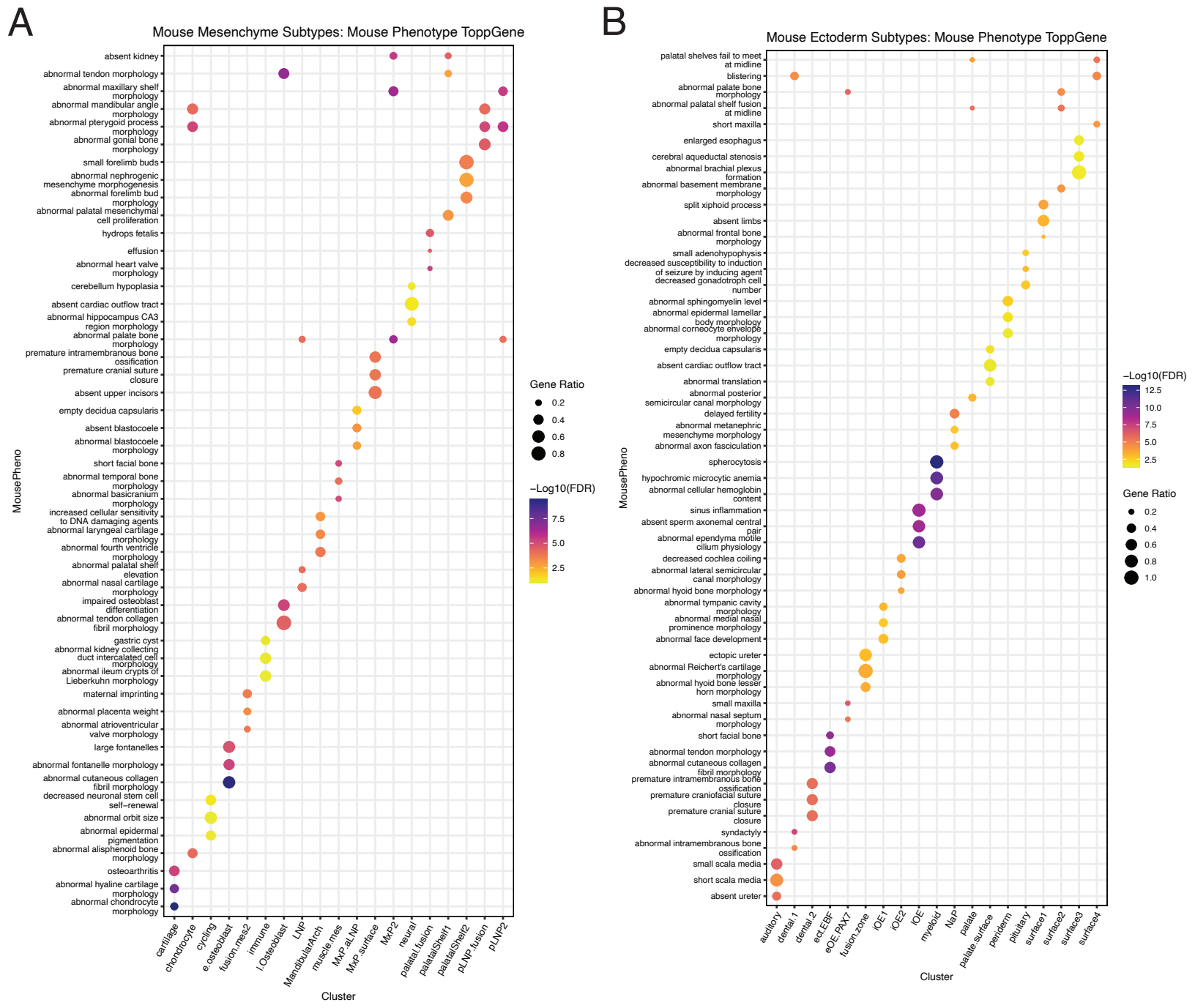
Supplementary Figure 20. Characterizing mouse ectodermal subtypes.

A). Elbow plot with optimal number of subclusters for mouse ectoderm. B). Average and percent expression of the top 5 DEGs for the mouse ectodermal subtypes. C). Distribution of mouse ectodermal cells from each stage across the UMAP projection.


A
Mouse Ectoderm Markers
Slice1
Slice2
Slice3
Grhl2
Esrp1
Trp63
Irf6
Tfap2a
Tfap2b
B
Mouse Ectoderm Subtype Module Scores
auditory
dental.1
dental.2
ect.EBF
eOE.PAX7
fusion.zone
iOE1
iOE2
IOE
myeloid
NaP
palate
palate.surface
periderm
pituitary
surface1
surface2
surface3
surface4

Supplementary Figure 21. Spatial feature plots of mouse ectodermal genes and module scores from 3 sections of mouse E11.5 embryos[11].

A). Mouse ectodermal gene markers. B). Mouse ectodermal subtype module scores.


A
Mouse Mesenchyme Subtypes: Mouse Phenotype ToppGene
absent kidney
abnormal tendon morphology
abnormal maxillary shelf morphology
abnormal mandibular angle morphology
abnormal pterygoid process morphology
abnormal gonial bone morphology
small forelimb buds
abnormal nephrogenic mesenchyme morphogenesis
abnormal forelimb bud morphology
abnormal palatal mesenchymal cell proliferation
hydrops fetalis
effusion
abnormal heart valve morphology
cerebellum hypoplasia
absent cardiac outflow tract
abnormal hippocampus CA3 region morphology
abnormal palate bone morphology
premature intramembranous bone ossification
premature cranial suture closure
absent upper incisors
empty decidua capsularis
absent blastocoele
abnormal blastocoele morphology
short facial bone
abnormal temporal bone morphology
abnormal basicranium morphology
increased cellular sensitivity to DNA damaging agents
abnormal laryngeal cartilage morphology
abnormal fourth ventricle morphology
abnormal palatal shelf elevation
abnormal nasal cartilage morphology
impaired osteoblast differentiation
abnormal tendon collagen fibril morphology
gastric cyst
abnormal kidney collecting duct intercalated cell morphology
abnormal ileum crypts of Lieberkuhn morphology
maternal imprinting
abnormal placenta weight
abnormal atrioventricular valve morphology
large fontanelles
abnormal fontanelle morphology
abnormal cutaneous collagen fibril morphology
decreased neuronal stem cell self−renewal
abnormal orbit size
abnormal epidermal pigmentation
abnormal alisphenoid bone morphology
osteoarthritis
abnormal hyaline cartilage morphology
abnormal chondrocyte morphology
MousePheno
cartilage
chondrocyte
cycling
e.osteoblast
fusion.mes2
immune
l.Osteoblast
LNP
MandibularArch
muscle.mes
MxP.aLNP
MxP.surface
MxP2
neural
palatal.fusion
palatalShelf1
palatalShelf2
pLNP.fusion
pLNP2
Cluster
Gene Ratio
0.2
0.4
0.6
0.8
−Log10(FDR)
7.5
5.0
2.5
B
Mouse Ectoderm Subtypes: Mouse Phenotype ToppGene
palatal shelves fail to meet at midline
blistering
abnormal palate bone morphology
abnormal palatal shelf fusion at midline
short maxilla
enlarged esophagus
cerebral aqueductal stenosis
abnormal brachial plexus formation
abnormal basement membrane morphology
split xiphoid process
absent limbs
abnormal frontal bone morphology
small adenohypophysis
decreased susceptibility to induction of seizure by inducing agent
decreased gonadotroph cell number
abnormal sphingomyelin level
abnormal epidermal lamellar body morphology
abnormal corneocyte envelope morphology
empty decidua capsularis
absent cardiac outflow tract
abnormal translation
abnormal posterior semicircular canal morphology
delayed fertility
abnormal metanephric mesenchyme morphology
abnormal axon fasciculation
spherocytosis
hypochromic microcytic anemia
abnormal cellular hemoglobin content
sinus inflammation
absent sperm axonemal central pair
abnormal ependyma motile cilium physiology
decreased cochlea coiling
abnormal lateral semicircular canal morphology
abnormal hyoid bone morphology
abnormal tympanic cavity morphology
abnormal medial nasal prominence morphology
abnormal face development
ectopic ureter
abnormal Reichert's cartilage morphology
abnormal hyoid bone lesser horn morphology
small maxilla
abnormal nasal septum morphology
short facial bone
abnormal tendon morphology
abnormal cutaneous collagen fibril morphology
premature intramembranous bone ossification
premature craniofacial suture closure
premature cranial suture closure
syndactyly
abnormal intramembranous bone ossification
small scala media
short scala media
absent ureter
MousePheno
auditory
dental.1
dental.2
ect.EBF
eOE.PAX7
fusion.zone
iOE1
iOE2
lOE
myeloid
NaP
palate
palate.surface
periderm
pituitary
surface1
surface2
surface3
surface4
Cluster
−Log10(FDR)
12.5
10.0
7.5
5.0
2.5
Gene Ratio
0.2
0.4
0.6
0.8
1.0

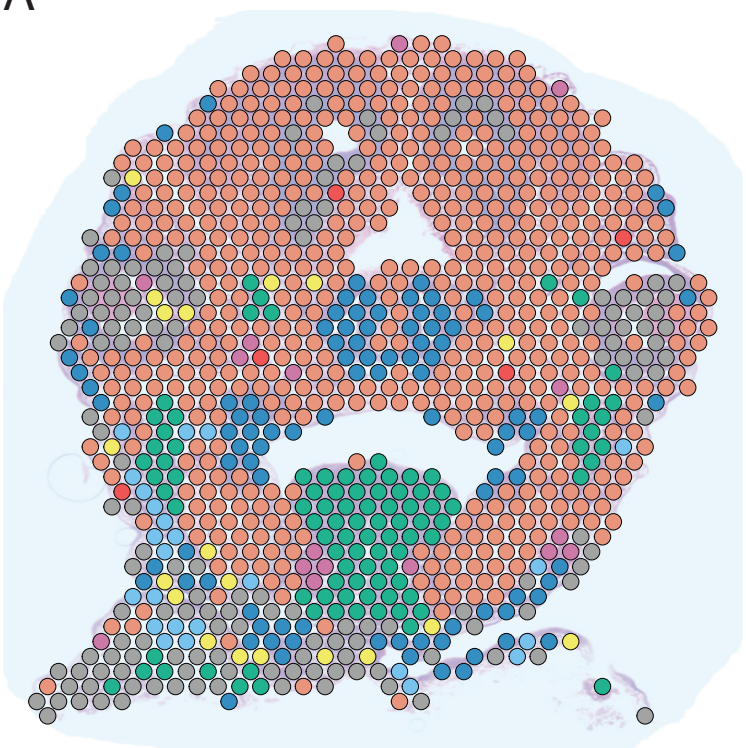
Supplementary Figure 22. Confirming mouse subtype labels using ToppGene[12].

Gene ratio and -log10(FDR) of the top mouse phenotypes for A). mouse mesenchymal subtypes and B). mouse ectodermal subtypes.

Human to Mouse CCA

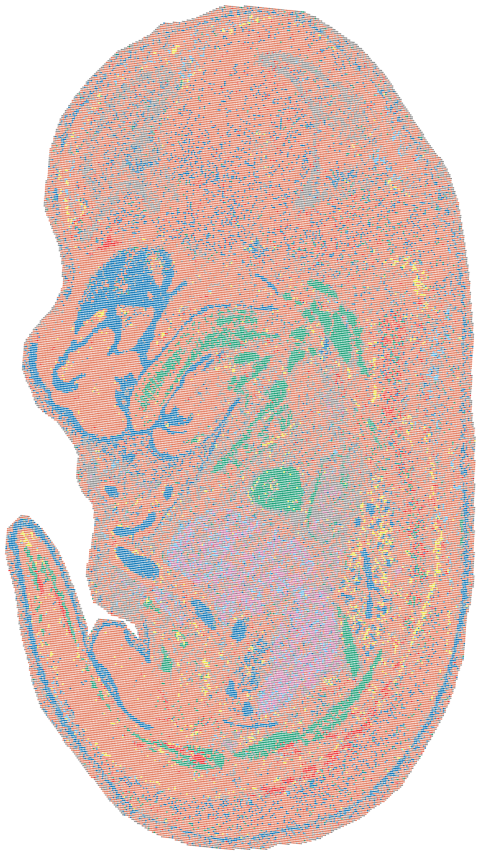
E15.5 craniofacial coronal cross-section
(Pina et al. 2024)

A



E15.5 embryo
(Chen et al. 2022)

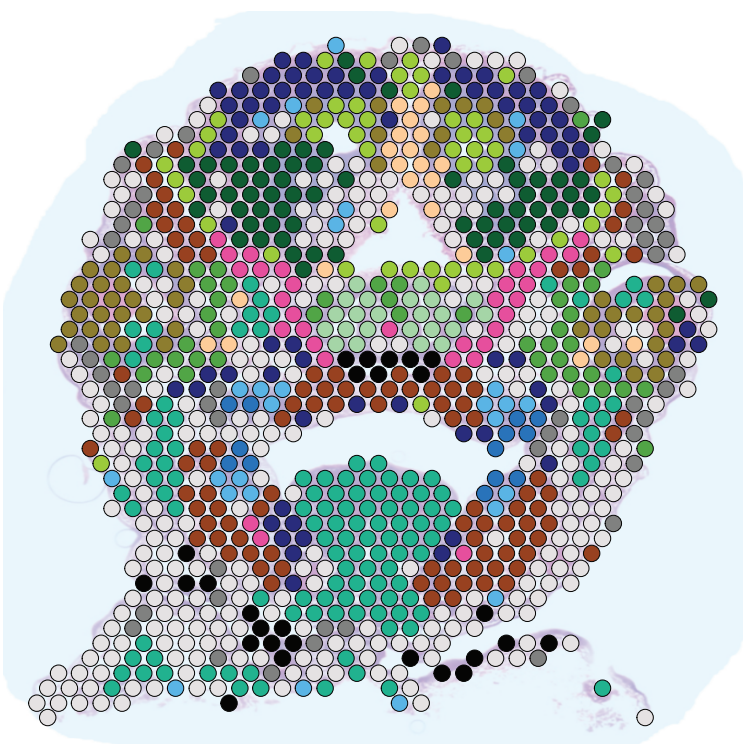
B



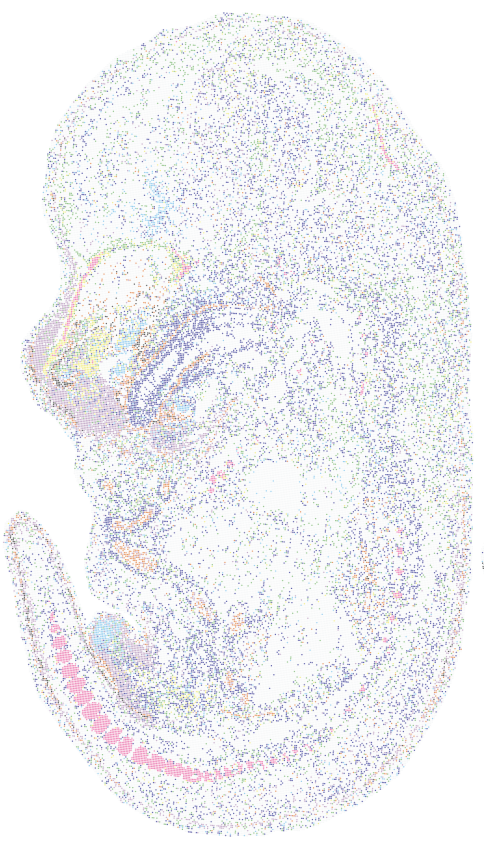
Main Cell Types

- mesenchyme
- immune
- endothelium
- erythrocytes
- muscle
- ectoderm
- *SOX2-/SOX10+*
- *SOX2+/SOX10-*

C



D

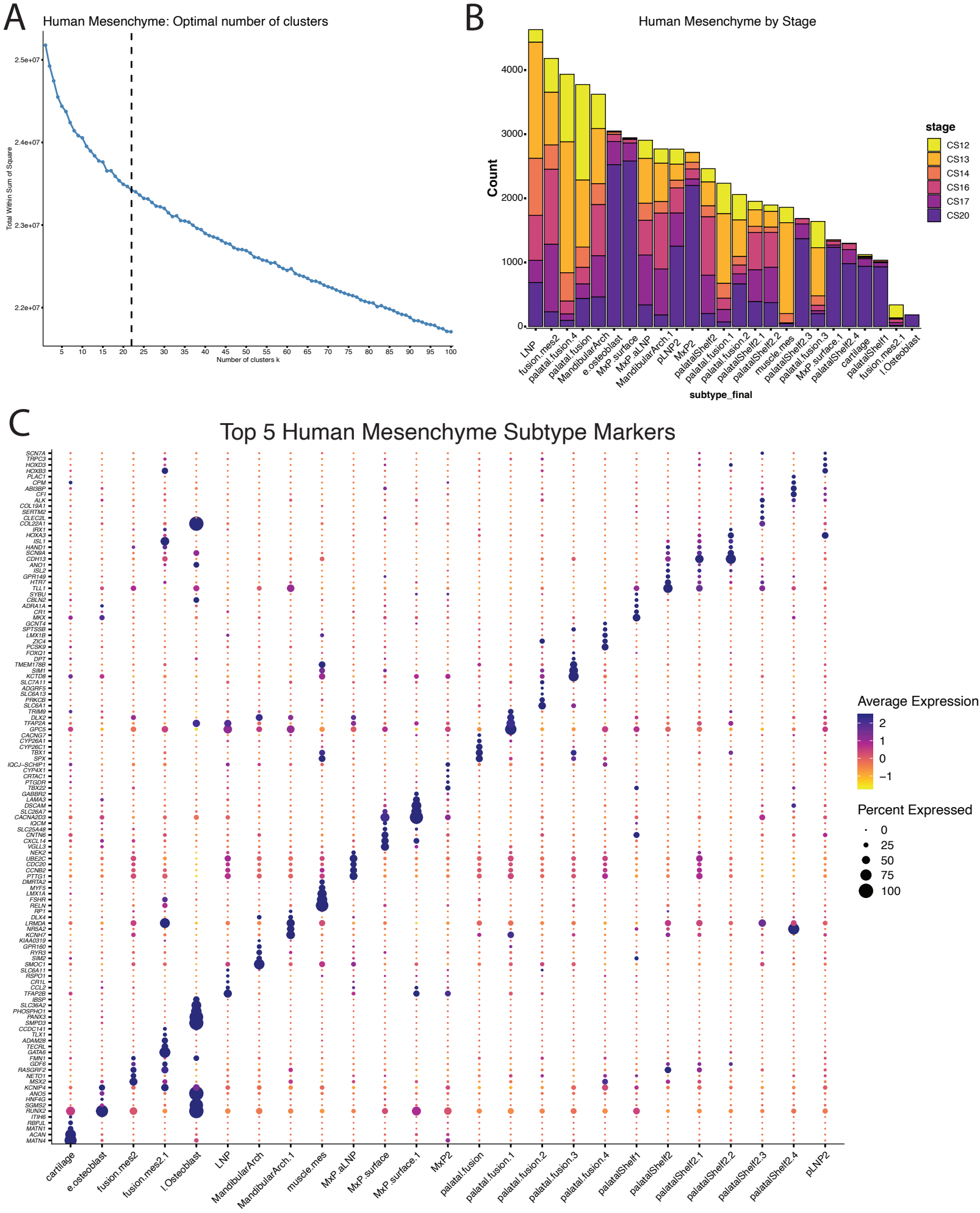


Cell Subtypes

- cartilage
- dental1
- e.osteoblast
- fusion.mes2
- LNP
- MandibularArch
- muscle
- muscle.mes
- MxP2
- MxP.surface
- NaP
- NeuralProg
- palatal.fusion
- palatalShelf
- palate
- periderm
- surface
- other cell types

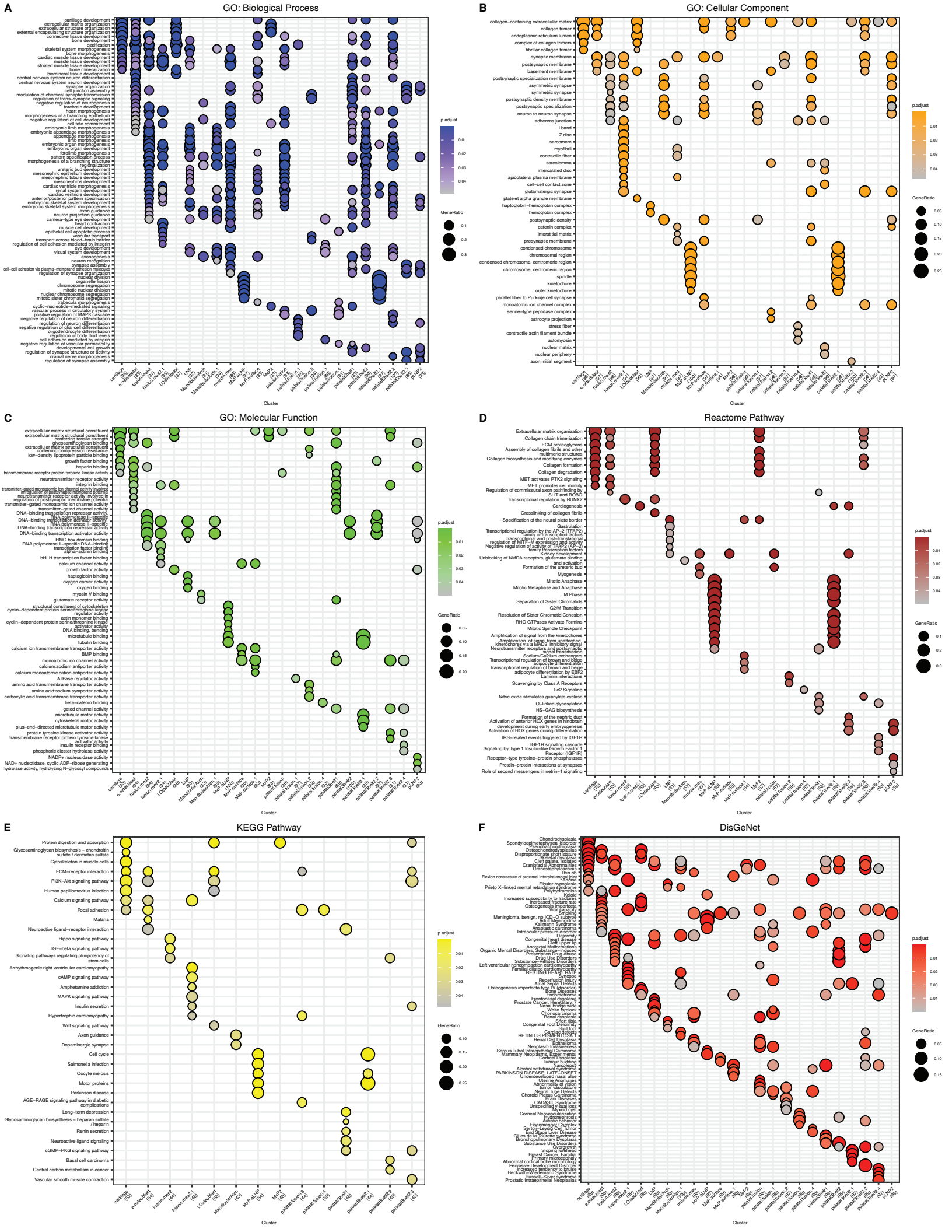
Supplementary Figure 23. Mapping human craniofacial main cell types and subtypes to mouse spatial transcriptomics data by canonical correlation analysis (CCA).

Transferring human main cell types to mouse spatial transcriptomics data for A). an E15.5 craniofacial coronal cross-section[13] and B). and a E15.5 embryo[14]. Transferring human cell subtypes to mouse spatial transcriptomics data for C). an E15.5 craniofacial coronal cross-section[13] and D). and a E15.5 embryo[14].


A
Human Mesenchyme: Optimal number of clusters
Total Within Sum of Square
Number of clusters k
B
Human Mesenchyme by Stage
Count
stage
CS12
CS13
CS14
CS16
CS17
CS20
subtype_final
C
Top 5 Human Mesenchyme Subtype Markers
Average Expression
Percent Expressed

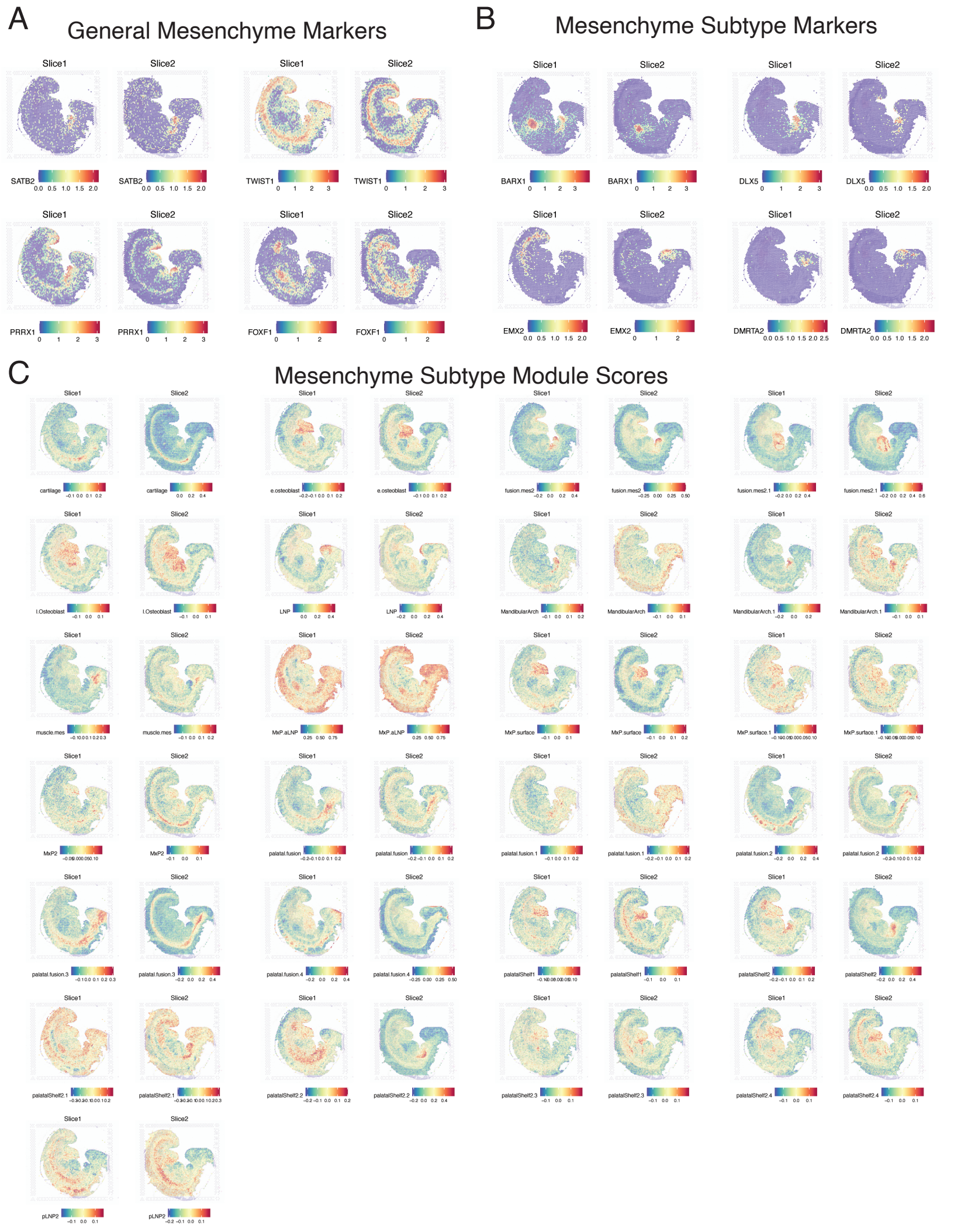
Supplementary Figure 24. Characterizing human mesenchymal subtypes.

A). Elbow plot with optimal number of subclusters for human mesenchyme. B). Number of cells obtained at each CS stage for each human mesenchymal subtype. C). Average and percent expression of the top 5 DEGs for the human mesenchymal subtypes.


A
GO: Biological Process
cartilage development
extracellular matrix organization
extracellular structure organization
external encapsulating structure organization
connective tissue development
bone development
ossification
skeletal system morphogenesis
bone morphogenesis
cardiac muscle tissue development
muscle tissue development
striated muscle tissue development
bone mineralization
biomineral tissue development
central nervous system neuron differentiation
central nervous system neuron development
synapse organization
cell junction assembly
modulation of chemical synaptic transmission
regulation of trans−synaptic signaling
negative regulation of neurogenesis
forebrain development
heart morphogenesis
morphogenesis of a branching epithelium
negative regulation of cell development
cell fate commitment
embryonic limb morphogenesis
embryonic appendage morphogenesis
appendage morphogenesis
limb morphogenesis
embryonic organ morphogenesis
embryonic organ development
forelimb morphogenesis
pattern specification process
morphogenesis of a branching structure
regionalization
ureteric bud development
mesonephric epithelium development
mesonephric tubule development
mesonephros development
cardiac ventricle morphogenesis
renal system development
cardiac ventricle development
anterior/posterior pattern specification
embryonic skeletal system development
embryonic skeletal system morphogenesis
axon guidance
neuron projection guidance
camera−type eye development
heart contraction
muscle cell development
epithelial cell apoptotic process
vascular transport
transport across blood−brain barrier
regulation of cell adhesion mediated by integrin
eye development
visual system development
axonogenesis
neuron recognition
synapse assembly
cell−cell adhesion via plasma−membrane adhesion molecules
regulation of synapse organization
nuclear division
organelle fission
chromosome segregation
mitotic nuclear division
nuclear chromosome segregation
mitotic sister chromatid segregation
trabecula morphogenesis
cyclic−nucleotide−mediated signaling
vascular process in circulatory system
positive regulation of MAPK cascade
negative regulation of neuron differentiation
regulation of neuron differentiation
negative regulation of glial cell differentiation
oligodendrocyte differentiation
regulation of body fluid levels
cell adhesion mediated by integrin
negative regulation of vascular permeability
developmental cell growth
regulation of synapse structure or activity
cranial nerve morphogenesis
regulation of synapse assembly
p.adjust
0.01
0.02
0.03
0.04
GeneRatio
0.1
0.2
0.3
cartilage (98)
e.osteoblast (65)
fusion.mes2 (97)
fusion.mes1 (96)
i.Osteoblast (97)
LMP (98)
MandibularArch (97)
MandibularArch.1 (97)
muscle.mes (98)
MyP.pLMP (100)
MyP.surface (97)
MyP.surface.1 (96)
MyP2 (98)
palatal.fusion (98)
palatal.fusion.1 (97)
palatal.fusion.2 (98)
palatal.fusion.3 (98)
palatal.fusion.4 (98)
palatalSheet (98)
palatalSheet.1 (98)
palatalSheet.2 (100)
palatalSheet.3 (98)
palatalSheet.4 (98)
pLMP2 (98)
Cluster
B
GO: Cellular Component
collagen−containing extracellular matrix
collagen trimer
endoplasmic reticulum lumen
complex of collagen trimers
fibrillar collagen trimer
synaptic membrane
postsynaptic membrane
basement membrane
postsynaptic specialization membrane
asymmetric synapse
symmetric synapse
postsynaptic density membrane
postsynaptic specialization
neuron to neuron synapse
adherens junction
I band
Z disc
sarcomere
myofibril
contractile fiber
sarcolemma
intercalated disc
apicolateral plasma membrane
cell−cell contact zone
glutamatergic synapse
platelet alpha granule membrane
haptoglobin−hemoglobin complex
hemoglobin complex
postsynaptic density
catenin complex
interstitial matrix
presynaptic membrane
condensed chromosome
chromosomal region
condensed chromosome, centromeric region
chromosome, centromeric region
spindle
kinetochore
outer kinetochore
parallel fiber to Purkinje cell synapse
monoatomic ion channel complex
serine−type peptidase complex
astrocyte projection
stress fiber
contractile actin filament bundle
actomyosin
nuclear matrix
nuclear periphery
axon initial segment
p.adjust
0.01
0.02
0.03
0.04
GeneRatio
0.05
0.10
0.15
0.20
0.25
cartilage (98)
e.osteoblast (65)
fusion.mes2 (97)
fusion.mes1 (96)
i.Osteoblast (97)
LMP (98)
MandibularArch (97)
muscle.mes (98)
MyP.pLMP (100)
MyP.surface (97)
MyP.surface.1 (96)
MyP2 (98)
palatal.fusion (98)
palatal.fusion.1 (97)
palatal.fusion.2 (98)
palatal.fusion.3 (98)
palatal.fusion.4 (98)
palatalSheet (98)
palatalSheet.1 (98)
palatalSheet.2 (100)
palatalSheet.3 (98)
palatalSheet.4 (98)
pLMP2 (98)
Cluster
C
GO: Molecular Function
extracellular matrix structural constituent
extracellular matrix structural constituent conferring tensile strength
glycosaminoglycan binding
extracellular matrix structural constituent conferring compression resistance
low−density lipoprotein particle binding
growth factor binding
heparin binding
transmembrane receptor protein tyrosine kinase activity
neurotransmitter receptor activity
integrin binding
transmitter−gated monoatomic ion channel activity involved in regulation of postsynaptic membrane potential
neurotransmitter receptor activity involved in regulation of postsynaptic membrane potential
transmitter−gated monoatomic ion channel activity involved in regulation of postsynaptic membrane potential
transmitter−gated channel activity
DNA−binding transcription repressor activity, RNA polymerase II−specific
DNA−binding transcription activator activity, RNA polymerase II−specific
DNA−binding transcription repressor activity
DNA−binding transcription activator activity
HMG box domain binding
RNA polymerase II−specific DNA−binding transcription factor binding
alpha−actinin binding
bHLH transcription factor binding
calcium channel activity
growth factor activity
haptoglobin binding
oxygen carrier activity
oxygen binding
myosin V binding
glutamate receptor activity
structural constituent of cytoskeleton
cyclin−dependent protein serine/threonine kinase regulator activity
actin monomer binding
cyclin−dependent protein serine/threonine kinase activator activity
DNA binding, bending
microtubule binding
tubulin binding
calcium ion transmembrane transporter activity
BMP binding
monoatomic ion channel activity
calcium:sodium antiporter activity
calcium:monoatomic cation antiporter activity
ATPase regulator activity
amino acid transmembrane transporter activity
amino acid:sodium symporter activity
carboxylic acid transmembrane transporter activity
beta−catenin binding
gated channel activity
microtubule motor activity
cytoskeletal motor activity
plus−end−directed microtubule motor activity
protein tyrosine kinase activator activity
transmembrane receptor protein tyrosine kinase activator activity
insulin receptor binding
phosphoric diester hydrolase activity
NADP+ nucleotidase activity
NAD+ nucleotidase, cyclic ADP−ribose generating
hydrolase activity, hydrolyzing N−glycosyl compounds
p.adjust
0.01
0.02
0.03
0.04
GeneRatio
0.05
0.10
0.15
0.20
cartilage (98)
e.osteoblast (65)
fusion.mes2 (97)
fusion.mes1 (96)
i.Osteoblast (97)
LMP (98)
MandibularArch (97)
MandibularArch.1 (97)
muscle.mes (98)
MyP.pLMP (100)
MyP.surface (97)
MyP.surface.1 (96)
MyP2 (98)
palatal.fusion (98)
palatal.fusion.1 (97)
palatal.fusion.2 (98)
palatal.fusion.3 (98)
palatal.fusion.4 (98)
palatalSheet (98)
palatalSheet.1 (98)
palatalSheet.2 (100)
palatalSheet.3 (98)
palatalSheet.4 (98)
pLMP2 (98)
Cluster
D
Reactome Pathway
Extracellular matrix organization
Collagen chain trimerization
ECM proteoglycans
Assembly of collagen fibrils and other multimeric structures
Collagen biosynthesis and modifying enzymes
Collagen formation
Collagen degradation
MET activates PTK2 signaling
MET promotes cell motility
Regulation of commissural axon pathfinding by SLIT and ROBO
Transcriptional regulation by RUNX2
Cardiogenesis
Crosslinking of collagen fibrils
Specification of the neural plate border
Gastrulation
Transcriptional regulation by the AP−2 (TFAP2) family of transcription factors
Transcriptional and post−translational regulation of MITF−M expression and activity
Negative regulation of activity of TFAP2 (AP−2) family transcription factors
Kidney development
Unblocking of NMDA receptors, glutamate binding and activation
Formation of the ureteric bud
Myogenesis
Mitotic Anaphase
Mitotic Metaphase and Anaphase
M Phase
Separation of Sister Chromatids
G2/M Transition
Resolution of Sister Chromatid Cohesion
RHO GTPases Activate Formins
Mitotic Spindle Checkpoint
Amplification of signal from the kinetochores
Amplification of signal from unattached kinetochores via a MAD2 inhibitory signal
Neurotransmitter receptors and postsynaptic signal transmission
Sodium/Calcium exchangers
Transcriptional regulation of brown and beige adipocyte differentiation
Transcriptional regulation of brown and beige adipocyte differentiation by EBF2
Laminin interactions
Scavenging by Class A Receptors
Tie2 Signaling
Nitric oxide stimulates guanylate cyclase
O−linked glycosylation
HS−GAG biosynthesis
Formation of the nephric duct
Activation of anterior HOX genes in hindbrain development during early embryogenesis
Activation of HOX genes during differentiation
IRS−related events triggered by IGF1R
IGF1R signaling cascade
Signaling by Type 1 Insulin−like Growth Factor 1 Receptor (IGF1R)
Receptor−type tyrosine−protein phosphatases
Protein−protein interactions at synapses
Role of second messengers in netrin−1 signaling
p.adjust
0.01
0.02
0.03
0.04
GeneRatio
0.1
0.2
0.3
cartilage (98)
e.osteoblast (72)
fusion.mes2 (98)
fusion.mes1 (55)
i.Osteoblast (63)
LMP (81)
MandibularArch (97)
muscle.mes (97)
MyP.pLMP (47)
MyP.surface (65)
MyP.surface.1 (54)
MyP2 (57)
palatal.fusion (98)
palatal.fusion.1 (59)
palatal.fusion.2 (59)
palatal.fusion.3 (59)
palatal.fusion.4 (59)
palatalSheet (98)
palatalSheet.1 (98)
palatalSheet.2 (59)
palatalSheet.3 (59)
palatalSheet.4 (69)
pLMP2 (59)
Cluster
E
KEGG Pathway
Protein digestion and absorption
Glycosaminoglycan biosynthesis − chondroitin sulfate / dermatan sulfate
Cytoskeleton in muscle cells
ECM−receptor interaction
PI3K−Akt signaling pathway
Human papillomavirus infection
Calcium signaling pathway
Focal adhesion
Malaria
Neuroactive ligand−receptor interaction
Hippo signaling pathway
TGF−beta signaling pathway
Signaling pathways regulating pluripotency of stem cells
Arrhythmogenic right ventricular cardiomyopathy
cAMP signaling pathway
Amphetamine addiction
MAPK signaling pathway
Insulin secretion
Hypertrophic cardiomyopathy
Wnt signaling pathway
Axon guidance
Dopaminergic synapse
Cell cycle
Salmonella infection
Oocyte meiosis
Motor proteins
Parkinson disease
AGE−RAGE signaling pathway in diabetic complications
Long−term depression
Glycosaminoglycan biosynthesis − heparan sulfate / heparin
Renin secretion
Neuroactive ligand signaling
cGMP−PKG signaling pathway
Basal cell carcinoma
Central carbon metabolism in cancer
Vascular smooth muscle contraction
p.adjust
0.01
0.02
0.03
0.04
GeneRatio
0.10
0.15
0.20
0.25
cartilage (53)
e.osteoblast (54)
fusion.mes2 (44)
fusion.mes1 (48)
i.Osteoblast (58)
MandibularArch (49)
MyP.pLMP (54)
MyP2 (46)
palatal.fusion (44)
palatal.fusion.3 (44)
palatal.fusion.4 (55)
palatalSheet (48)
palatalSheet.1 (44)
palatalSheet.2 (45)
palatalSheet.3 (42)
Cluster
F
DisGeNet
Chondrodysplasia
Spondyloepimetaphyseal disorder
Pseudochondroplasia
Osteochondrodysplasias
Disproportionate short stature
Skeletal dysplasia
Cleft palate, isolated
Craniofacial Abnormalities
Craniosynostosis
Thin rib
Flexion contracture of proximal interphalangeal joint
Amelia
Fibular hypoplasia
Prieto X−linked mental retardation syndrome
Polyhydramnios
Keloid
Increased susceptibility to fractures
Increased fracture rate
Osteogenesis imperfecta
Vital capacity
Stricture
Meningioma, benign, no ICD−O subtype
Adult Meningioma
Kallmann Syndrome
Anaplastic carcinoma
Intraocular pressure disorder
Deformity
Congenital heart disease
Keloid scar
Anorectal Malformations
Organic Mental Disorders, Substance−Induced
Prescription Drug Abuse
Drug Use Disorders
Substance−Related Disorders
Left ventricular noncompaction cardiomyopathy
Familial dilated cardiomyopathy
RESTING HEART RATE
Syncope
Reperfusion injury
Atrial septal defect
Osteogenesis imperfecta type IV (disorder)
Bone Diseases
Endometriosis
Frontonasal dysplasia
Prostate Cancer, Hereditary, 7
Nasal bridge wide
White forelock
Choriocarcinoma
Renal dysplasia
Short stature
Congenital Foot Deformities
Split foot
Cardiac Defects
RETINITIS PIGMENTOSA 1
Renal Cell Dysplasia
Epithelioma
Neoplasm Invasiveness
Serpus Tubal Intraepithelial Carcinoma
Mammary Neoplasms, Experimental
Cortical Dysplasia
tumour budding
Hypertrophy
Alcohol withdrawal syndrome
PARKINSON DISEASE, LATE−ONSET
Underdeveloped nasal alae
Uterine Anomalies
Abnormality of vision
tumor vasculature
Neural Tube Defects
Choroid Plexus Carcinoma
Mental Diseases
CADASIL Syndrome
Unspecified Juvenile Diabetes
Thyroid cyst
Corneal Neovascularization
Hydronephrosis
Autistic behavior
Eisenmenger Complex
Sertoli−Leydig Cell Tumor
End Stage Liver Disease
Gilles de la Tourette syndrome
Bronchopulmonary Dysplasia
Substance Use Disorders
Overgrowth
Sloping forehead
Breast Cancer, Familial
Primary microcephaly
Abnormal cortical bone morphology
Pervasive Development Disorder
Increased tendency to bruise
Beckwith−Wiedemann Syndrome
Russell−Silver syndrome
Prostatic Intraepithelial Neoplasias
p.adjust
0.01
0.02
0.03
0.04
GeneRatio
0.05
0.10
0.15
cartilage (98)
e.osteoblast (66)
fusion.mes2 (98)
fusion.mes1 (96)
i.Osteoblast (56)
LMP (98)
MandibularArch (98)
MandibularArch.1 (98)
muscle.mes (98)
MyP.pLMP (100)
MyP.surface (97)
MyP.surface.1 (96)
MyP2 (97)
palatal.fusion (98)
palatal.fusion.1 (98)
palatal.fusion.2 (97)
palatal.fusion.3 (98)
palatal.fusion.4 (98)
palatalSheet (98)
palatalSheet.1 (98)
palatalSheet.2 (97)
palatalSheet.3 (98)
palatalSheet.4 (97)
pLMP2 (98)
Cluster

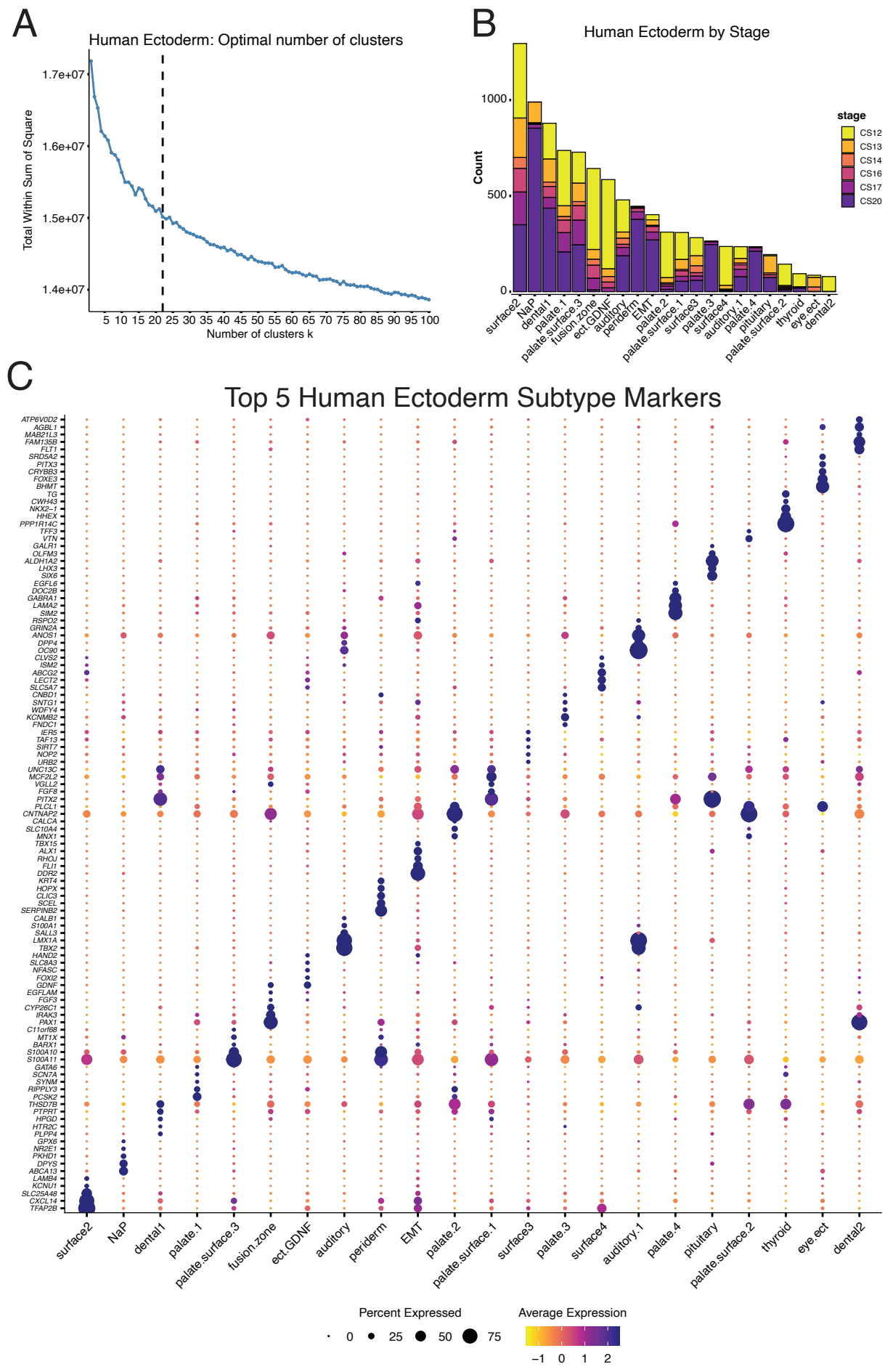
Supplementary Figure 25. Functional annotation enrichment for human mesenchymal subtypes using the top 100 marker genes.

A). Gene Ontology for Biological Processes. B). Gene Ontology for Cellular Components. C). Gene Ontology for Molecular Functions. D). Reactome Pathways. E). KEGG pathways. F). DisGeNet.


A
General Mesenchyme Markers
B
Mesenchyme Subtype Markers
C
Mesenchyme Subtype Module Scores
Slice1
Slice2
SATB2
TWIST1
BARX1
DLX5
PRRX1
FOXF1
EMX2
DMRTA2
cartilage
e.osteoblast
fusion.mes2
fusion.mes2.1
l.Osteoblast
LNP
MandibularArch
MandibularArch.1
muscle.mes
MxP.aLNP
MxP.surface
MxP.surface.1
MxP2
palatal.fusion
palatal.fusion.1
palatal.fusion.2
palatal.fusion.3
palatal.fusion.4
palatalShelf1
palatalShelf2
palatalShelf2.1
palatalShelf2.2
palatalShelf2.3
palatalShelf2.4
pLNP2

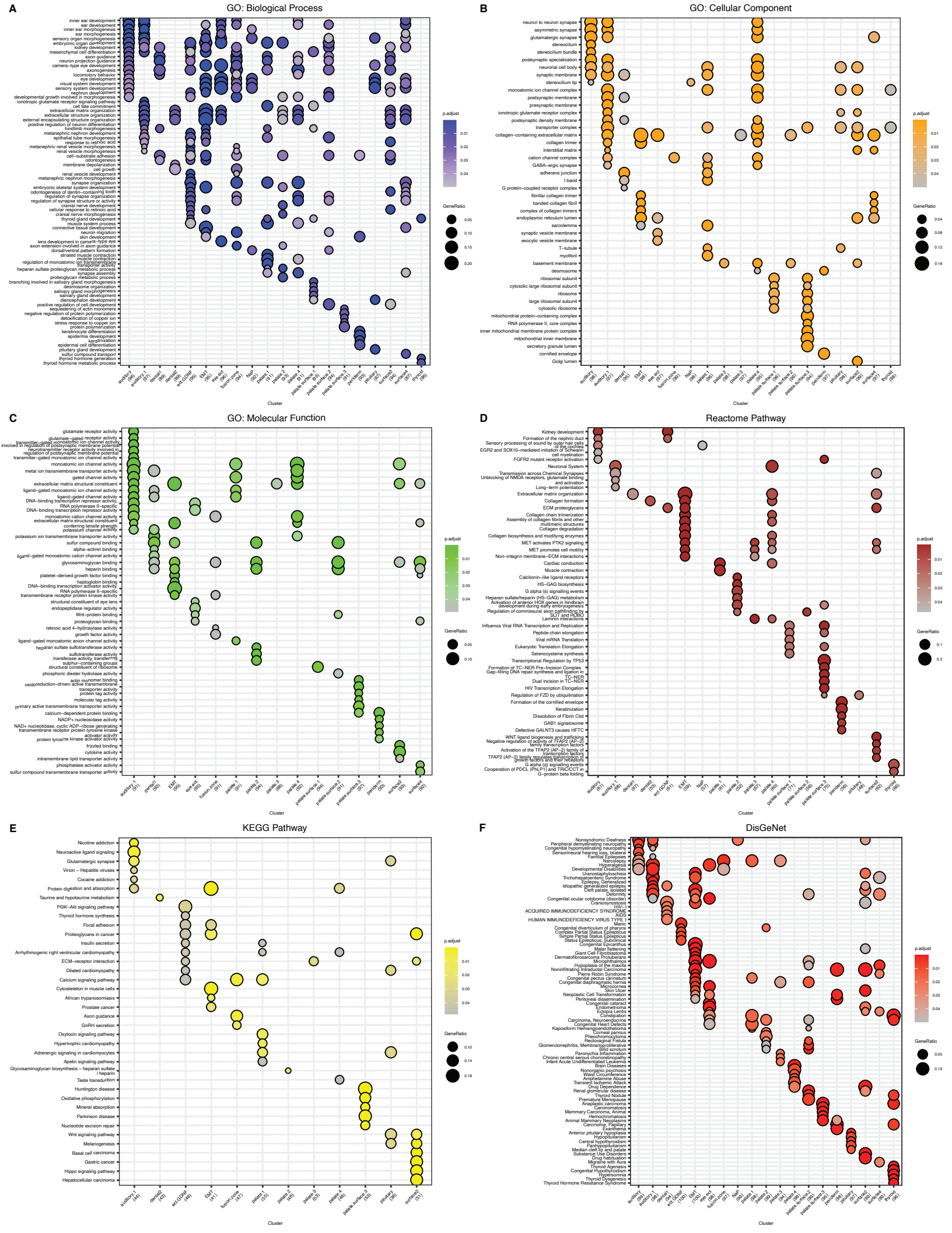
Supplementary Figure 26. Spatial feature plots of human mesenchymal genes and module scores from two sections of a human CS13 embryo[10].

A). General mesenchymal gene markers. B). Human mesenchymal subtype markers. C). Human mesenchymal subtype module scores.


A
Human Ectoderm: Optimal number of clusters
Total Within Sum of Square
1.7e+07
1.6e+07
1.5e+07
1.4e+07
5 10 15 20 25 30 35 40 45 50 55 60 65 70 75 80 85 90 95 100
Number of clusters k
B
Human Ectoderm by Stage
Count
1000
500
0
stage
CS12
CS13
CS14
CS16
CS17
CS20
surface2
NaP
dental1
palate.1
palate.surface.3
fusion.zone
ect.GDNF
auditory
periderm
EMT
palate.2
palate.surface.1
surface3
palate.3
surface4
auditory.1
palate.4
pituitary
palate.surface.2
thyroid
eye.ect
dental2
C
Top 5 Human Ectoderm Subtype Markers
ATP6V0D2
AGBL1
MAB21L3
FAM135B
FLT1
SRD5A2
PITX3
CRYBB3
FOXE3
BHMT
TG
CWH43
NKX2–1
HHEX
PPP1R14C
TFF3
VTN
GALR1
OLFM3
ALDH1A2
LHX3
SIX6
EGFL6
DOC2B
GABRA1
LAMA2
SIM2
RSPO2
GRIN2A
ANOS1
DPP4
OC90
CLVS2
ISM2
ABCG2
LECT2
SLC5A7
CNBD1
SNTG1
WDFY4
KCNMB2
FNDC1
IER5
TAF13
SIRT7
NOP2
URB2
UNC13C
MCF2L2
VGLL2
FGF8
PITX2
PLCL1
CNTNAP2
CALCA
SLC10A4
MNX1
TBX15
ALX1
RHOJ
FLI1
DDR2
KRT4
HOPX
CLIC3
SCEL
SERPINB2
CALB1
S100A1
SALL3
LMX1A
TBX2
HAND2
SLC8A3
NFASC
FOXI2
GDNF
EGFLAM
FGF3
CYP26C1
IRAK3
PAX1
C11orf68
MT1X
BARX1
S100A10
S100A11
GATA6
SCN7A
SYNM
RIPPLY3
PCSK2
THSD7B
PTPRT
HPGD
HTR2C
PLPP4
GPX6
NR2E1
PKHD1
DPYS
ABCA13
LAMB4
KCNU1
SLC25A48
CXCL14
TFAP2B
surface2
NaP
dental1
palate.1
palate.surface.3
fusion.zone
ect.GDNF
auditory
periderm
EMT
palate.2
palate.surface.1
surface3
palate.3
surface4
auditory.1
palate.4
pituitary
palate.surface.2
thyroid
eye.ect
dental2
Percent Expressed
0
25
50
75
Average Expression
–1
0
1
2

Supplementary Figure 27. Characterizing human ectodermal subtypes.

A). Elbow plot with optimal number of subclusters for human ectoderm. B). Number of cells obtained at each CS stage for each human ectodermal subtype. C). Average and percent expression of the top 5 DEGs for the human ectodermal subtypes.


A
GO: Biological Process
inner ear development
ear development
inner ear morphogenesis
ear morphogenesis
sensory organ morphogenesis
embryonic organ development
kidney development
mesenchymal cell differentiation
axon guidance
neuron projection guidance
camera-type eye development
axonogenesis
locomotory behavior
eye development
visual system development
sensory system development
nephron development
developmental growth involved in morphogenesis
ionotropic glutamate receptor signaling pathway
cell fate commitment
extracellular matrix organization
extracellular structure organization
external encapsulating structure organization
positive regulation of neuron differentiation
hindlimb morphogenesis
metanephric nephron development
epithelial tube morphogenesis
response to retinoic acid
metanephric renal vesicle morphogenesis
renal vesicle morphogenesis
cell-substrate adhesion
odontogenesis
membrane depolarization
cell growth
renal vesicle development
metanephric nephron morphogenesis
synapse organization
embryonic skeletal system development
odontogenesis of dentin-containing tooth
regulation of synapse organization
regulation of synapse structure or activity
cranial nerve development
cellular response to retinoic acid
cranial nerve morphogenesis
thyroid gland development
muscle system process
connective tissue development
neuron migration
skin development
lens development in camera-type eye
axon extension involved in axon guidance
dorsal/ventral pattern formation
striated muscle contraction
muscle contraction
regulation of monoatomic ion transmembrane
heparan sulfate proteoglycan metabolic process
synapse assembly
proteoglycan metabolic process
branching involved in salivary gland morphogenesis
desmosome organization
salivary gland morphogenesis
salivary gland development
diencephalon development
positive regulation of cell development
sequestering of actin monomers
negative regulation of protein polymerization
detoxification of copper ion
stress response to copper ion
protein polymerization
keratinocyte differentiation
epidermis development
keratinization
epidermal cell differentiation
pituitary gland development
sulfur compound transport
thyroid hormone generation
thyroid hormone metabolic process
auditory 1 (56)
auditory 2 (57)
dental1 (89)
dental2 (88)
ect.GDNF (99)
EMT (95)
eye ect (96)
fusion zone (94)
NaP (92)
palate 1 (91)
palate 2 (93)
palate 3 (90)
palate 4 (91)
palate surface 1 (95)
palate surface 2 (94)
palate surface 3 (91)
periderm (93)
pituitary (87)
surface2 (96)
surface4 (87)
thyroid (96)
Cluster
p.adjust
0.01
0.02
0.03
0.04
GeneRatio
0.05
0.10
0.15
0.20
B
GO: Cellular Component
neuron to neuron synapse
asymmetric synapse
glutamatergic synapse
stereocilium
stereocilium bundle
postsynaptic specialization
neuronal cell body
synaptic membrane
stereocilium tip
monoatomic ion channel complex
postsynaptic membrane
presynaptic membrane
ionotropic glutamate receptor complex
postsynaptic density membrane
transporter complex
collagen-containing extracellular matrix
collagen trimer
interstitial matrix
cation channel complex
GABA-ergic synapse
adherens junction
I band
G protein-coupled receptor complex
fibrillar collagen trimer
banded collagen fibril
complex of collagen trimers
endoplasmic reticulum lumen
sarcolemma
synaptic vesicle membrane
exocytic vesicle membrane
T-tubule
myofibril
basement membrane
desmosome
ribosomal subunit
cytosolic large ribosomal subunit
ribosome
large ribosomal subunit
cytosolic ribosome
mitochondrial protein-containing complex
RNA polymerase II, core complex
inner mitochondrial membrane protein complex
mitochondrial inner membrane
secretory granule lumen
cornified envelope
Golgi lumen
auditory (98)
auditory 1 (97)
dental1 (95)
dental2 (95)
EMT (98)
eye ect (97)
fusion zone (99)
NaP (98)
palate 1 (96)
palate 2 (98)
palate 3 (97)
palate 4 (95)
palate surface 1 (96)
palate surface 2 (96)
palate surface 3 (96)
periderm (97)
pituitary (98)
surface2 (96)
surface4 (97)
thyroid (98)
Cluster
p.adjust
0.01
0.02
0.03
0.04
GeneRatio
0.04
0.08
0.12
0.16
C
GO: Molecular Function
glutamate receptor activity
glutamate-gated receptor activity
transmitter-gated monoatomic ion channel activity involved in regulation of postsynaptic membrane potential
neurotransmitter receptor activity involved in regulation of postsynaptic membrane potential
transmitter-gated monoatomic ion channel activity
monoatomic ion channel activity
metal ion transmembrane transporter activity
gated channel activity
extracellular matrix structural constituent
ligand-gated monoatomic ion channel activity
ligand-gated channel activity
DNA-binding transcription repressor activity, RNA polymerase II-specific
DNA-binding transcription repressor activity
monoatomic cation channel activity
extracellular matrix structural constituent conferring tensile strength
potassium channel activity
potassium ion transmembrane transporter activity
sulfur compound binding
ligand-gated monoatomic cation channel activity
alpha-actinin binding
glycosaminoglycan binding
heparin binding
platelet-derived growth factor binding
haptoglobin binding
DNA-binding transcription activator activity, RNA polymerase II-specific
transmembrane receptor protein kinase activity
structural constituent of eye lens
endopeptidase regulator activity
Wnt-protein binding
proteoglycan binding
retinoic acid 4-hydroxylase activity
growth factor activity
ligand-gated monoatomic anion channel activity
heparan sulfate sulfotransferase activity
sulfotransferase activity
transferase activity, transferring sulphur-containing groups
structural constituent of ribosome
phosphoric diester hydrolase activity
actin monomer binding
oxidoreduction-driven active transmembrane transporter activity
protein tag activity
molecular tag activity
primary active transmembrane transporter activity
calcium-dependent protein binding
NADP+ nucleosidase activity
NAD+ nucleotidase, cyclic ADP-ribose generating
transmembrane receptor protein tyrosine kinase activator activity
protein tyrosine kinase activator activity
frizzled binding
cytokine activity
intramembrane lipid transporter activity
phosphatase activator activity
sulfur compound transmembrane transporter activity
auditory 1 (91)
dental1 (82)
EMT (93)
eye ect (95)
fusion zone (91)
palate 1 (91)
palate 2 (94)
palate 3 (88)
palate 4 (92)
palate surface 1 (94)
palate surface 2 (91)
palate surface 3 (97)
periderm (93)
surface2 (93)
surface4 (92)
Cluster
p.adjust
0.01
0.02
0.03
0.04
GeneRatio
0.05
0.10
D
Reactome Pathway
Kidney development
Formation of the nephric duct
Sensory processing of sound by outer hair cells of the cochlea
EGR2 and SOX10-mediated initiation of Schwann cell myelination
FGFR2 mutant receptor activation
Neuronal System
Transmission across Chemical Synapses
Unblocking of NMDA receptors, glutamate binding and activation
Long-term potentiation
Extracellular matrix organization
Collagen formation
ECM proteoglycans
Collagen chain trimerization
Assembly of collagen fibrils and other multimeric structures
Collagen degradation
Collagen biosynthesis and modifying enzymes
MET activates PTK2 signaling
MET promotes cell motility
Non-integrin membrane-ECM interactions
Cardiac conduction
Muscle contraction
Calcitonin-like ligand receptors
HS-GAG biosynthesis
G alpha (s) signalling events
Heparan sulfate/heparin (HS-GAG) metabolism
Activation of anterior HOX genes in hindbrain development during early embryogenesis
Regulation of commissural axon pathfinding by SLIT and ROBO
Laminin interactions
Influenza Viral RNA Transcription and Replication
Peptide chain elongation
Viral mRNA Translation
Eukaryotic Translation Elongation
Selenocysteine synthesis
Transcriptional Regulation by TP53
Formation of TC-NER Pre-Incision Complex
Gap-filling DNA repair synthesis and ligation in TC-NER
Dual incision in TC-NER
HIV Transcription Elongation
Regulation of FZD by ubiquitination
Formation of the cornified envelope
Keratinization
Dissolution of Fibrin Clot
GAB1 signalosome
Defective GALNT3 causes HFTC
WNT ligand biogenesis and trafficking
Negative regulation of activity of TFAP2 (AP-2) family transcription factors
Activation of the TFAP2 (AP-2) family of transcription factors
TFAP2 (AP-2) family regulates transcription of growth factors and their receptors
G alpha (q) signalling events
Cooperation of PDCL (PhLP1) and TRiC/CCT in G-protein beta folding
auditory (61)
auditory 1 (68)
dental1 (67)
dental2 (53)
ect.GDNF (61)
EMT (59)
NaP (57)
palate 1 (61)
palate 2 (52)
palate 3 (67)
palate 4 (60)
palate surface 1 (71)
palate surface 2 (56)
palate surface 3 (75)
periderm (56)
pituitary (48)
surface2 (63)
thyroid (66)
Cluster
p.adjust
0.01
0.02
0.03
0.04
GeneRatio
0.1
0.2
E
KEGG Pathway
Nicotine addiction
Neuroactive ligand signaling
Glutamatergic synapse
Virion - Hepatitis viruses
Cocaine addiction
Protein digestion and absorption
Taurine and hypotaurine metabolism
PI3K-Akt signaling pathway
Thyroid hormone synthesis
Focal adhesion
Proteoglycans in cancer
Insulin secretion
Arrhythmogenic right ventricular cardiomyopathy
ECM-receptor interaction
Dilated cardiomyopathy
Calcium signaling pathway
Cytoskeleton in muscle cells
African trypanosomiasis
Prostate cancer
Axon guidance
GnRH secretion
Oxytocin signaling pathway
Hypertrophic cardiomyopathy
Adrenergic signaling in cardiomyocytes
Apelin signaling pathway
Glycosaminoglycan biosynthesis - heparan sulfate / heparin
Taste transduction
Huntington disease
Oxidative phosphorylation
Mineral absorption
Parkinson disease
Nucleotide excision repair
Wnt signaling pathway
Melanogenesis
Basal cell carcinoma
Gastric cancer
Hippo signaling pathway
Hepatocellular carcinoma
auditory 1 (44)
dental2 (45)
ect.GDNF (49)
EMT (61)
fusion zone (47)
palate 1 (55)
palate 2 (46)
palate 3 (53)
palate 4 (46)
palate surface 3 (55)
pituitary (56)
surface2 (51)
Cluster
p.adjust
0.01
0.02
0.03
0.04
GeneRatio
0.10
0.14
0.18
F
DisGeNet
Nonsyndromic Deafness
Peripheral demyelinating neuropathy
Congenital hypomyelinating neuropathy
Sensorineural hearing loss, bilateral
Familial Epilepsies
Narcolepsy
Hyperalgesia
Developmental Disabilities
Uranostaphyloschisis
Trichohepatoenteric Syndrome
Epilepsy, Generalized
Idiopathic generalized epilepsy
Cleft palate, isolated
Deformity
Congenital ocular coloboma (disorder)
Craniosynostosis
Cleft Lip
ACQUIRED IMMUNODEFICIENCY SYNDROME
AIDS
HUMAN IMMUNODEFICIENCY VIRUS TYPE 1
Manic
Congenital diverticulum of pharynx
Complex Partial Status Epilepticus
Simple Partial Status Epilepticus
Status Epilepticus, Subclinical
Congenital Epicanthus
Malar flattening
Giant Cell Fibroblastoma
Dermatofibrosarcoma Protuberans
Microphthalmos
Hypoplasia of the maxilla
Noninfiltrating Intraductal Carcinoma
Pierre Robin Syndrome
Congenital pectus carinatum
Congenital diaphragmatic hernia
Microcornea
Skin Ulcer
Neoplastic Cell Transformation
Peritoneal dissemination
Congenital cataract
Endometrioma
Ectopia Lentis
Constipation
Carcinoma, Neuroendocrine
Congenital Heart Defects
Kaposiform Hemangioendothelioma
Corneal pannus
Pheochromocytoma
Rectovaginal Fistula
Glomerulonephritis, Membranoproliferative
Bifid scrotum
Paronychia Inflammation
Chronic central serous chorioretinopathy
Infant Acute Undifferentiated Leukemia
Brain Diseases
Nonorganic psychosis
Waist Circumference
Amphetamine Abuse
Transient Ischemic Attack
Drug Dependence
Renal glomerular disease
Thyroid Nodule
Premature Menopause
Anaplastic carcinoma
Carcinomatosis
Mammary Carcinoma, Animal
Hemochromatosis
Animal Mammary Neoplasms
Carcinoma, Papillary
Exanthema
Anterior pituitary hypoplasia
Hypopituitarism
Central hypothyroidism
Panhypopituitarism
Median cleft lip and palate
Substance Use Disorders
Drug habituation
Migraine with Aura
Thyroid Agenesis
Congenital Hypothyroidism
Hypersomnia
Thyroid Dysgenesis
Thyroid Hormone Resistance Syndrome
auditory (90)
auditory 1 (86)
dental1 (84)
dental2 (84)
ect.GDNF (100)
EMT (100)
eye ect (96)
fusion zone (97)
NaP (96)
palate 1 (96)
palate 2 (96)
palate 3 (96)
palate 4 (96)
palate surface 2 (96)
palate surface 3 (96)
periderm (98)
pituitary (97)
surface2 (96)
surface4 (97)
thyroid (98)
Cluster
p.adjust
0.01
0.02
0.03
0.04
GeneRatio
0.05
0.10

Supplementary Figure 28. Functional annotation enrichment for human ectodermal subtypes using the top 100 marker genes.

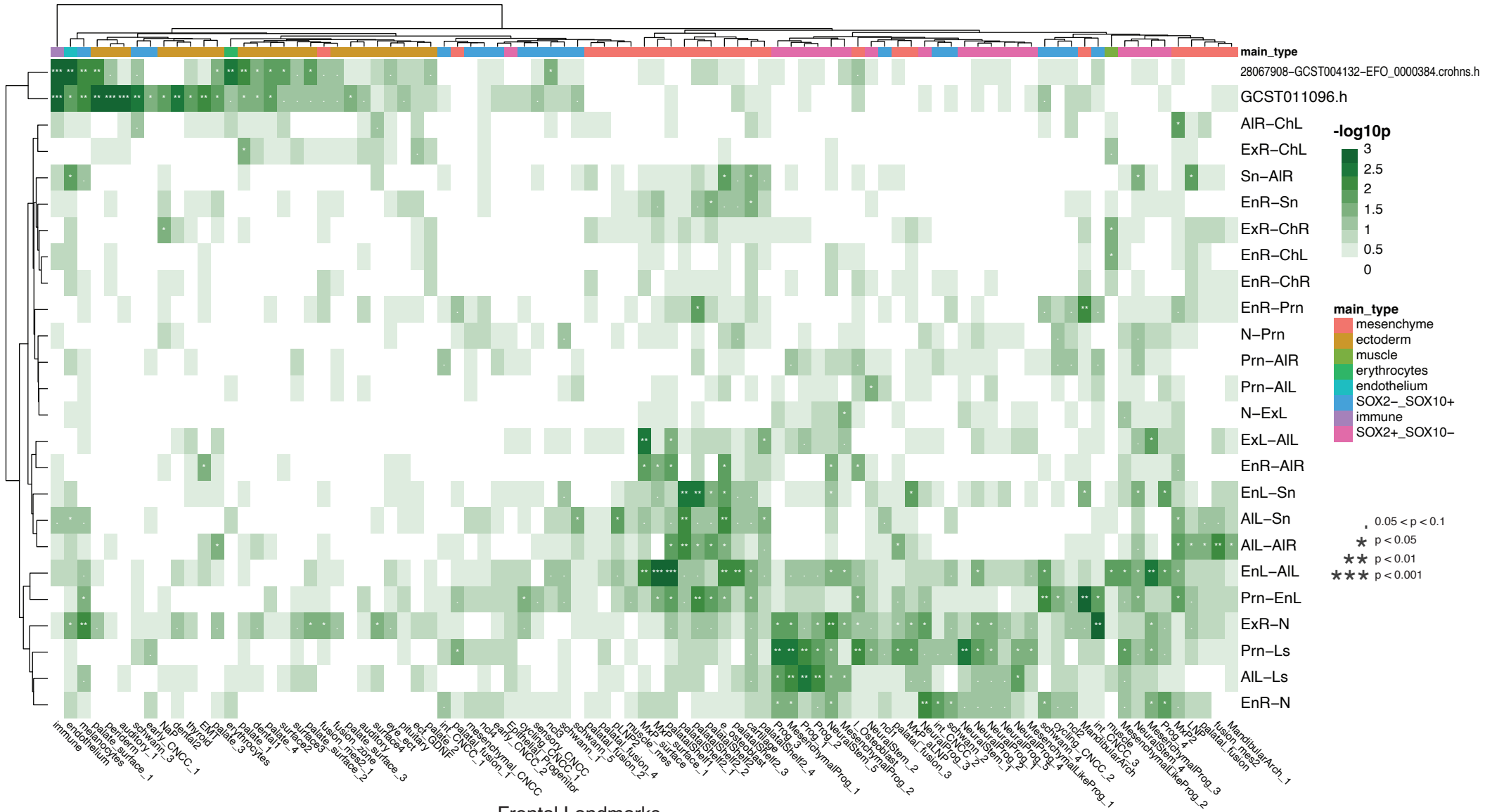
A). Gene Ontology for Biological Processes. B). Gene Ontology for Cellular Components. C). Gene Ontology for Molecular Functions. D). Reactome Pathways. E). KEGG pathways. F). DisGeNet.


A
General Ectoderm Markers
Slice1
Slice2
TFAP2A
GRHL2
ESRP1
KLF5
B
Ectoderm Subtype Markers
SIX2
NR2E1
SIX6
NKX2−1
C
Ectoderm Subtype Module Scores
auditory
auditory.1
dental1
dental2
ect.GDNF
EMT
eye.ect
fusion.zone
NaP
palate.1
palate.2
palate.3
palate.4
palate.surface.1
palate.surface.2
palate.surface.3
palate.surface.4
periderm
pituitary
surface2
surface3
surface4
thyroid

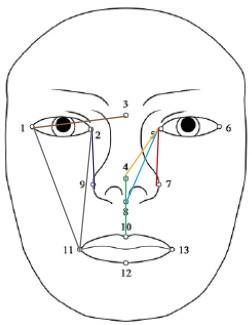
Supplementary Figure 29. Spatial feature plots of human ectodermal genes and module scores from two sections of a human CS13 embryo[10].

A). General ectodermal gene markers. B). Human ectodermal subtype markers. C). Human ectodermal subtype module scores.

Craniofacial Variation

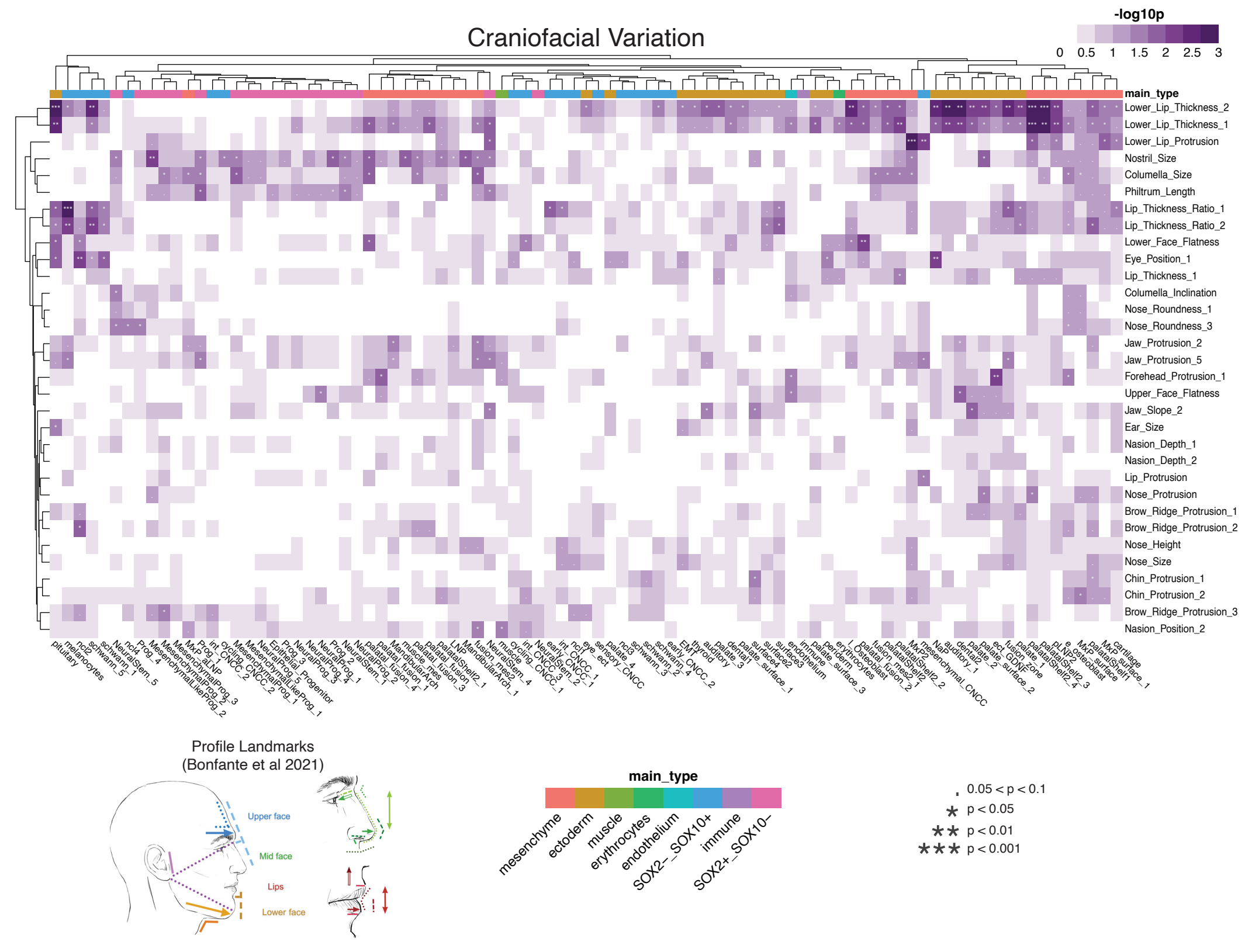


Frontal Landmarks
(Xiong et al 2019)

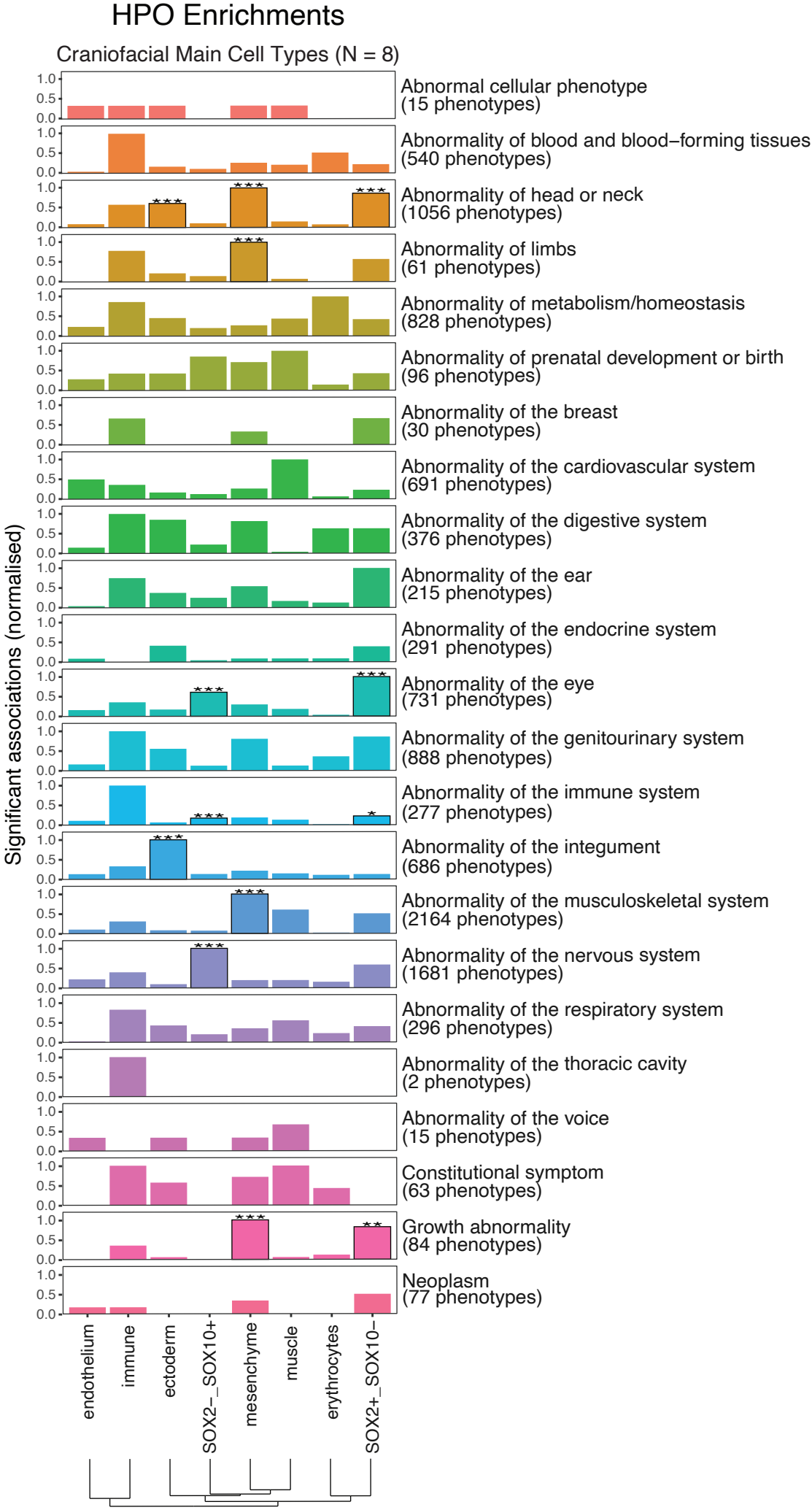


No	Abbreviation	Name
1	ExR	Right Exocanthion
2	EnR	Right Endocanthion
3	N	Nasion
4	Prn	Pronasale
5	EnL	Left Endocanthion
6	ExL	Left Exocanthion
7	AlL	Left Alare
8	Sn	Subnasale
9	AlR	Right Alare
10	Ls	Labliale superius
11	ChR	Right Cheilion
12	Li	Labiale inferius
13	ChL	Left Cheilion

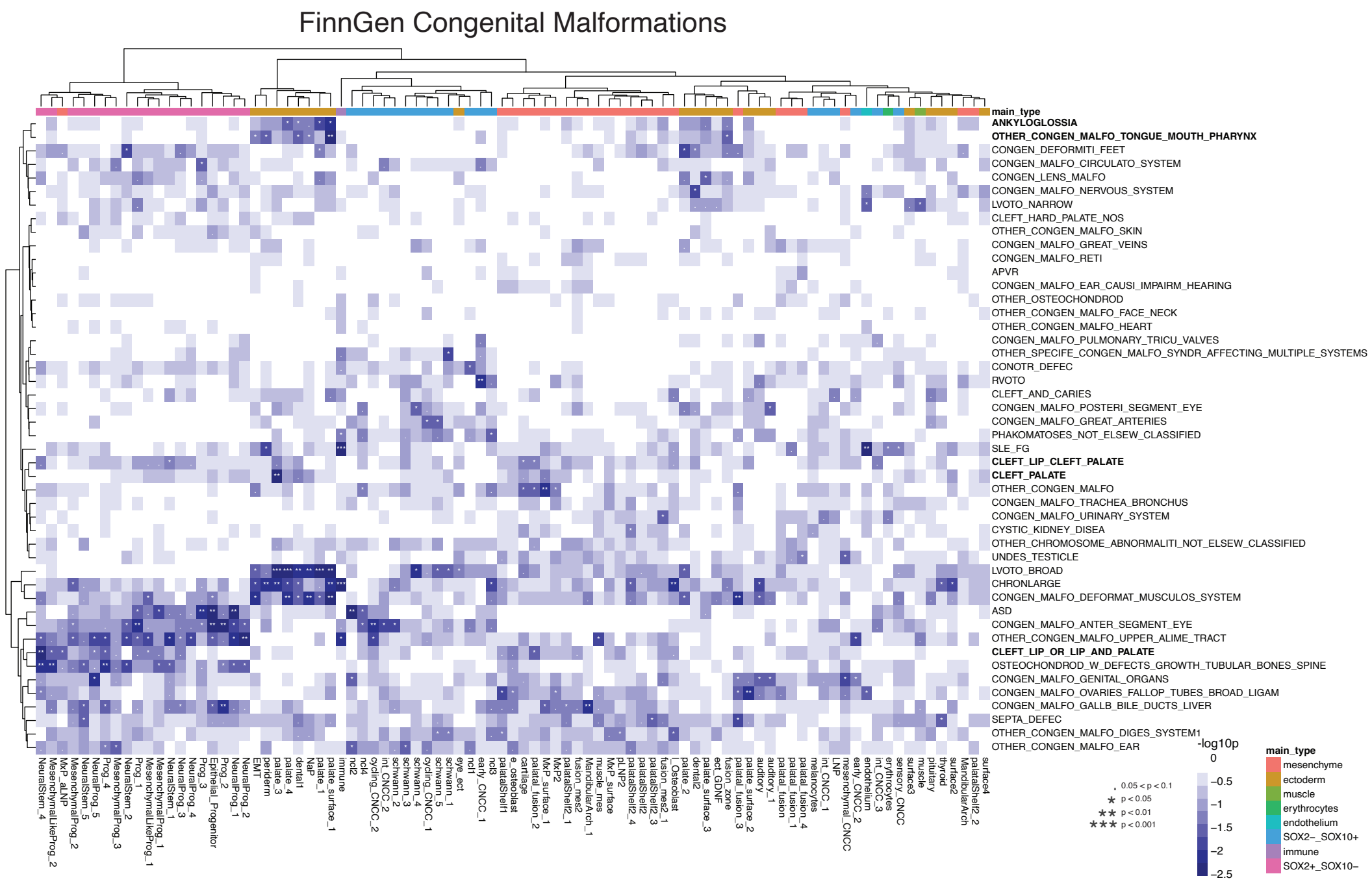
Supplementary Figure 30. Clustered heatmap of significance values calculated by MAGMA.Celltyping[15] for all frontal landmark facial variation traits[16] and cell subtypes. Crohn's (28067908–GCST004132–EFO_0000384.crohns.h) and Systemic Lupus Erythematosus (GCST011096.h) traits were also included as controls. Colors along top of heatmap indicate main cell type classification. Facial trait measures were obtained from Xiong et al 2019 and combinatorial code is indicated in coded legend (e.g., EnL-AIL indicates landmark segment 5 to 7). Levels of significance indicated by asterisks or period according to figure.


Craniofacial Variation
-log10p
0 0.5 1 1.5 2 2.5 3
main_type
Lower_Lip_Thickness_2
Lower_Lip_Thickness_1
Lower_Lip_Protrusion
Nostril_Size
Columella_Size
Philtrum_Length
Lip_Thickness_Ratio_1
Lip_Thickness_Ratio_2
Lower_Face_Flatness
Eye_Position_1
Lip_Thickness_1
Columella_Inclination
Nose_Roundness_1
Nose_Roundness_3
Jaw_Protrusion_2
Jaw_Protrusion_5
Forehead_Protrusion_1
Upper_Face_Flatness
Jaw_Slope_2
Ear_Size
Nasion_Depth_1
Nasion_Depth_2
Lip_Protrusion
Nose_Protrusion
Brow_Ridge_Protrusion_1
Brow_Ridge_Protrusion_2
Nose_Height
Nose_Size
Chin_Protrusion_1
Chin_Protrusion_2
Brow_Ridge_Protrusion_3
Nasion_Position_2
pituitary
melanocytes
ncl2
schwann_1
schwann_5
NeuralStem_5
ncl4
Prog_4
MesenchymalProg_3
MesenchymalLikeProg_2
MxP_aLNP
Prog_1
int_cycling_CNCC_2
cycling_CNCC_2
MesenchymalProg_2
MesenchymalProg_1
NeuralProg_5
Epithelial_Progenitor
Prog_3
NeuralProg_3
NeuralProg_4
Prog_2
NeuralProg_1
NeuralStem_1
palatal_fusion_2
palatal_fusion_4
MandibularArch_1
muscle_mes
palatal_fusion_1
palatal_fusion_3
LNP
palatalShelf2_1
MandibularArch_1
fusion_mes2
NeuralStem_4
muscle_2
cycling_CNCC_1
int_CNCC_3
NeuralStem_2
early_CNCC_1
int_CNCC_1
eye_ect
sensory_CNCC
palate_4
ncl3
schwann_3
schwann_2
schwann_4
EMT_CNCC_2
thyroid
auditory_3
dental1
palate_surface_1
surface4
surface2
surface3
endothelium
immune
periderm
palate_surface_3
erythrocytes
Osteoblast
palatal_fusion_2
fusion_mes1
palatalShelf2_1
MxP2
palatalShelf2_2
mesenchymal_CNCC
NaP
auditory_1
dental2
palate_2
palate_surface_2
ect_GDNF_zone
fusion_zone
palate_1
palatalShelf2_3
pLNP2
palatalShelf2_4
e_osteoblast
MxP_surface
palatalShelf1
MxP_surface_1
cartilage
Profile Landmarks
(Bonfante et al 2021)
Upper face
Mid face
Lips
Lower face
main_type
mesenchyme
ectoderm
muscle
erythrocytes
endothelium
SOX2−_SOX10+
immune
SOX2+_SOX10−
. 0.05 < p < 0.1
* p < 0.05
** p < 0.01
*** p < 0.001

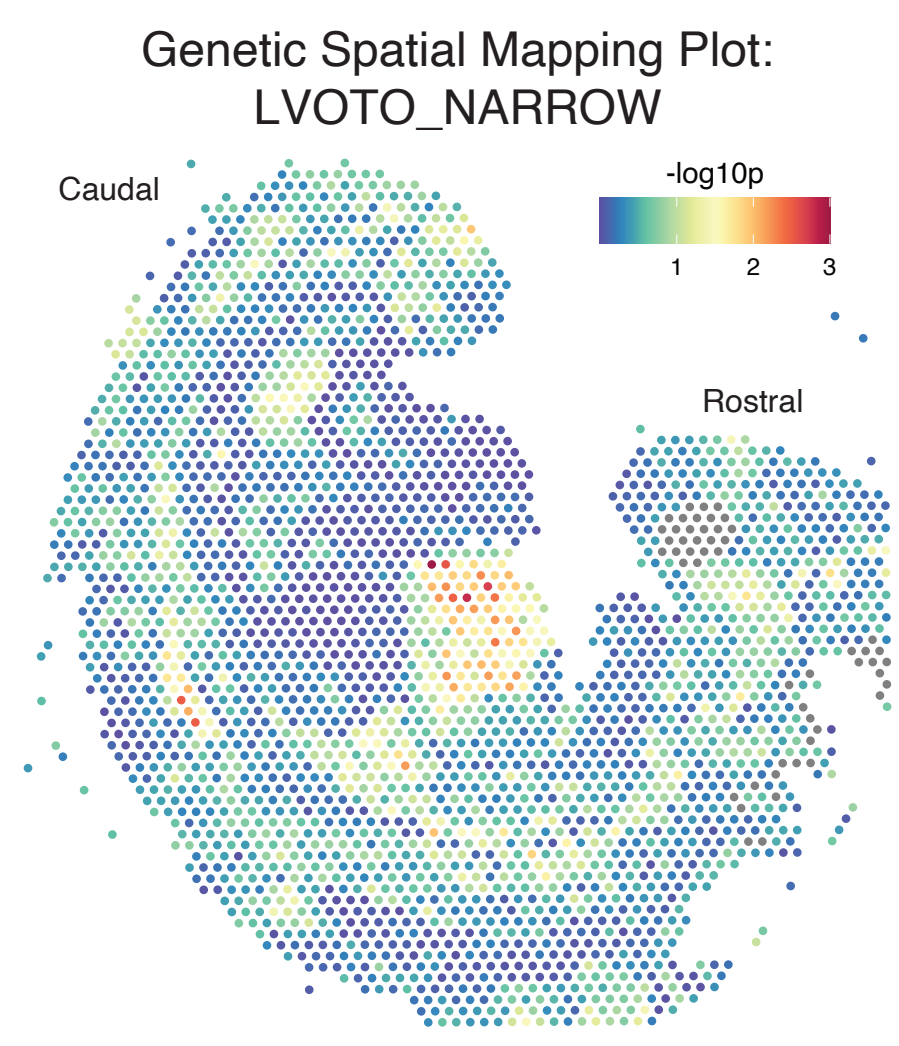
Supplementary Figure 31. Clustered heatmap of significance values calculated by MAGMA.Celltyping[15] for all profile landmark facial variation traits[78] and cell subtypes. Colors along top of heatmap indicate main cell type classification. Facial trait measures were obtained from Bonfante et al 2021 and the facial regions measured are shown in the legend. Levels of significance indicated by asterisks or period according to figure.

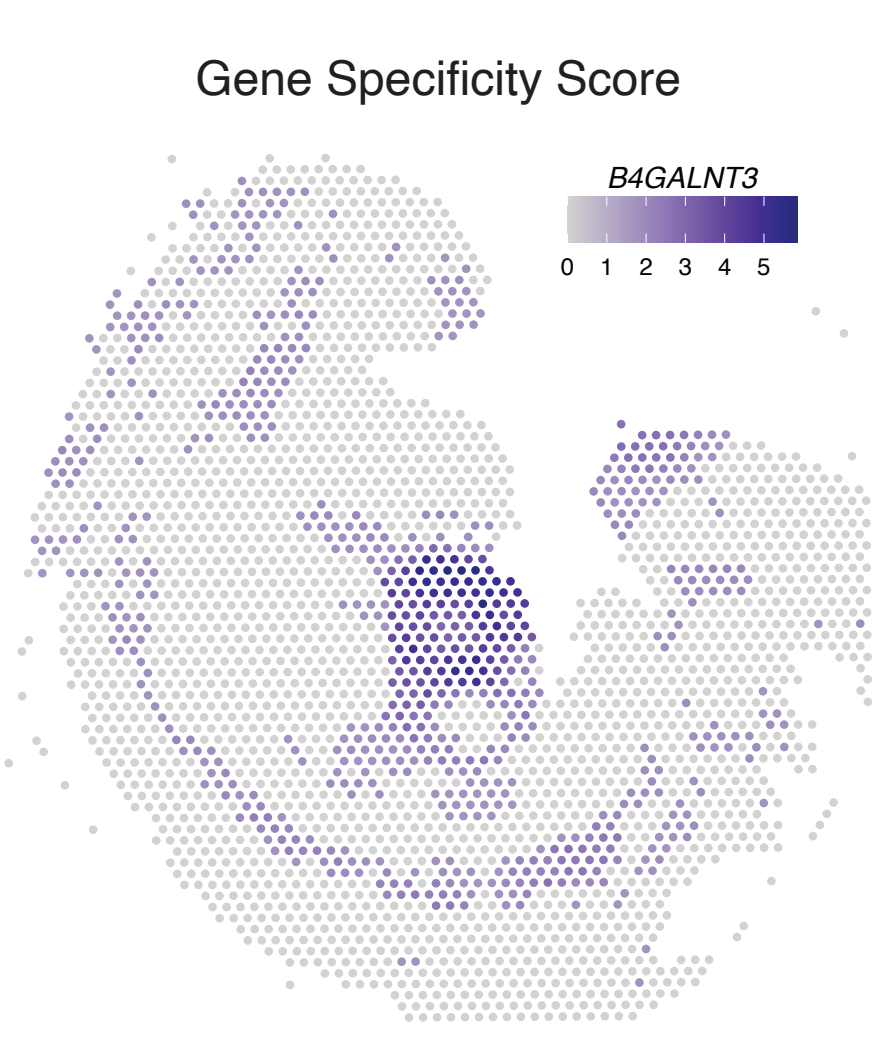

HPO Enrichments
Craniofacial Main Cell Types (N = 8)
Significant associations (normalised)
Abnormal cellular phenotype (15 phenotypes)
Abnormality of blood and blood−forming tissues (540 phenotypes)
Abnormality of head or neck (1056 phenotypes)
Abnormality of limbs (61 phenotypes)
Abnormality of metabolism/homeostasis (828 phenotypes)
Abnormality of prenatal development or birth (96 phenotypes)
Abnormality of the breast (30 phenotypes)
Abnormality of the cardiovascular system (691 phenotypes)
Abnormality of the digestive system (376 phenotypes)
Abnormality of the ear (215 phenotypes)
Abnormality of the endocrine system (291 phenotypes)
Abnormality of the eye (731 phenotypes)
Abnormality of the genitourinary system (888 phenotypes)
Abnormality of the immune system (277 phenotypes)
Abnormality of the integument (686 phenotypes)
Abnormality of the musculoskeletal system (2164 phenotypes)
Abnormality of the nervous system (1681 phenotypes)
Abnormality of the respiratory system (296 phenotypes)
Abnormality of the thoracic cavity (2 phenotypes)
Abnormality of the voice (15 phenotypes)
Constitutional symptom (63 phenotypes)
Growth abnormality (84 phenotypes)
Neoplasm (77 phenotypes)
endothelium
immune
ectoderm
SOX2−_SOX10+
mesenchyme
muscle
erythrocytes
SOX2+_SOX10−

Supplementary Figure 32. Bar plot showing number of enriched human phenotypes (max-normalized from 0-1 within each branch) for main cell types as calculated by MSTExplorer::run_phenomix. Significance of the proportion tests, testing for disproportionate numbers of phenotype enrichments for a given cell type within a given HPO branch, is denoted with asterisks (FDR<0.001=***, FDR<0.01=**, FDR<0.05=*).


FinnGen Congenital Malformations
main_type
ANKYLOGLOSSIA
OTHER_CONGEN_MALFO_TONGUE_MOUTH_PHARYNX
CONGEN_DEFORMITI_FEET
CONGEN_MALFO_CIRCULATO_SYSTEM
CONGEN_LENS_MALFO
CONGEN_MALFO_NERVOUS_SYSTEM
LVOTO_NARROW
CLEFT_HARD_PALATE_NOS
OTHER_CONGEN_MALFO_SKIN
CONGEN_MALFO_GREAT_VEINS
CONGEN_MALFO_RETI
APVR
CONGEN_MALFO_EAR_CAUSI_IMPAIRM_HEARING
OTHER_OSTEOCHONDROD
OTHER_CONGEN_MALFO_FACE_NECK
OTHER_CONGEN_MALFO_HEART
CONGEN_MALFO_PULMONARY_TRICU_VALVES
OTHER_SPECIFE_CONGEN_MALFO_SYNDR_AFFECTING_MULTIPLE_SYSTEMS
CONOTR_DEFEC
RVOTO
CLEFT_AND_CARIES
CONGEN_MALFO_POSTERI_SEGMENT_EYE
CONGEN_MALFO_GREAT_ARTERIES
PHAKOMATOSES_NOT_ELSEW_CLASSIFIED
SLE_FG
CLEFT_LIP_CLEFT_PALATE
CLEFT_PALATE
OTHER_CONGEN_MALFO
CONGEN_MALFO_TRACHEA_BRONCHUS
CONGEN_MALFO_URINARY_SYSTEM
CYSTIC_KIDNEY_DISEA
OTHER_CHROMOSOME_ABNORMALITI_NOT_ELSEW_CLASSIFIED
UNDES_TESTICLE
LVOTO_BROAD
CHRONLARGE
CONGEN_MALFO_DEFORMAT_MUSCULOS_SYSTEM
ASD
CONGEN_MALFO_ANTER_SEGMENT_EYE
OTHER_CONGEN_MALFO_UPPER_ALIME_TRACT
CLEFT_LIP_OR_LIP_AND_PALATE
OSTEOCHONDROD_W_DEFECTS_GROWTH_TUBULAR_BONES_SPINE
CONGEN_MALFO_GENITAL_ORGANS
CONGEN_MALFO_OVARIES_FALLOP_TUBES_BROAD_LIGAM
CONGEN_MALFO_GALLB_BILE_DUCTS_LIVER
SEPTA_DEFEC
OTHER_CONGEN_MALFO_DIGES_SYSTEM1
OTHER_CONGEN_MALFO_EAR
NeuralStem_4
MesenchymalLikeProg_2
MxP_aLNP
MesenchymalProg_2
NeuralStem_5
NeuralProg_5
Prog_4
MesenchymalProg_3
NeuralStem_2
Prog_1
MesenchymalLikeProg_1
MesenchymalProg_1
NeuralStem_1
NeuralProg_3
Prog_3
Epithelial_Progenitor
Prog_2
NeuralProg_1
NeuralProg_2
EMT
periderm
palate_3
palate_4
dental1
NaP
palate_1
palate_surface_1
immune
ncl2
ncl4
cycling_CNCC_2
int_CNCC_2
schwann_2
schwann_3
schwann_4
cycling_CNCC_1
schwann_5
schwann_1
eye_ect
ncl1
early_CNCC_1
ncl3
palatalShelf1
e_osteoblast
cartilage
palatal_fusion_2
MxP_surface_1
MxP2
palatalShelf2_1
fusion_mes2
MandibularArch_1
muscle_mes
MxP_surface
pLNP2
palatalShelf2_4
palatalShelf2
palatalShelf2_3
fusion_mes2_1
l_Osteoblast
palate_2
dental2
palate_surface_3
ect_GDNF
fusion_zone
palatal_fusion_3
palate_surface_2
auditory
auditory_1
palatal_fusion
palatal_fusion_1
palatal_fusion_4
melanocytes
int_CNCC_1
LNP
mesenchymal_CNCC
early_CNCC_2
endothelium
int_CNCC_3
erythrocytes
sensory_CNCC
surface3
muscle
pituitary
thyroid
surface2
MandibularArch
palatalShelf2_2
surface4
-log10p
0
−0.5
−1
−1.5
−2
−2.5
. 0.05 < p < 0.1
* p < 0.05
** p < 0.01
*** p < 0.001
main_type
mesenchyme
ectoderm
muscle
erythrocytes
endothelium
SOX2−_SOX10+
immune
SOX2+_SOX10−

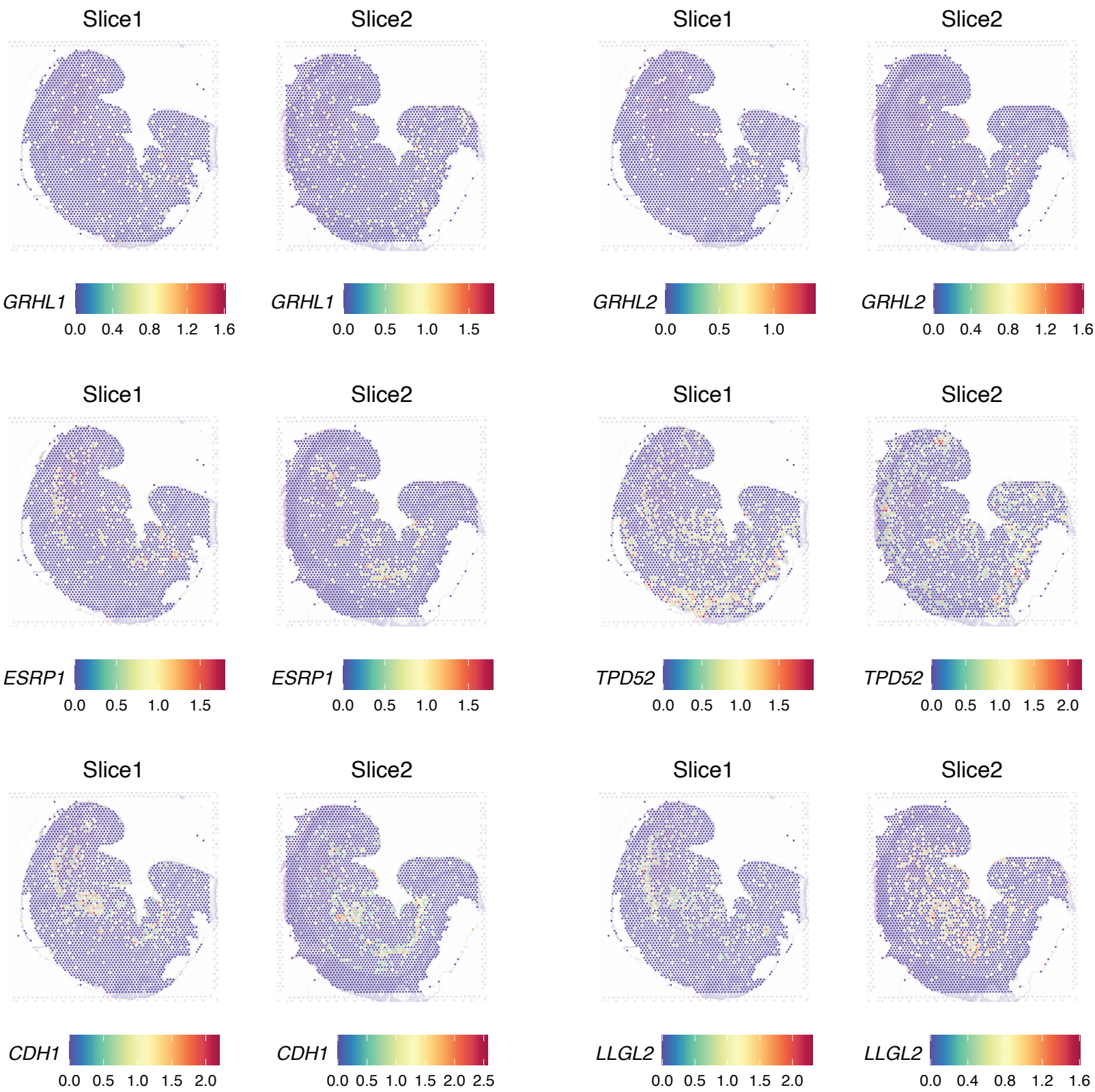
Supplementary Figure 33. Clustered heatmap of significance values calculated by MAGMA.Celltyping[15] for all FinnGen[17] congenital abnormalities or diseases and cell subtypes. Colors along top of heatmap indicate main cell type classification. Levels of significance indicated by asterisks or period according to figure.


Genetic Spatial Mapping Plot:
LVOTO_NARROW
Caudal
-log10p
1
2
3
Rostral

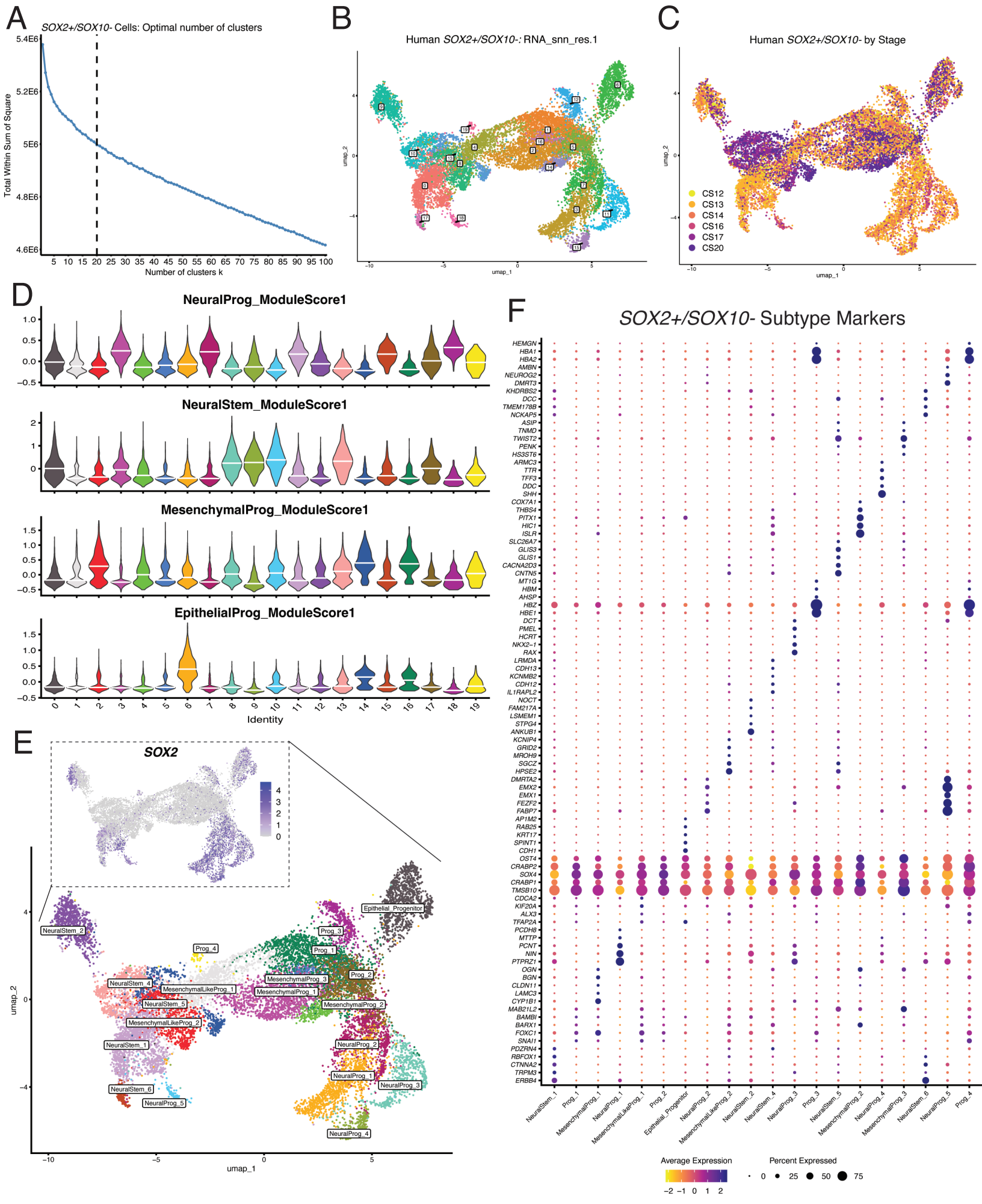

Gene Specificity Score
B4GALNT3
0
1
2
3
4
5

Supplementary Figure 34. Spatial mapping of GWAS variants associated with narrow left ventricular outflow tract obstruction (LVOTO Narrow) and *B4GALNT3* gene specificity scores on Slice 1 of the CS13 human embryo as calculated by gsMAP[18].

Gene Drivers for *de novo* Variants in Probands with Cleft Palate

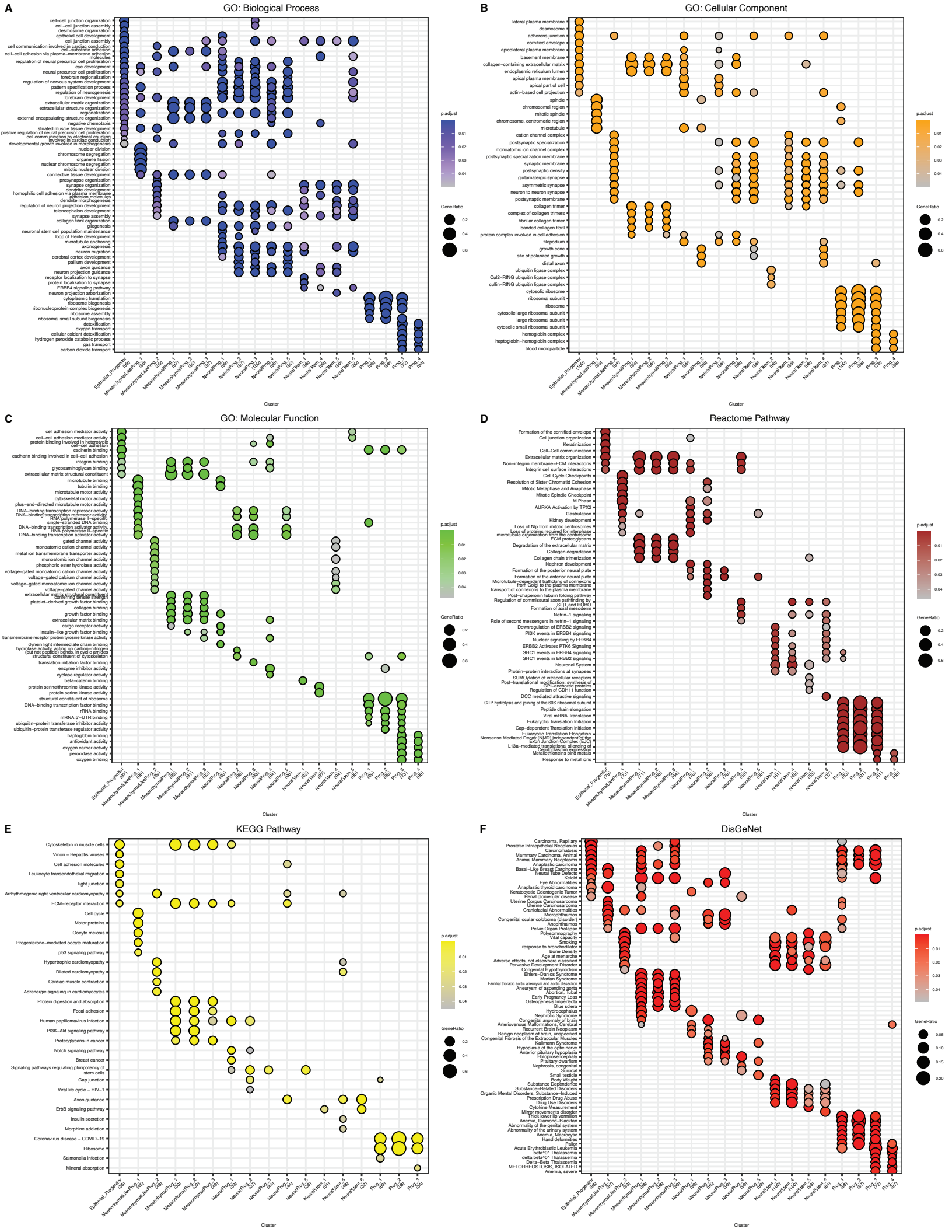


Supplementary Figure 35. Spatial feature plots of genes driving *de novo* variants in probands with cleft palate from two sections of a human CS13 embryo[10].


A
SOX2+/SOX10- Cells: Optimal number of clusters
Total Within Sum of Square
Number of clusters k
B
Human SOX2+/SOX10-: RNA_snn_res.1
umap_1
umap_2
C
Human SOX2+/SOX10- by Stage
CS12
CS13
CS14
CS16
CS17
CS20
D
NeuralProg_ModuleScore1
NeuralStem_ModuleScore1
MesenchymalProg_ModuleScore1
EpithelialProg_ModuleScore1
Identity
E
SOX2
NeuralStem_2
Prog_4
Prog_3
Prog_1
Epithelial_Progenitor
NeuralStem_4
MesenchymalLikeProg_1
MesenchymalProg_3
MesenchymalProg_1
Prog_2
NeuralStem_5
MesenchymalProg_2
MesenchymalLikeProg_2
NeuralStem_1
NeuralProg_2
NeuralProg_1
NeuralProg_3
NeuralStem_6
NeuralProg_5
NeuralProg_4
F
SOX2+/SOX10- Subtype Markers
HEMGN
HBA1
HBA2
AMBN
NEUROG2
DMRT3
KHDRBS2
DCC
TMEM178B
NCKAP5
ASIP
TNMD
TWIST2
PENK
HS3ST6
ARMC3
TTR
TFF3
DDC
SHH
COX7A1
THBS4
PITX1
HIC1
ISLR
SLC26A7
GLIS3
GLIS1
CACNA2D3
CNTN5
MT1G
HBM
AHSP
HBZ
HBE1
DCT
PMEL
HCRT
NKX2-1
RAX
LRMDA
CDH13
KCNMB2
CDH12
IL1RAPL2
NOCT
FAM217A
LSMEM1
STPG4
ANKUB1
KCNIP4
GRID2
MROH9
SGCZ
HPSE2
DMRTA2
EMX2
EMX1
FEZF2
FABP7
AP1M2
RAB25
KRT17
SPINT1
CDH1
OST4
CRABP2
SOX4
CRABP1
TMSB10
CDCA2
KIF20A
ALX3
TFAP2A
PCDH8
MTTP
PCNT
NIN
PTPRZ1
OGN
BGN
CLDN11
LAMC3
CYP1B1
MAB21L2
BAMBI
BARX1
FOXC1
SNAI1
PDZRN4
RBFOX1
CTNNA2
TRPM3
ERBB4
NeuralStem_1
Prog_1
MesenchymalProg_1
NeuralProg_1
MesenchymalLikeProg_1
Prog_2
Epithelial_Progenitor
NeuralProg_2
MesenchymalLikeProg_2
NeuralStem_2
NeuralProg_3
Prog_3
NeuralStem_5
MesenchymalProg_2
NeuralProg_4
MesenchymalProg_3
NeuralStem_6
NeuralProg_5
Prog_4
Average Expression
Percent Expressed

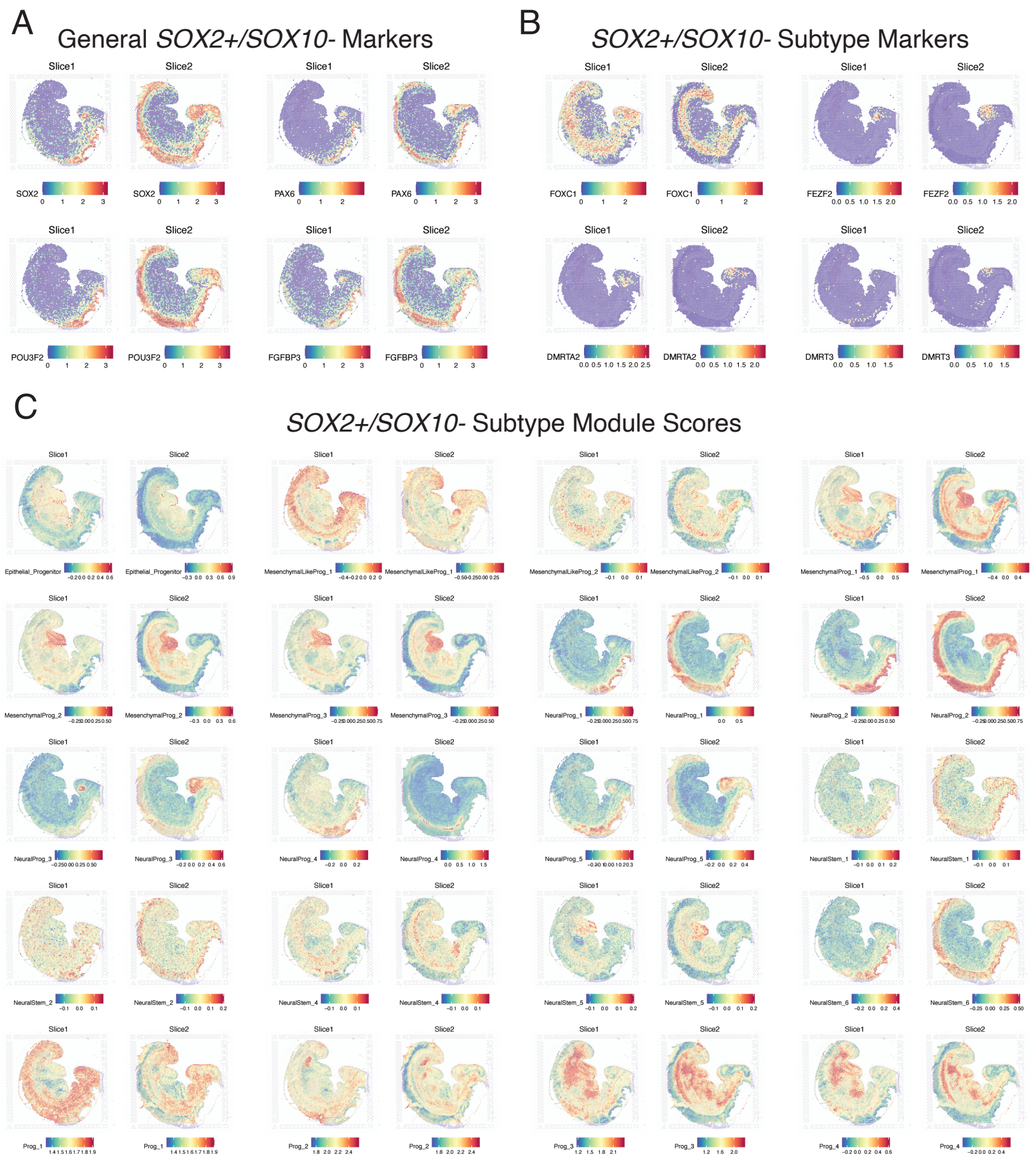
Supplementary Figure 36. Characterizing human *SOX2+/SOX10-* putative early progenitor subtypes.

A). Elbow plot with optimal number of subclusters for human *SOX2+/SOX10-* putative early progenitors. B). UMAP projection of clustered *SOX2+/SOX10-* putative early progenitor cells with resolution parameter set to 1. C). Distribution of cells from each stage across the UMAP projection. D). Neural progenitor, neural stem, mesenchymal progenitor, and epithelial progenitor module scores across *SOX2+/SOX10-* putative early progenitor subclusters. E). UMAP projection with *SOX2+/SOX10-* putative early progenitor cell subtype labels and *SOX2* expression (inset). F). Average and percent expression of the top 5 DEGs for the human *SOX2+/SOX10-* putative early progenitor subtypes.


A
GO: Biological Process
cell−cell junction organization
cell−cell junction assembly
desmosome organization
epithelial cell development
cell junction assembly
cell communication involved in cardiac conduction
cell−substrate adhesion
cell−cell adhesion via plasma−membrane adhesion molecules
regulation of neural precursor cell proliferation
eye development
neural precursor cell proliferation
forebrain regionalization
regulation of nervous system development
pattern specification process
regulation of neurogenesis
forebrain development
extracellular matrix organization
extracellular structure organization
regionalization
external encapsulating structure organization
negative chemotaxis
striated muscle tissue development
positive regulation of neural precursor cell proliferation
cell communication by electrical coupling involved in cardiac conduction
developmental growth involved in morphogenesis
nuclear division
chromosome segregation
organelle fission
nuclear chromosome segregation
mitotic nuclear division
connective tissue development
presynapse organization
synapse organization
dendrite development
homophilic cell adhesion via plasma membrane adhesion molecules
dendrite morphogenesis
regulation of neuron projection development
telencephalon development
synapse assembly
collagen fibril organization
gliogenesis
neuronal stem cell population maintenance
loop of Henle development
microtubule anchoring
axonogenesis
neuron migration
cerebral cortex development
pallium development
axon guidance
neuron projection guidance
receptor localization to synapse
protein localization to synapse
ERBB4 signaling pathway
neuron projection arborization
cytoplasmic translation
ribosome biogenesis
ribonucleoprotein complex biogenesis
ribosome assembly
ribosomal small subunit biogenesis
detoxification
oxygen transport
cellular oxidant detoxification
hydrogen peroxide catabolic process
gas transport
carbon dioxide transport
Epithelial_Progenitor (99)
MesenchymalLikeProg_1 (95)
MesenchymalLikeProg_2 (89)
MesenchymalProg_1 (97)
MesenchymalProg_2 (90)
MesenchymalProg_3 (97)
NeuralProg_1 (98)
NeuralProg_2 (97)
NeuralProg_3 (100)
NeuralProg_4 (95)
NeuralProg_5 (90)
NeuralStem_1 (98)
NeuralStem_4 (95)
NeuralStem_5 (95)
NeuralStem_6 (90)
Prog_1 (99)
Prog_2 (98)
Prog_3 (73)
Prog_4 (94)
Cluster
p.adjust
0.01
0.02
0.03
0.04
GeneRatio
0.2
0.4
0.6
B
GO: Cellular Component
lateral plasma membrane
desmosome
adherens junction
cornified envelope
apicolateral plasma membrane
basement membrane
collagen−containing extracellular matrix
endoplasmic reticulum lumen
apical plasma membrane
apical part of cell
actin−based cell projection
spindle
chromosomal region
mitotic spindle
chromosome, centromeric region
microtubule
cation channel complex
postsynaptic specialization
monoatomic ion channel complex
postsynaptic specialization membrane
synaptic membrane
postsynaptic density
glutamatergic synapse
asymmetric synapse
neuron to neuron synapse
postsynaptic membrane
collagen trimer
complex of collagen trimers
fibrillar collagen trimer
banded collagen fibril
protein complex involved in cell adhesion
filopodium
growth cone
site of polarized growth
distal axon
ubiquitin ligase complex
Cul2−RING ubiquitin ligase complex
cullin−RING ubiquitin ligase complex
cytosolic ribosome
ribosomal subunit
ribosome
cytosolic large ribosomal subunit
large ribosomal subunit
cytosolic small ribosomal subunit
hemoglobin complex
haptoglobin−hemoglobin complex
blood microparticle
Epithelial_Progenitor (100)
MesenchymalLikeProg_1 (99)
MesenchymalLikeProg_2 (94)
MesenchymalProg_1 (98)
MesenchymalProg_2 (98)
MesenchymalProg_3 (98)
NeuralProg_1 (96)
NeuralProg_2 (96)
NeuralProg_3 (98)
NeuralProg_4 (96)
NeuralStem_1 (98)
NeuralStem_2 (98)
NeuralStem_4 (95)
NeuralStem_5 (96)
NeuralStem_6 (91)
Prog_1 (100)
Prog_2 (99)
Prog_3 (73)
Prog_4 (98)
Cluster
p.adjust
0.01
0.02
0.03
0.04
GeneRatio
0.2
0.4
0.6
C
GO: Molecular Function
cell adhesion mediator activity
cell−cell adhesion mediator activity
protein binding involved in heterotypic cell−cell adhesion
cadherin binding
cadherin binding involved in cell−cell adhesion
integrin binding
glycosaminoglycan binding
extracellular matrix structural constituent
microtubule binding
tubulin binding
microtubule motor activity
cytoskeletal motor activity
plus−end−directed microtubule motor activity
DNA−binding transcription repressor activity
DNA−binding transcription repressor activity, RNA polymerase II−specific
single−stranded DNA binding
DNA−binding transcription activator activity
DNA−binding transcription activator activity, RNA polymerase II−specific
gated channel activity
monoatomic cation channel activity
metal ion transmembrane transporter activity
monoatomic ion channel activity
phosphoric ester hydrolase activity
voltage−gated monoatomic cation channel activity
voltage−gated calcium channel activity
voltage−gated monoatomic ion channel activity
voltage−gated channel activity
extracellular matrix structural constituent conferring tensile strength
platelet−derived growth factor binding
collagen binding
growth factor binding
extracellular matrix binding
cargo receptor activity
insulin−like growth factor binding
transmembrane receptor protein tyrosine kinase activity
dynein light intermediate chain binding
hydrolase activity, acting on carbon−nitrogen (but not peptide) bonds, in cyclic amides
structural constituent of cytoskeleton
translation initiation factor binding
enzyme inhibitor activity
cyclase regulator activity
beta−catenin binding
protein serine/threonine kinase activity
protein serine kinase activity
structural constituent of ribosome
DNA−binding transcription factor binding
rRNA binding
mRNA 5'−UTR binding
ubiquitin−protein transferase inhibitor activity
ubiquitin−protein transferase regulator activity
haptoglobin binding
antioxidant activity
oxygen carrier activity
peroxidase activity
oxygen binding
Epithelial_Progenitor (97)
MesenchymalLikeProg_1 (96)
MesenchymalLikeProg_2 (88)
MesenchymalProg_1 (96)
MesenchymalProg_2 (91)
MesenchymalProg_3 (92)
NeuralProg_1 (98)
NeuralProg_2 (98)
NeuralProg_3 (98)
NeuralProg_4 (94)
NeuralProg_5 (96)
NeuralStem_1 (92)
NeuralStem_2 (97)
NeuralStem_4 (94)
NeuralStem_5 (95)
NeuralStem_6 (90)
Prog_1 (99)
Prog_2 (98)
Prog_3 (73)
Prog_4 (94)
Cluster
p.adjust
0.01
0.02
0.03
0.04
GeneRatio
0.2
0.4
0.6
D
Reactome Pathway
Formation of the cornified envelope
Cell junction organization
Keratinization
Cell−Cell communication
Extracellular matrix organization
Non−integrin membrane−ECM interactions
Integrin cell surface interactions
Cell Cycle Checkpoints
Resolution of Sister Chromatid Cohesion
Mitotic Metaphase and Anaphase
Mitotic Spindle Checkpoint
M Phase
AURKA Activation by TPX2
Gastrulation
Kidney development
Loss of Nlp from mitotic centrosomes
Loss of proteins required for interphase microtubule organization from the centrosome
ECM proteoglycans
Degradation of the extracellular matrix
Collagen degradation
Collagen chain trimerization
Nephron development
Formation of the posterior neural plate
Formation of the anterior neural plate
Microtubule−dependent trafficking of connexons from Golgi to the plasma membrane
Transport of connexons to the plasma membrane
Post−chaperonin tubulin folding pathway
Regulation of commissural axon pathfinding by SLIT and ROBO
Formation of axial mesoderm
Netrin−1 signaling
Role of second messengers in netrin−1 signaling
Downregulation of ERBB2 signaling
PI3K events in ERBB4 signaling
Nuclear signaling by ERBB4
ERBB2 Activates PTK6 Signaling
SHC1 events in ERBB4 signaling
SHC1 events in ERBB2 signaling
Neuronal System
Protein−protein interactions at synapses
SUMOylation of intracellular receptors
Post−translational modification: synthesis of GPI−anchored proteins
Regulation of CDH11 function
DCC mediated attractive signaling
GTP hydrolysis and joining of the 60S ribosomal subunit
Peptide chain elongation
Viral mRNA Translation
Eukaryotic Translation Initiation
Cap−dependent Translation Initiation
Eukaryotic Translation Elongation
Nonsense Mediated Decay (NMD) independent of the Exon Junction Complex (EJC)
L13a−mediated translational silencing of Ceruloplasmin expression
Metallothioneins bind metals
Response to metal ions
Epithelial_Progenitor (79)
MesenchymalLikeProg_1 (73)
MesenchymalProg_1 (71)
MesenchymalProg_2 (62)
MesenchymalProg_3 (64)
NeuralProg_1 (70)
NeuralProg_2 (66)
NeuralProg_3 (70)
NeuralProg_4 (65)
NeuralProg_5 (60)
NeuralStem_1 (61)
NeuralStem_4 (65)
NeuralStem_5 (65)
NeuralStem_6 (51)
Prog_1 (63)
Prog_2 (61)
Prog_3 (61)
Prog_4 (66)
Cluster
p.adjust
0.01
0.02
0.03
0.04
GeneRatio
0.2
0.4
0.6
E
KEGG Pathway
Cytoskeleton in muscle cells
Virion − Hepatitis viruses
Cell adhesion molecules
Leukocyte transendothelial migration
Tight junction
Arrhythmogenic right ventricular cardiomyopathy
ECM−receptor interaction
Cell cycle
Motor proteins
Oocyte meiosis
Progesterone−mediated oocyte maturation
p53 signaling pathway
Hypertrophic cardiomyopathy
Dilated cardiomyopathy
Cardiac muscle contraction
Adrenergic signaling in cardiomyocytes
Protein digestion and absorption
Focal adhesion
Human papillomavirus infection
PI3K−Akt signaling pathway
Proteoglycans in cancer
Notch signaling pathway
Breast cancer
Signaling pathways regulating pluripotency of stem cells
Gap junction
Viral life cycle − HIV−1
Axon guidance
ErbB signaling pathway
Insulin secretion
Morphine addiction
Coronavirus disease − COVID−19
Ribosome
Salmonella infection
Mineral absorption
Epithelial_Progenitor (68)
MesenchymalLikeProg_1 (66)
MesenchymalLikeProg_2 (43)
MesenchymalProg_1 (60)
MesenchymalProg_2 (58)
MesenchymalProg_3 (58)
NeuralProg_1 (59)
NeuralProg_2 (57)
NeuralProg_3 (64)
NeuralProg_4 (44)
NeuralProg_5 (56)
NeuralStem_1 (51)
NeuralStem_4 (46)
NeuralStem_5 (56)
NeuralStem_6 (50)
Prog_1 (68)
Prog_2 (68)
Prog_3 (54)
Cluster
p.adjust
0.01
0.02
0.03
0.04
GeneRatio
0.2
0.4
0.6
F
DisGeNet
Carcinoma, Papillary
Prostatic Intraepithelial Neoplasias
Carcinomatosis
Mammary Carcinoma, Animal
Animal Mammary Neoplasms
Anaplastic carcinoma
Basal−Like Breast Carcinoma
Neural Tube Defects
Keloid
Eye Abnormalities
Anaplastic thyroid carcinoma
Keratocystic Odontogenic Tumor
Renal glomerular disease
Uterine Corpus Carcinosarcoma
Uterine Carcinosarcoma
Craniofacial Abnormalities
Microphthalmos
Congenital ocular coloboma (disorder)
Anophthalmos
Pelvic Organ Prolapse
Polysomnography
Vital capacity
Smoking
response to bronchodilator
Bone Density
Age at menarche
Adverse effects, not elsewhere classified
Pervasive Development Disorder
Congenital Hypothyroidism
Ehlers−Danlos Syndrome
Marfan Syndrome
Familial thoracic aortic aneurysm and aortic dissection
Aneurysm of ascending aorta
Abortion, Tubal
Early Pregnancy Loss
Osteogenesis Imperfecta
Blue sclera
Hydrocephalus
Nephrotic Syndrome
Congenital anomaly of brain
Arteriovenous Malformations, Cerebral
Recurrent Brain Neoplasm
Benign neoplasm of brain, unspecified
Congenital Fibrosis of the Extraocular Muscles
Kallmann Syndrome
Hypoplasia of the optic nerve
Anterior pituitary hypoplasia
Holoprosencephaly
Pituitary dwarfism
Nephrosis, congenital
Suicidal
Small testicle
Body Weight
Substance Dependence
Substance−Related Disorders
Organic Mental Disorders, Substance−Induced
Prescription Drug Abuse
Drug Use Disorders
Cytokine Measurement
Mirror movements disorder
Thick lower lip vermilion
Anemia, Diamond−Blackfan
Abnormality of the genital system
Abnormality of the urinary system
Anemia, Macrocytic
Hand deformities
Pallor
Acute Erythroblastic Leukemia
beta*0^ Thalassemia
delta beta*0^ Thalassemia
Delta−Beta Thalassemia
MELORHEOSTOSIS, ISOLATED
Anemia, severe
Epithelial_Progenitor (68)
MesenchymalLikeProg_1 (67)
MesenchymalLikeProg_2 (62)
MesenchymalProg_1 (68)
MesenchymalProg_2 (68)
MesenchymalProg_3 (68)
NeuralProg_1 (68)
NeuralProg_2 (68)
NeuralProg_3 (68)
NeuralProg_4 (68)
NeuralProg_5 (63)
NeuralStem_1 (68)
NeuralStem_4 (68)
NeuralStem_5 (68)
NeuralStem_6 (61)
Prog_1 (68)
Prog_2 (67)
Prog_3 (73)
Prog_4 (61)
Cluster
p.adjust
0.01
0.02
0.03
0.04
GeneRatio
0.05
0.10
0.15
0.20

Supplementary Figure 37. Functional annotation enrichment for human *SOX2+/SOX10-* putative early progenitor subtypes using the top 100 marker genes.

A). Gene Ontology for Biological Processes. B). Gene Ontology for Cellular Components. C). Gene Ontology for Molecular Functions. D). Reactome Pathways. E). KEGG pathways. F). DisGeNet.


A
General SOX2+/SOX10- Markers
Slice1
Slice2
SOX2
PAX6
POU3F2
FGFBP3
B
SOX2+/SOX10- Subtype Markers
FOXC1
FEZF2
DMRTA2
DMRT3
C
SOX2+/SOX10- Subtype Module Scores
Epithelial_Progenitor
MesenchymalLikeProg_1
MesenchymalLikeProg_2
MesenchymalProg_1
MesenchymalProg_2
MesenchymalProg_3
NeuralProg_1
NeuralProg_2
NeuralProg_3
NeuralProg_4
NeuralProg_5
NeuralStem_1
NeuralStem_2
NeuralStem_4
NeuralStem_5
NeuralStem_6
Prog_1
Prog_2
Prog_3
Prog_4

Supplementary Figure 38. Spatial feature plots of human *SOX2+/SOX10-* putative early progenitor genes and module scores from two sections of a human CS13 embryo[10].

A). General *SOX2+/SOX10-* putative early progenitor gene markers. B). Human *SOX2+/SOX10-* putative early progenitor subtype markers. C). Human *SOX2+/SOX10-* putative early progenitor subtype module scores.

3. Supplementary References

1. Li, M. *et al.* Integrative functional genomic analysis of human brain development and neuropsychiatric risks. *Science (New York, NY)* **362**, eaat7615 (2018).
2. Rajderkar, S.S. *et al.* Dynamic enhancer landscapes in human craniofacial development. *Nat Commun* **15**, 2030 (2024).
3. Yankee, T.N. *et al.* Integrative analysis of transcriptome dynamics during human craniofacial development identifies candidate disease genes. *Nat Commun* **14**, 4623 (2023).
4. Eze, U.C., Bhaduri, A., Haeussler, M., Nowakowski, T.J. & Kriegstein, A.R. Single-cell atlas of early human brain development highlights heterogeneity of human neuroepithelial cells and early radial glia. *Nat Neurosci* **24**, 584-594 (2021).
5. Liberzon, A. *et al.* The Molecular Signatures Database (MSigDB) hallmark gene set collection. *Cell Syst* **1**, 417-425 (2015).
6. Leland, M., Healy, J. & Melville, J. UMAP: Uniform Manifold Approximation and Projection for Dimension Reduction. *arXiv* **1802.03426**(2020).
7. Ianevski, A., Giri, A.K. & Aittokallio, T. Fully-automated and ultra-fast cell-type identification using specific marker combinations from single-cell transcriptomic data. *Nat Commun* **13**, 1246 (2022).
8. Wang, C. *et al.* Single-cell RNA sequencing analysis of human embryos from the late Carnegie to fetal development. *Cell Biosci* **14**, 118 (2024).
9. Hu, C. *et al.* CellMarker 2.0: an updated database of manually curated cell markers in human/mouse and web tools based on scRNA-seq data. *Nucleic Acids Res* **51**, D870-D876 (2023).
10. Xu, Y. *et al.* A single-cell transcriptome atlas profiles early organogenesis in human embryos. *Nature Cell Biology* **25**, 604-615 (2023).
11. Chen, A. *et al.* Spatiotemporal transcriptomic atlas of mouse organogenesis using DNA nanoball-patterned arrays. *Cell* **185**, 1777-1792.e21 (2022).
12. Chen, J., Bardes, E.E., Aronow, B.J. & Jegga, A.G. ToppGene Suite for gene list enrichment analysis and candidate gene prioritization. *Nucleic Acids Research* **37**, W305-W311 (2009).
13. Pina, J.O. *et al.* Multimodal spatiotemporal transcriptomic resolution of embryonic palate osteogenesis. *Nat Commun* **14**, 5687 (2023).
14. Chen, A. *et al.* Spatiotemporal transcriptomic atlas of mouse organogenesis using DNA nanoball-patterned arrays. *Cell* **185**, 1777-1792 e21 (2022).
15. Skene, N.G. *et al.* Genetic identification of brain cell types underlying schizophrenia. *Nature Genetics* **50**, 825-833 (2018).
16. Xiong, Z. *et al.* Novel genetic loci affecting facial shape variation in humans. *eLife* **8**, e49898 (2019).
17. Kurki, M.I. *et al.* FinnGen provides genetic insights from a well-phenotyped isolated population. *Nature* **613**, 508-518 (2023).
18. Song, L., Chen, W., Hou, J., Guo, M. & Yang, J. Spatially resolved mapping of cells associated with human complex traits. *Nature* **641**, 932-941 (2025).